



**EUROPEAN SCHOOL OF MOLECULAR MEDICINE
SEDE DI NAPOLI
UNIVERSITA' DEGLI STUDI DI NAPOLI "FEDERICO II"**

**Ph.D. in Molecular Medicine – Ciclo III/XXI
Curriculum Human Genetics**



"Mechanisms of transcriptional regulation by Tbx1"

**Tutor:
Prof. Antonio Baldini**

**Internal Supervisor:
Prof. Michele Studer**

**External Supervisor:
Prof. Peter Scambler**

**Coordinator:
Prof. Francesco Salvatore**

**Ph.D. student:
Dr. Luna Simona Pane**

Academic Year: 2008-2009

ACKNOWLEDGMENTS

I would like to thank my supervisor, Professor Antonio Baldini, for his guidance and training.

I would like to thank Dr. Elizabeth Illingworth for her useful suggestions and discussions.

I would like to thank the past and present members of the Baldini lab, who have provided an intellectually stimulating and entertaining work environment.

Finally, I would like to thank my family and friends, for their love, support and encouragement.

ABSTRACT

Deletion 22q11.2 syndrome (22q11DS) is the most common microdeletion syndrome in man, with an incidence of approximately 1:4000 live births (1); the major malformations include congenital heart defects such as truncus arteriosus (TA) and interrupted aortic arch type B (IAA-B), hypo/aplasia of the parathyroid and thymus glands, and craniofacial dysmorphism. Velo-cardio-facial (VCFS) and DiGeorge syndromes (DGS) are other diagnoses commonly made in affected individuals (1). The gene encoding the T-box transcription factor *Tbx1*, which is required for pharyngeal and cardiovascular development, has been identified as the gene haploinsufficient in mouse and human.

We and others have identified a number of genes potentially targeted by *Tbx1*, but the mechanisms by which it can regulate the transcription of these genes and how it controls developmental pathways, are mostly unclear.

One of the best studied molecular functions of *Tbx1* is in heart development, where it is required to sustain proliferation of mesodermally-derived precursors of the second heart field (SHF), a cardiac progenitor cell population that contributes to the development of most of the heart, including the outflow tract and right ventricle.

To better understand how it works during embryonic development, we evaluated *Tbx1*-dosage dependent gene expression changes in vivo using a novel dosage gradient approach. Among genes sensitive to *Tbx1* level, we found the one encoding the cardiogenic transcription factor Mef2c which is involved in cardiomyocyte differentiation. Interestingly, this gene was anti-correlated to *Tbx1* dosage; in situ hybridization on mutant mouse embryos also corroborated quantitative expression data. These results suggest that *Tbx1* may negatively regulate cardiac muscle cell differentiation through a mechanism involving *Mef2c* transcriptional repression; this would be consistent with recent data showing that loss of function of *Tbx1* is associated with increased expression of differentiation markers of the myocardium.

It has also been shown that *Mef2c* is a direct transcriptional target of Gata4 in the SHF, during mouse embryonic development (2); accordingly our *in vitro* data, suggest that *Tbx1* could negatively regulate *Mef2c* expression, somehow interfering with Gata4-dependent *Mef2c* activation. Virtually all the mechanistic data obtained so far derive from murine models of 22q11DS; there is the need of a system to validate these data on human material. Since human Embryonic Stem cells can differentiate *in vitro*, into multiple somatic tissues, including cardiac progenitors, we

generated DiGeorge syndrome-specific Pluripotent Stem cells by reprogramming adult patient fibroblasts. Developing of this system as human model of the disease, will help us to investigate its underlying molecular mechanism on a cellular level. *Tbx1* loss of function in mice, and, to a lesser extent, *TBX1* haploinsufficiency in DiGeorge syndrome patients, is associated with hypoplasia or aplasia of several organs and tissues; so it is possible that *Tbx1* function in regulating the balance between proliferation and differentiation in the SHF, may also apply to other tissues where *Tbx1* is expressed. Availability of DiGeorge syndrome-specific Pluripotent Stem cells, will help us to speculate whether that dysregulation of the balance between proliferation and differentiation of different types of progenitor cells or stem cells, may be a basic pathogenic mechanism for the loss of function phenotype.

TABLE OF CONTENTS

ACKNOWLEDGMENTS.....	2
ABSTRACT.....	3
LIST OF FIGURES.....	11
CHAPTER 1: Introduction.....	14
1.1 T-box genes.....	14
1.2 T-box transcription factors and human disorders... 	16
1.3 <i>TBX1</i> and Del22q11.2/DiGeorge syndrome.....	24
1.4 <i>Tbx1</i> roles during mouse embryonic development....	29
1.5 The emerging <i>Tbx1</i> genetic pathway.....	43
CHAPTER 2: Materials and methods.....	48
2.1 Mouse lines, breeding and genotyping.....	48
2.2 Cloning, plasmids and mutagenesis.....	48
2.3 Cell culture and transfections.....	49
2.4 Microarray analysis.....	50
2.5 T-box binding element (TBE) analysis.....	51
2.6 Quantitative Real-Time PCR (qRT-PCR).....	52
2.7 In situ hybridization.....	53
2.8 Western Blotting.....	55
2.9 Luciferase assays.....	55

2.10 RNA interference.....	56
CHAPTER 3: Results.....	58
3.1 Microarray analysis of <i>Tbx1</i> dosage-dependent gene expression changes <i>in vivo</i>	58
3.2 Conserved T-box binding element analysis.....	62
3.3 Selection of <i>Tbx1</i> candidate transcriptional targets..	63
3.4 Validation of selected <i>Tbx1</i> candidate transcriptional targets.....	64
3.4.1 <i>Pex2: peroxin2</i>	64
3.4.2 <i>Vps33a: vacuolar protein sorting 33A</i>	65
3.4.3 <i>Morf4l1: mortality factor 4 like 1</i>	67
3.4.4 <i>Tgfbr3: transforming growth factor, beta receptor III</i>	70
3.4.5 <i>Mef2c: myocyte enhancer factor 2C</i>	73
3.5 <i>Mef2c</i> is specifically overexpressed in the second heart field of <i>Tbx1</i> ^{-/-} mutant embryos.....	82
3.6 <i>Mef2c</i> expression is <i>Tbx1</i> dosage-dependent in transfected C2C12 myoblasts.....	82
3.7 <i>Mef2c</i> protein level is affected by <i>Tbx1</i> dosage in transfected C2C12 myoblasts.....	85

3.8 Conserved T-box binding element analysis of <i>Mef2c</i> locus.....	89
3.9 <i>Mef2c</i> regulation by Tbx1 seems to be mediated by Gata4.....	93
3.10 <i>Mef2c</i> regulation by Tbx1 does not require its direct binding to the SHF-specific enhancer of <i>Mef2c</i> locus.....	96
3.11 <i>Tbx1</i> dosage does not affect <i>Mef2c</i> expression in the absence of Gata4 in transfected C1C12 myoblasts.....	98
3.12 <i>Mef2c</i> is negatively regulated by Tbx1 in skeletal muscle cells <i>in vivo</i>	101
3.13 <i>Mef2c</i> is negatively regulate by Tbx1 during <i>in vitro</i> C2C12 myoblast differentiation.....	108
CHAPTER 4: Discussion.....	111
4.1 <i>Pex2</i> and <i>Vps33a</i> : cytoplasmic organelle biogenesis and brain abnormalities.....	113
4.2 <i>Morf4l1</i> and <i>TgfrbIII</i> : positive regulation of cell proliferation.....	118
4.3 <i>Mef2c</i> : negative regulation of cardiac and skeletal muscle cell differentiation.....	120
CHAPTER 5: Appendix.....	129

5.1 Towards a human model of DiGeorge syndrome...	129
5.2 Material and methods.....	132
5.2.1 Cell culture.....	132
5.2.2 Genomic DNA analysis.....	133
5.2.3 Expression analysis.....	133
5.2.4 Alkaline Phosphatase Staining, Immunofluorescence and DAPI staining.....	133
5.2.5 Fluorescence-activated cell sorting analysis.....	135
5.3 Results and discussion.....	136
5.3.1 Generation of human induced Pluripotent Stem (hiPS) cells from DGS fibroblasts.....	136
5.3.2 Characterization of hiPS cells generated from DGS fibroblasts.....	139
5.3.2.I Alkaline Phosphatase staining.....	139
5.3.2.II Genotype analysis.....	139
5.3.2.III ES cell marker expression analysis.....	141
5.3.2.IV OCT3/4 expression analysis.....	143
5.3.2.V SSEA-4 surface antigen expression analysis... 	143
5.3.2.VI Fluorescence-activated cell sorting analysis... 	146
5.3.3 Human induced Pluripotent Stem cells and disease	

modeling.....	148
CHAPTER 6: Bibliography.....	152

LIST OF FIGURES

Figure 1: <i>Tbx1</i> mRNA dosage in E9.5 wt and mutant embryos.....	60
Figure 2: genes differentially expressed across the <i>Tbx1</i> allelic series...	61
Figure 3: <i>Pex2</i> and <i>Morf4l1</i> are down-regulated in <i>Tbx1</i> null mutant embryos at E9.5, while <i>Vps33a</i> and <i>Mef2c</i> are up-regulated.....	76
Figure 4: the ROSA-TET system.....	79
Figure 5: induction of expression in the <i>Tbx1</i> -ROSA-TET system.....	79
Figure 6: <i>Mef2c</i> , <i>Vps33a</i> and <i>Tgfbr3</i> are down-regulated in <i>Tbx1</i> over-expressing ES cells, while <i>Morf4l1</i> and <i>Pex2</i> are up-regulated.....	81
Figure 7: <i>Mef2c</i> is specifically over-expressed in the second heart field of <i>Tbx1</i> null mutant embryos at E9.5.....	83
Figure 8: <i>Mef2c</i> expression is <i>Tbx1</i> dosage-dependent in transfected C2C12 myoblasts.....	84
Figure 9: <i>Tbx1</i> dosage affects <i>Mef2c</i> protein level in transfected C2C12 myoblasts.....	86
Figure 10: <i>Tbx1</i> interferes with Gata4-dependent <i>Mef2c</i> activity in transfected C2C12 myoblasts.....	88
Figure 11: schematic representation of the second heart field-specific enhancer of <i>Mef2c</i> locus.....	92
Figure 12: <i>Tbx1</i> interferes with Gata4-dependent activation of <i>Mef2c</i>	

second heart field-specific enhancer.....	95
Figure 13: <i>Mef2c</i> regulation by Tbx1 does not require its direct binding to the TBE in the second heart field enhancer of <i>Mef2c</i> locus.....	97
Figure 14: endogenous <i>Gata4</i> RNAi in C2C12 myoblasts.....	100
Figure 15: in the absence of Gata4, Tbx1 is not able to regulate <i>Mef2c</i> expression.....	100
Figure 16: <i>Tbx1</i> over-expression in COET; <i>Mesp1</i> ^{Cre/+} mutant embryos at E9.5.....	102
Figure 17: <i>Mef2c</i> is down-regulated in the second heart field and inflow tract of COET; <i>Mesp1</i> ^{Cre/+} mutant embryos at E9.5.....	104
Figure 18: <i>Mef2c</i> is down-regulated in the somite compartment of COET; <i>Mesp1</i> ^{Cre/+} mutant embryos at E9.5.....	105
Figure 19: <i>Gata4</i> is down-regulated in the heart of COET; <i>Mesp1</i> ^{Cre/+} mutant embryos at E8.5 and E9.5.....	107
Figure 20: Tbx1 inhibits <i>in vitro</i> C2C12 myoblast differentiation.....	109
Figure 21: induced Pluripotent Stem (iPS) cells from DiGeorge syndrome (DGS) fibroblasts show a human embryonic stem cell-like morphology.....	138
Figure 22: iPS cells induced from DGS fibroblasts are positive for alkaline phosphatase staining.....	140

Figure 23: The genome of iPS cells induced from DGS fibroblasts, shows integration of all the retroviruses used for reprogramming.....	140
Figure 24: iPS cells induced from DGS fibroblasts express several human embryonic stem cell marker genes.....	142
Figure 25: iPS cells induced from DGS fibroblasts strongly express OCT3/4.....	144
Figure 26: iPS cells induced from DGS fibroblasts strongly express the surface antigen SSEA-4.....	145
Figure 27: FACS analysis shows the presence of a significant number of OCT3/4-SSEA-4 double positive cells in iPS clones induced from DGS fibroblasts.....	147

CHAPTER 1

Introduction

1.1 T-box genes

Tbx1 belongs to the T-box gene family, which consists of at least seventeen different members in Mammals, organized into five distinct subfamilies based on phylogenetic analyses and presumed gene duplication events during evolution. T-box genes encode a group of phylogenetically conserved transcription factors, defined by a common DNA binding domain, the T-box sequence, the T-site or T-box binding element (TBE), that was first defined as the sequence with the highest affinity for Brachyury (3). Brachyury binds this palindromic sequence as a dimer (4), with each monomer of Brachyury binding half of the sequence, or T-half site (5'-AGGTGTGAAATT-3'). Extensive studies have demonstrated that all T-box proteins tested are capable of binding the T-half site as monomers (4-10), although some have different optimal target sequences (11, 12). Comparisons between T-box proteins have shown reference for different synthetic combinations of T-half sites in varying orientations, numbers, and spacing (9, 13), which may help to create promoter specificity for target genes.

As well as binding DNA, T-box genes have been shown to regulate transcription. Activation domains have been mapped to the C-terminal domains of several T-box proteins (10, 14, 15). T-box proteins can also repress transcription, as has been shown for Tbx2, Tbx3 and Tbx20 (12, 16-19). Some T-box genes contain both activation and repression domains in their C-terminal domains (10, 14) and Tbx2 has been reported to act in either fashion, depending on promoter context (8). Although some T-box gene targets appear to be regulated by T-box proteins alone (20), there is a growing body of work demonstrating that target genes are controlled in combination with other transcription factors. Cooperative binding of promoters and synergistic upregulation of target gene expression is seen with T-box factors and homeodomain (7, 10), GATA zinc finger (10, 21, 22), and LIM domain proteins (23). Frequently, these interactions enhance target gene activation, and probably contribute to promoter specificity. Some of these interactions can be generalized to transcription factor subfamilies while others are exquisitely specific; Tbx20, for example, interacts with GATA5 but not the related transcription factor GATA4 (10). In an even more extreme case of specificity, LMP4 binds both of the most closely related vertebrate T-box

proteins, Tbx4 and Tbx5, but interacts with each via a different LIM domain repeat (23).

1.2 T-box transcription factors and human disorders

Members of the evolutionarily conserved T-box family of transcription factors are important players in developmental processes that include mesoderm formation and patterning and organogenesis both in vertebrates and invertebrates. The importance of T-box genes for human development is illustrated by the association between mutations in several of the seventeen human family members and congenital errors of morphogenesis that include cardiac, craniofacial, and limb malformations (24, 25).

Ulnar-mammary syndrome (UMS, OMIM 181450) is caused by mutations in *TBX3*, (26-28). It affects the ulnar ray of the limb with phenotypes ranging from hypoplasia of the terminal phalanx of the fifth digit, to the complete absence of forearm and hand (28). Patients with UMS also have abnormal development of breasts, teeth and genitalia (29, 30). Male patients typically have delayed onset of puberty (31). *TBX3* is expressed in a wide range of tissues including those where developmental abnormalities occur in UMS (27, 32, 33). There does appear to be a correlation between *TBX3* mutations and UMS symptoms, suggesting that

haploinsufficiency of *TBX3* causes UMS. *TBX3* has a role in specification of posterior limb mesoderm and in setting up the dorso/ventral limb axis. In some cases of UMS, posterior structures are lost or duplicated, and in others the ventral surface of posterior digits becomes dorsalized (28). Breast, tooth and genital development all rely on inductive interactions between epithelial tissue and underlying mesenchyme (34-36) and *TBX3* may have a common role in these developmental processes.

Holt–Oram syndrome (HOS, OMIM 142900) is an autosomal dominant disorder affecting 1 in 100000 live births. It is completely penetrant with a highly variable expression and causes both cardiac and skeletal congenital abnormalities. The skeletal abnormalities affect the forelimb, and include clinodactyly, limited supination, sloping shoulders and phocomelia. They affect the radial ray and are bilateral and asymmetrical, affecting the left side more severely than the right. Defects observed in the heart affect the conduction system, atrial and ventricular septation and tetralogy of Fallot. A high proportion of patients have an absence of the pectoralis major and an ocular defect (37). Mutations in *TBX5* have been identified in both familial and sporadic cases of HOS (38-43). The majority of mutations in *TBX5* are null alleles that cause the HOS phenotype by haploinsufficiency; they cause both severe cardiac and

skeletal phenotypes. A mouse model of Holt–Oram syndrome has been made (5); heterozygous *Tbx5*^{del/+} mice show both cardiac and forelimb defects, having enlarged hearts with atrial septal defects and conduction defects as well as hypoplastic falciformis bones in the wrist and elongated phalanges in the first digit of the forelimb.

Tbx19, also known as *Tpit*, was identified as required for expression of pro-opiomelanocortin (POMC) in the corticotroph and melanotroph pituitary lineages (7). Expression is restricted to the ventral aspects of the anterior pituitary and the ventral diencephalon (7, 44). In humans the absence of pituitary POMC leads to a lack of adrenocorticotrophin (ACTH) resulting in adrenal insufficiency (OMIM 201400). *TBX19* (45) was screened in patients with this phenotype and seven different mutations were identified (7, 46). Isolated ACTH deficiency is transmitted recessively; in all cases, except for one compound heterozygote, the patients were homozygous for a *TBX19* mutation while their unaffected parents were heterozygous carriers (46). The missense mutations identified had severely reduced ability to bind their DNA target and activate transcription while the other mutations generated prematurely terminated transcripts. This suggests that the *TBX19* mutations described were loss-of-function alleles. *Tbx19* activates the

POMC promoter synergistically with the homeodomain protein *Pitx1* (7); this activation requires both transcription factors to be bound to the DNA. Ectopic expression of *Tbx19* in cells expressing high levels of *Pitx1* is sufficient to activate POMC, suggesting that it may act as a signal to initiate POMC cell differentiation (7). *Tpit*-deficient mice model isolated ACTH deficiency (46) and should facilitate understanding of differentiation of the pituitary corticotroph lineage.

Cleft palate affects 1 in 1500 births and is caused by failure of the paired palatal shelves to make contact and form the midline seam which later disappears, allowing the palate to become confluent. Cleft palate causes problems with feeding, speech, hearing, dental and also psychological development, and requires corrective surgery. It is usually sporadic and involves both genetic and environmental factors (47, 48). However, cleft palate with ankyloglossia (CPX, OMIM 303400) is a semi-dominant X-linked condition mapping to Xq21 in which environmental factors play little part (49-52). *TBX22* was identified on Xq21 during the human genome project (53, 54). It maps to the CPX critical region and is expressed at the correct time and in the appropriate tissue for palatogenesis (55-57). Screening of individuals with CPX has identified eight point mutations in *TBX22* including splice site, missense and

nonsense mutations (55, 58). These segregate with the disorder in their respective families confirming *TBX22* as the causative gene for CPX.

Mutations in the human *TBX4* gene underlie Small Patella Syndrome (SPS) also referred to as “Scott-Taor syndrome”, “ischio-pubicpatellar syndrome”, “coxo-podo patellar syndrome” or “ischiopatellar dysplasia”, which is a rare autosomal-dominant disorder affecting skeletal structures of the lower limb and the pelvis (59-63). Essential features for the clinical diagnosis of SPS are patellar aplasia or hypoplasia, associated with absent, delayed, or irregular ossification of the ischiopubic junctions and/or the infra-acetabular axe-cut notches (64). In addition, femur and foot anomalies and pes planus, may accompany SPS. Craniofacial dysmorphisms have been described in reports of four sporadic individuals with SPS and one familial case of SPS including micrognathia and/or cleft palate (64-68). The SPS phenotype suggests that human *TBX4* mutations do not affect early steps in limb development, such as limb-bud initiation, but do have a profound effect at later stages. The late effect of *TBX4* mutations is manifested by patellar aplasia/hypoplasia and anomalies of the posterior structures of the foot, such as short fourth and fifth rays. Completion of ischiopubic formation is another very late process in human development, that is disrupted in individuals with SPS

(69).

Laush et al. (70) identified two unrelated individuals affected by Cousin syndrome, a complex cranial, cervical, auricular, and skeletal malformation syndrome with scapular and pelvic hypoplasia (Cousin syndrome) that recapitulates the dysmorphic phenotype seen in the *Tbx15*-deficient mice, *droopy ear*. *Droopy ear* exhibits a complex craniofacial malformation including small, widely spaced eyes with short palpebral fissures, a broad nasal area, a shortened skull held in an elevated position, misshapen and rotated external ears, and an abnormal coat-color patterning (71, 72). The skeletal phenotype of *Tbx15*-inactivated mice includes small overall size, hypoplastic scapulae, moderate shortening of several long bones, and a dysmorphogenesis of cranial bones and cervical vertebrae, including vertical displacement of the supraoccipital bone, a small basiooccipital bone, a small foramen magnum, and changes in the shape of the squamosum and of the first and second vertebrae (73, 74). Both affected individuals shared an identical phenotype consisting of short stature and macrocephaly; their dysmorphic features included frontal bossing, narrow palpebral fissures with deep set globes and hypertelorism, strabismus, low-set ears with posterior rotation and dysplasia of the conchae, narrow auditory canals and hypoacusis, a

short neck with redundant skinfolds, and a low hairline. The main radiographic features were hypoplastic scapulae and iliac bones, short femurs, humeroradial synostosis, and moderate brachydactyly. Both patients were homozygous for genomic *TBX15* mutations that resulted in truncation of the protein and addition of a stretch of missense amino acids. Although the mutant proteins had an intact T-box and were able to bind to their target DNA sequence *in vitro*, the missense amino acid sequence directed them to early degradation, and cellular levels were markedly reduced, suggesting that Cousin syndrome is caused by *TBX15* insufficiency and is thus the human counterpart of the *droopy ear* mouse.

TBX20 is an ancient member of the T-box transcription factor family, related to *TBX1*. In mice, it is expressed in cardiac progenitor cells, as well as in the developing myocardium and endothelial cells associated with endocardial cushions, the precursor structures for the cardiac valves and the atrioventricular septum (10, 18). Loss of *Tbx20* in mice is catastrophic for heart development; homozygous mutants show a rudimentary heart that is poorly proliferative and lacks chamber myocardium (18, 19, 75). *Tbx20* also has later functions in atrioventricular valve development: adult heterozygous *Tbx20*-knockout mice show mild atrial septal abnormalities, including an increased

prevalence of patent foramen ovale (PFO) and aneurismal atrial septum primum, as well as mild dilated cardiomyopathy (DCM) and a genetic predisposition to frank ASD (18). The essential roles of *Tbx20* in heart development and adult heart function in mice, raised the possibility that mutations in human contribute to congenital heart disease (CHD), structural malformations of the heart which are extremely common, present in nearly 1 in 100 live births and 1 in 10 stillborns. Kirk et al., in fact, identified *TBX20* mutations in two white CHD-affected families; both mutations occurred in the T-box domain affecting the protein DNA-binding ability and were associated with a complex spectrum of developmental and functional abnormalities, including defects in septation, valvulogenesis, and chamber growth as well as cardiomyopathy, so establishing the first link between *TBX20* mutation and human disease (76).

Finally *TBX2* maps to 17q23 region which is frequently altered in ovarian carcinomas (77), and is amplified in about 20% of breast cancers (78). *TBX2* is amplified in some breast cancer cell lines, with about 4.5% of sporadic breast cancers having a dosage increase equivalent to one extra copy of the *TBX2* allele. A screen designed to identify immortalizing genes in breast cancer showed that *TBX2* affects the p53 tumour

suppressor pathway by repressing the *cdkn2a* (p19ARF) promoter (79), implying a role for this T-box gene in cancer.

1.3 *TBX1* and Del22q11.2/DiGeorge syndrome

TBX1 is the major candidate gene for the Del22q11.2 syndrome; del22q11.2 is an interstitial deletion of chromosome 22 associated with a characteristic phenotype clinically recognizable as DiGeorge syndrome, velocardiofacial syndrome or conotruncal anomaly face, which are collectively referred to as 22q11.2 deletion syndromes (22q11.2DS) which is estimated to be the most common microdeletion syndrome in humans, affecting about 1 in 4000 live births. Microdeletion syndromes are genetic disorders caused by the loss of a small chromosomal segment, usually spanning multiple genes, but too small to be detected by standard cytogenetic analysis. There are actually several versions of del22q11.2 and the most common version eliminates 3 Mb of genomic DNA, including approximately 40 genes; smaller deletions are associated with essentially identical phenotypes.

Long-range DNA mapping analysis, molecular cytogenetics, and, more recently, genome sequencing have identified stretches of DNA sequences repeated multiple times along the chromosomal band 22q11.2. Some of these sequences, referred to as *low copy repeats* (LCRs), localize at or

near the break points of del22q11. Therefore, LCRs are thought to provide the substrate for aberrant DNA recombination leading to chromosomal deletions. LCRs have been found in all the human chromosomes, and they have been implicated in a number of chromosomal rearrangements, including deletions, duplications, and translocations. Thus, the genomic architecture of 22q11 explains the homogeneity of the deletion across patients and perhaps also the high incidence of this rearrangement. It has been shown, in fact, that del22q11 originates predominantly through aberrant interchromosomal exchange at LCR sites (80-85).

Patients who carry del22q11 seek treatment with a complex clinical picture including the DiGeorge, velocardiofacial, and conotruncal anomaly face phenotypes. Clinical findings can be classified in three categories: (1) pharyngeal phenotype, related to developmental defects of the embryonic pharyngeal apparatus; (2) neurobehavioral phenotype, mostly learning disabilities and psychiatric disorders; and (3) a heterogeneous group of clinical signs or developmental defects such as kidney abnormalities, non craniofacial skeletal defects, and vascular abnormalities. Most patients have clinical signs from at least two of these three categories of phenotypes.

The embryonic pharyngeal system is a transient, vertebrate-specific structure comprising alternating bulges (arches) and indentations (pouches and clefts) that develops sequentially along the body axis in a head-to-tail direction. The pharyngeal arches are overlaid by surface ectoderm and lined by endoderm, which we refer to together as the pharyngeal epithelia. Between the epithelial layers of the pharyngeal apparatus, there is mesenchyme of mesodermal origin that is later infiltrated by ectomesenchyme of neural crest origin. The pharyngeal system contributes, among other organs and structures, to the formation and/or morphogenesis of the thymus, thyroid, parathyroids, maxilla, mandible, aortic arch, cardiac outflow tract, external and middle ear. Many birth defects, including a large fraction of congenital heart disease cases, derive from developmental problems of the pharyngeal system; so the research interest in the del22q11.2 syndrome is driven not only by the obvious clinical significance of the disease, but also by a broader biological importance: this syndrome is the most typical developmental defect of the embryonic pharyngeal system. The pharyngeal phenotype comprises in fact, physical signs derived from developmental abnormalities of the pharyngeal arches and pouches: specifically, craniofacial (including external and middle ear) abnormalities, thymus,

parathyroid and, in some cases, thyroid hypoplasia or aplasia (86, 87), aortic arch and cardiac outflow tract abnormalities (interrupted aortic arch type B, abnormal origin of the right subclavian artery, right sided aortic arch, tetralogy of Fallot), ventricular and atrial septal defects (VSD, ASD).

Investigators have used the power of mouse genetics to determine which of the many genes deleted in patients could be required for the development of the pharyngeal apparatus. The first genetic model of del22q11DS was a mouse mutant with an engineered deletion of most of the mouse genomic region homologous to the region deleted in del22q11 patients (88). These mice, carrying a heterozygous deletion named *Df1/+*, have aortic arch defects and parathyroid, thymic, and neurobehavioral abnormalities, reminiscent of those found in human patients (88-90). Additional targeted mutations of the mouse genome allowed investigators to attribute most of these phenotypic findings to haploinsufficiency (a situation in which a single copy of the normal gene is insufficient to assure normal function) of a single gene, precisely *Tbx1* (91-93). To determine whether *TBX1* haploinsufficiency was the main cause of the 22q11.2DS phenotype also in humans, investigators performed mutational analysis in patients with a 22q11.2DS-like phenotype but

without the chromosomal deletion. An initial report (93) analyzed the *TBX1* coding region in 100 patients but did not find mutations. Subsequently, Gong et al. (94) tested 105 patients and found several rare variants, mostly located in exon 9 coding for the C-terminal region of the TBX1 protein. Unfortunately, the authors could not definitively link these variants to the disease status. Later, Yagi et al. (95) reported a family segregating frame-shift mutation (1223delC) located 51 bp upstream of the one reported by Gong et al (94). Family members carrying this mutation presented with a variable but characteristic 22q11.2DS phenotype ranging from severe to very mild. This is the strongest evidence available to date that links *TBX1* mutations to the del22q11.2DS phenotype. Yagi et al. (95) also identified two additional mutations in patients with typical phenotypes. These were de novo missense mutations, F148Y and G310S; the first was located in the highly conserved T-box domain, and the other was located immediately downstream to the T-box domain, also in a highly conserved region. The effect of all of the reported mutations on protein function is still unknown. The mutation affecting the T-box domain is likely to impair DNA binding activity of the TBX1 protein, but the effect of the other mutations are less predictable as we do not have a catalog of functional

domains of the protein. The identification of functional domains is, of course, an important subject for future research.

1.4 *Tbx1* roles during mouse embryonic development

DiGeorge syndrome phenotype, both in mice and humans, suggests critical roles for *Tbx1* during pharyngeal system development; *Tbx1* expression pattern is highly dynamic during development and is mainly localized in the head mesenchyme, pharyngeal endoderm (PE), core mesenchyme of the cranial pharyngeal arches, outflow tract of the heart, mesenchyme surrounding the dorsal aortae, otocyst and sclerotome. Pharyngeal arches develop one after the other, in a cranial–caudal order, and surround the embryonic pharynx, which is lined by the PE. The PE of the pouches contributes to the development of the parathyroids and thymus, and the ventral PE contributes to the development of the thyroid. The first pharyngeal arches form the maxilla and mandible; the second form the hyoid bone. *Tbx1*^{-/-} have severe developmental defects of the pharyngeal apparatus: the characteristic segmented arrangement is lost, the embryonic pharynx is severely hypoplastic and lacks pouches, hence presenting a tube-like morphology. The first pharyngeal arch is abnormally patterned (96), the second is very hypoplastic, and the third, fourth and sixth are not identifiable (91, 97). Pharyngeal arch arteries

(PAAs) run inside the pharyngeal arches, surrounded by mesenchymal cells, most of neural crest and some of paraxial mesoderm origin. *Tbx1* haploinsufficiency causes early growth and remodeling defects of the fourth PAAs, first evident at embryonic day (E) 10.5. The caudal PAAs (third, fourth and sixth) form sequentially as symmetric vessels connecting the aortic sac with the dorsal aortae. From ~E11.5, the PAAs undergo a major, asymmetric remodeling that leads to the mature aortic arch and great vessel patterning (98). In particular, the left fourth PAA contributes to the section of the mature aortic arch between the origins of the left common carotid artery and the left subclavian artery. Developmental failure of the left fourth PAA causes interruption of the aortic arch type B (IAA-B). The right fourth PAA provides the connection of the right subclavian artery with the innominate artery. Developmental failure of the right fourth PAA causes aberrant origin of the right subclavian artery, most commonly from the descending aorta, via a retroesophageal vessel. Thus, all pharyngeal segments are affected, but the caudal segments are more severely affected. This is consistent with dynamic expression of *Tbx1* in the pharyngeal endoderm, which tends to increase in intensity along cranial–caudal and medial–lateral directions. These are also the directions of growth/extension of the

pharyngeal endoderm during E9 to 10.5 in mice (99, 100). Expression of *Tbx1* in other pharyngeal tissues (core mesoderm and head mesenchyme) is less dynamic in nature and less suggestive of a role in pharyngeal system growth and segmentation.

Because the pharyngeal pouches do not form in *Tbx1*^{-/-} mice, it is possible that one of the functions of *Tbx1*, perhaps the earliest during development, is to initiate and maintain the invagination of the endoderm, cell autonomously. The invagination then extends to form the pharyngeal pouch; in principle, this mechanism would be similar to those proposed for the formation of other ‘tubular’ organs such as the lung (101). The cranial–caudal ‘wave’ of *Tbx1* expression may drive the order in which the pouches form. It would be very interesting to establish how this process is regulated upstream of *Tbx1*. Perhaps the notochord could provide the appropriate signals. Indeed, Sonic hedgehog (Shh), which is highly expressed in the notochord, has been shown to activate *Tbx1* expression in chick, while in *Shh*^{-/-} mice, *Tbx1* is downregulated (102). However, *Shh*^{-/-} mice have less severe defects of the caudal pharyngeal arches and pouches than *Tbx1*^{-/-} mice, suggesting that the regulation of *Tbx1* by Shh may be more important for the most-cranial pharyngeal segments. Initial migration of cranial neural crest cells, their proliferation

and survival appear normal in *Tbx1*^{-/-} embryos; however, migration streams, especially the caudal ones, become abnormal and disordered as cells enter the pharyngeal area, and cranial nerves, derived from neural crest cells, are misdirected (97). We speculated that normally the endodermal pouches provide guidance to the migrating neural crest cell streams; in the absence of pouches, migration is affected and pharyngeal arches do not develop. *Tbx1* is expressed in the endoderm that surrounds the 4th PAAs but not in the arteries themselves. Therefore, it has been hypothesized that *Tbx1* affects the growth of the artery through a non-cell-autonomous mechanism involving a diffusible signal triggered in endodermal cells of the pouches and directed toward the artery (97); so a key question is how *Tbx1* expression in the pharyngeal endoderm can trigger molecular signals to the underlying mesenchyme to support vessel growth. FGF signaling has been shown to interact with other T-box genes and therefore it is possible that FGF molecules may mediate the role of *Tbx1* in fourth PAA growth. The *Fgf8* gene expression pattern overlaps with that of *Tbx1* in the pharyngeal endoderm around the time when the fourth PAA hypoplasia becomes apparent; in addition *Fgf8* expression in the pharyngeal endoderm of *Tbx1* null mutant embryos is lost, while the other expression domains are maintained (103). Loss of *Fgf8* in the

pharyngeal endoderm may be due to gene downregulation or lack of development/survival of endodermal cells expressing *Fgf8*; several endodermal markers (*Shh*, *Nkx2-5* and *Pax9*), are robustly expressed in homozygous mutants. In addition, using our *Tbx1-lacZ*-knock in allele, we demonstrated beta-gal activity in the endoderm of *Tbx1*^{-/-} embryos, indicating that *Tbx1* function is not required for the contribution of *Tbx1*-expressing cells to the endoderm (103). Overall, these data suggest that the endoderm of *Tbx1*^{-/-} embryos is properly specified. The gene expression data suggest that *Fgf8* may interact with *Tbx1* in the pharyngeal endoderm and be a mediator of the cell non-autonomous role of *Tbx1* in fourth pharyngeal arch artery development. Accordingly with this hypothesis *Tbx1*^{+/-};*Fgf8*^{+/-} mice presented with high penetrance of arch defects, significantly higher than that found in *Tbx1*^{+/-};*Fgf8*^{+/+} mutants; interestingly, the type of defects observed was not affected by *Fgf8* mutation, all defects were attributable to a failure of the fourth PAA development. In addition, the penetrance of fourth PAA abnormalities caused by *Tbx1* haploinsufficiency at E10.5 is much higher than the penetrance of aortic arch defects at E18.5, indicating a *Tbx1*-*Fgf8* genetic interaction during the early phases of fourth PAA development, consistent with the time of *Fgf8* and *Tbx1* expression overlap in the

pharyngeal endoderm. Double heterozygous mutants also showed an higher penetrance of thymic hypoplasia and/or lobe asymmetry mutants; and because the thymus primordia develop from the third pharyngeal pouch where both *Tbx1* and *Fgf8* are expressed, it is likely that the thymic phenotype in double heterozygous mutants is also a sign of *Tbx1*-*Fgf8* interaction in the pharyngeal endoderm.

Recently we showed that also early thyroid development requires a *Tbx1*-*Fgf8* pathway (104); the thyroid is an endocrine gland that secretes two types of hormones, thyroxin and calcitonin, which are produced by two distinct cell types, the thyroid follicular cells (TFC) and the parafollicular or C-cells, respectively. These two cell types derive from distinct regions of the pharyngeal endoderm, specifically the ventral pharyngeal endoderm provides the TFC progenitors, while the endoderm of the 4th pharyngeal pouches provides the C-cell progenitors. The TFC progenitor population constitutes the early primordium at approximately E8.5, when it appears as thickened epithelium on the ventral-medial wall of the pharynx, just caudal to the 1st pharyngeal arch. The early primordium then grows without further cell proliferation (105) presumably by recruiting cells from the adjacent endoderm, and forms a pit by invaginating into the pharyngeal mesenchyme. Between E11.5 and E13.5,

the primordium grows deeper into the mesenchyme, detaches from the pharyngeal endoderm, and begins to expand laterally. Later, the thyroid primordium reaches the trachea where it fuses with the 4th pouch-derived ultimobranchial bodies, which provide the C-cells of the mature organ. At around E15–E16, the thyroid gland acquires its final shape, i.e. two lobes connected by a narrow isthmus. From this stage, the organ grows and begins to express functional markers such as thyroglobulin (tg), thyroperoxidase (TPO) and Tshr (106). The signals that induce the initial events of specification and migration of thyroid precursor cells are still unknown. It has been postulated that the invagination process involves epithelial–mesenchyme transition. Congenital hypothyroidism has been reported in several cases of 22q11DS patients, although it is not a common feature of the syndrome (107). *Tbx1* mouse mutants present with a small thyroid, suggesting that the gene contributes, directly or indirectly, to thyroid development (108). The thyroid primordium and the ultimobranchial bodies, which derive from the 4th pharyngeal pouches, fuse at E13 and contribute to the mature gland. *Tbx1* null mutants do not have 4th pharyngeal pouches, thus thyroid hypoplasia in these mutants could be explained in part by the absence of the ultimobranchial bodies-derived component of the mature organ (108). However, loss of *Tbx1*

already affects thyroid development at E11.5 (105), indicating that loss of the 4th pharyngeal pouch is insufficient to explain the phenotype. It has been suggested that the bilobation defect of the thyroid in *Tbx1*-null mice could be due to failure of the thyroid primordium to establish a contact with the aortic sac, which normally occurs at around E11.5–12 (105), possibly through failed signaling between endothelial cells and primordium. So *Tbx1* seems to have a much earlier role in thyroid size, as the primordium is smaller from E9. In order to exclude a role of *Tbx1* in the endothelium adjacent to the primordium, we ablated the gene in endothelial cells using the Tie2-Cre driver, founding that the thyroid of Tie2-Cre; *Tbx1*^{fllox/-} embryos at E18.5 was of normal size. The role of *Tbx1* in the thyroid appears to be limited to regulating the number of cells of the primordium and does not appear to be involved in differentiation of thyroid precursors, as the expression of thyroid specific markers was not affected in *Tbx1* mutants. In addition, the mutant thyroid primordium does not regress and is still capable of growing, although it will never reach the normal, final size. This suggests that the primary defect is at or precedes primordium formation. Conditional ablation of *Tbx1* in the mesoderm is sufficient to recapitulate the null thyroid phenotype, thus indicating that the mesoderm plays a critical role in signaling to the

developing thyroid or their progenitors. We previously showed that loss of *Tbx1* in the mesoderm is associated with reduced cell proliferation in the pharyngeal endoderm of early embryos, thus providing a possible explanation as to why the primordium is small. Conditional ablation of *Fgf8* in *Tbx1*-expressing cells causes severe early and late thyroid hypoplasia, similarly to *Tbx1* ablation. Conversely, forced expression of *Fgf8* in the *Tbx1* expression domain, partially rescues the early and late *Tbx1*^{-/-} thyroid phenotype. Endogenous *Fgf8* expression in the mesoderm near the thyroid primordium is only detectable in early embryogenesis (up to approx. E9.0), consistent with the early appearance of the *Tbx1* mutant phenotype. Totally these data support a *Tbx1*-dependent role for *Fgf8* in thyroid development, and they are consistent with a report showing a critical role of this gene in zebrafish thyroid development (109). In addition, Olivieri et al. showed that pharyngeal mesoderm (including the cardiogenic mesoderm of the secondary heart field) supports thyroid development, thus providing a possible explanation for the frequent association between congenital heart disease and thyroid dysmorphogenesis (110).

Chromosome 22q11.2 deletion is one of the most common genetic causes of cardiac outflow tract (OFT) defects too. The OFT forms as a simple

vascular conduit that connects the embryonic right ventricle to the aortic sac, which is the site of confluence of the pharyngeal arch arteries. The embryonic OFT, which is divided into conal (proximal to the heart) and truncal (distal) segments, is soon lined by myocardial cells derived from migrating mesodermal cells. The myocardial layer of the embryonic OFT contracts and functions as a primitive valve. Septation separates the OFT into two channels, which direct the blood flow towards the aortic (systemic) and pulmonary circulation, and divides the primitive truncal valve into the aortic and pulmonary valves. Whereas the heart myocardium derives from lateral plate mesoderm precursors (the primary heart field), the OFT myocardium derives from the splanchnic mesoderm located caudal to the pharynx, the second heart field (SHF): in particular, the first lineage contributes to the left ventricle, atria, inflow region and partly to the right ventricle; the second one, which is characterized by the expression of the LIM-homeodomain protein *Isl1*, is thought to contribute mainly to the right ventricle and the outflow tract, but also the atria and the inflow region (111-114). The molecular mechanisms underlying induction and differentiation of myocardial precursors in the SHF are hypothesized to be similar to those of the primary heart field (113), but the genetics of SHF function and the phenotypic consequences of SHF

malfunction are uncertain. Neural crest-derived cells are also required for OFT septation and make up most of the aorto-pulmonary (AP) septum, a structure that originates from the dorsal wall of the aortic (115-118). Severe developmental defects of the OFT are tolerated during embryogenesis, provided that they do not compromise patency, but are lethal in post-natal life, when the pulmonary circulation is required for blood oxygenation. OFT developmental defects account for a high proportion of congenital heart disease cases and, consequently, are an important cause of morbidity and mortality in children.

Tbx1^{-/-} animals have severe OFT abnormalities including complete lack of septation and abnormal alignment of the truncus arteriosus with the ventricles (91, 97). These abnormalities seem to be because of a specific role of *Tbx1* in OFT development and not secondary to the severe defects of the pharyngeal apparatus associated with *Tbx1* loss of function.

Tbx1 is expressed in progenitors as well as in differentiated, resident myocytes and endothelial cells of the OFT. However, conditional deletion experiments indicate that *Tbx1* function is not required in myocardial or endothelial cells; instead, cell fate mapping experiments indicate that *Tbx1* regulates, but is not required for contribution of myocytes, and possibly other cell types, to the OFT. Most probably, *Tbx1* does not

directly regulate cell proliferation of progenitor cells because in chimeras, *Tbx1*^{-/-} cells do not have a proliferative disadvantage in the SHF. Thus, the *Tbx1* role in regulating cell contribution to the OFT is probably cell non-autonomous. *Fgf10* is a candidate mediator of this function because its expression in the SHF is abolished in *Tbx1*^{-/-} and Tbx1 can directly activate, through a conserved TBE, the *Fgf10* promoter in a tissue culture assay. Interestingly though, *Fgf10*^{-/-} animals do not have OFT defects, raising the question as to whether Tbx1 also activates other *Fgf* genes or other extracellular signaling systems critical for OFT morphogenesis. Alternatively, *Fgf10*^{-/-} animals may not have OFT defects because other *Fgf* genes compensate for the loss of *Fgf10*, as proposed by Kelly and Buckingham (119). *Tbx1* has an additional role in OFT morphogenesis; it is, in fact, required in cells expressing *Nkx2.5*, one of the first splanchnic mesodermal cell marker, for the formation of the aorto-pulmonary septum, which divides the aorta from the main pulmonary artery (120).

During mouse embryonic development, *Tbx1* is also required for inner ear morphogenesis; the inner ear derives from the otic placode, initially recognized as a thickened ectodermal patch near the hindbrain at E8 in mice. The otic placode undergoes invagination and becomes the otic pit, which in turn enlarges and closes off from the ectoderm to form the

otocyst by E9.5 (121). Cells in the otocyst undergo a series of cell fate specification events and differentiate into the various types of cells that populate the inner ear structures (122). From E9.5 to E12, neuronal precursors delaminate from a specific region of the otic epithelium, the neurogenic region, to contribute to the cochleo-vestibular ganglion (CVG). The neurogenic region is defined by activation of the Delta-Notch pathway and expression of proneural genes encoding bHLH transcription factors, including *Neurogenin1* (*Ngn1*) and *NeuroD* (123, 124). By E12, the delamination process is complete, and the otocyst exhibits recognizable primordial structures of sensory organs and endolymphatic duct (121). During otocyst development, *Tbx1* is expressed in a subregion of the otic epithelium and in the periotic mesenchyme (125, 126): it has been shown that both expression domains are essential for inner ear morphogenesis. *Tbx1* continues to be expressed in the primordial of the sensory organs and expression is evident until at least E13.5 (126). In *Tbx1*^{-/-} animals, the otocyst is small and the sensory organs do not form (125-127); in addition, the neurogenic region of the otic epithelium is expanded (125) and the endolymphatic duct appears to be enlarged (127). We previously (128) showed that *Tbx1* is required for localization, expansion and fate determination of a cell population that

forms most of the otocyst, excluding the neurogenic and the endolymphatic duct territories; delayed ablation of *Tbx1* partially rescued this cell population, but strongly reduced its proliferation in the otocyst. In addition, even if this *Tbx1*-dependent cell population does not normally contribute substantially to the cochleo-vestibular ganglion, timed deletion of *Tbx1* results in the expansion of the Delta-like1-Notch1 activation domain, and in change of fate of at least some of *Tbx1*-expressing cells towards a neurogenic fate. The molecular mechanisms that set the border of the neurogenic region in the otocyst are unknown. Delta-Notch signalling plays a role in determining the neurogenic versus non-neurogenic fate in other tissue contexts. Delta is positively regulated by proneural genes *Ngn1* and *NeuroD* (129), and in turn activates Notch in neighboring cells; aNotch finally suppresses proneural gene expression in those cells. Expression of *Dll1*, a Notch ligand, and the cleaved form of Notch1, are found at or near the neurogenic border region, suggesting that the Delta-aNotch signalling could play a role in setting or maintaining the border. *Tbx1* mutation is associated with a considerable expansion of the *Dll1*-aNotch domain, suggesting that it functions upstream of a possible Notch-mediated mechanism for selecting cells

undergoing neurogenic fate: so *Tbx1* may suppress *Ngn1* and/or *Dll1* expression.

1.5 The emerging *Tbx1* genetic pathway

Yamagishi and colleagues (130) identified a single *cis*-element upstream of *Tbx1* that recognized winged helix/forkhead box (Fox)-containing transcription factors (131, 132) and is essential for regulation of *Tbx1* transcription in the pharyngeal endoderm and head mesenchyme.

Forkhead proteins *Foxa2*, required for endoderm development (133), and *Foxc1* or *Foxc2*, required for head mesenchyme and aortic arch formation (134-138), bind and activate *Tbx1* transcription in their respective subdomains through this regulatory element. As mentioned above, *Tbx1* responds to signals initiated by the secreted morphogen Sonic hedgehog (Shh); interestingly both *Foxa2* and *Foxc2* are downregulated in *Shh* null mutants, which die soon after birth with severe craniofacial defects (139, 140) and fail to maintain *Tbx1* expression (102) suggesting a function for Forkhead proteins as an intermediary between Shh signalling and *Tbx1* regulation.

Maeda and colleagues showed that *Tbx1* expression in the SHF is also regulated by Forkhead proteins, through a combination of two evolutionary conserved Fox binding sites in a dose-dependent manner

(141); in addition Hu and colleagues (142) showed that mice hypomorphic for *Tbx1* failed to activate expression of the forkhead transcription factor *Foxa2* in the pharyngeal mesoderm, which contains cardiac outflow tract precursors, but not endoderm. They also identified a Fox-binding site upstream of *Tbx1* that interacted with *Foxa2* and was necessary for pharyngeal mesoderm and cardiac OFT expression of *Tbx1*, revealing an autoregulatory loop that may explain the increased cardiac sensitivity to *Tbx1* dosage.

Downstream of *Tbx1*, they found a *fibroblast growth factor 8* (*Fgf8*) enhancer that was dependent on *Tbx1* in vivo for regulating expression in the cardiac outflow tract, but not in pharyngeal arches (142). Consistent with its role in regulating cardiac outflow tract cells, *Tbx1* gain of function resulted in expansion of the cardiac outflow tract segment derived from the anterior heart field as marked by *Fgf10*. These findings reveal a *Tbx1*-dependent transcriptional and signaling network in the cardiac outflow tract that renders mouse cardiovascular development more susceptible than craniofacial development to a reduction in *Tbx1* dose, similar to humans with del22q11.

Thus, the genetic pathway emerging from available data is (*Foxc1*, *Foxc2*, *Foxa2*) → *Tbx1* → (*Fgf10*, *Fgf8*). The links in this pathway are

still uncertain because they are based on transgenic experiments with artificial constructs, gene expression studies and luciferase assays in cultured cells. Definitive evidence will come from modification of the endogenous genetic elements that establish the links in vivo. In addition, it is very likely that the list of regulators and targets of *Tbx1* will be extended considerably in the future.

So, even if a great amount of data has been accumulate to date, many outstanding questions remain about the *Tbx1* genetic pathway.

To reconstruct a more detailed picture of the *Tbx1* roles during embryonic development, the available knowledge concerning tissue and time-specific effects of *Tbx1* loss of function needs to be integrated with information about its targets, regulators and genetic interactors.

To this aim, we previously generated a series of genotypes associated with a nearly continuous variation of *Tbx1* mRNA dosage between 0 and 100% of the wild-type level, by combining two different hypomorphic alleles: *Tbx1*^{Neo2 (143)} and *Tbx1*^{Neo} (120) and a null allele: *Tbx1*⁻ (93). We have shown that the two hypomorphic alleles have uniformly low levels of expression across embryonic tissues. *Tbx1*^{Neo} is a ‘weak’ hypomorphic allele with an expression level around 2–3% of the wild-type allele. Consistently with this finding, phenotypic analysis demonstrated that

Tbx1^{Neo/Neo} embryos were nearly identical to *Tbx1* null embryos (120). However, remarkably, such a low level of *Tbx1* expression was sufficient to support palatogenesis, which is affected in null embryos, and to improve the alignment of the cardiac outflow tract (OFT) in some embryos (120). In contrast, the *Tbx1*^{Neo2} allele expressed 15–20% of the wildtype mRNA level. Both hypomorphic alleles were generated by inserting a PGKneo cassette into intron (120, 143), but in opposite orientation (Fig. 1A).

Phenotypic analysis of the nine different genotypes revealed, as expected, that penetrance and expressivity increase as the *Tbx1* level decreases, but the response is strikingly non-linear; the dynamic phenotypic response to dosage, in fact, is complex with different trends for different phenotypes, indicating that different developmental processes have different sensitivities to *Tbx1* mRNA level.

As part of the effort to identify new transcriptional targets of *Tbx1*, we performed a microarray-based transcriptome analysis through the above allelic series, in order to evaluate *Tbx1* dosage-dependent gene expression changes in vivo. This analysis allowed us to identify several genes affected by *Tbx1* expression levels; interestingly we found that the gene encoding the cardiogenic transcription factor *Mef2c*, is negatively

regulated by *Tbx1*, confirming recent reports. It has been uncovered, in fact, that different cell type populating the heart (e.g. cardiomyocytes, endothelial cells, smooth muscle cells) may derive from a single *Isl1*⁺ progenitor (144-146). Interestingly, *Tbx1* is expressed in these multipotent cardiac progenitors: it enhances their proliferation and inhibits their differentiation, thus ensuring the maintenance of the progenitor population (147). Because *Tbx1* can regulate *Fgf8* expression in the mesodermal region that includes the SHF, some of its mitogenic activity could be mediated by the FGF signalling; on the other hand a negative effect on differentiation could be explained by *Tbx1* negative regulation of the myogenic transcription factor *Srf* (Serum response factor), which, in turn, regulates the muscle transcription program (147). So our results suggest that *Mef2c* transcriptional repression could be another possible mechanism by which *Tbx1* regulates the balance between proliferation and differentiation in the SHF.

CHAPTER 2

Material and methods

2.1 Mouse lines, breeding and genotyping

All the mouse mutant alleles used in this study have been reported previously: *Tbx1*⁻ (93), *Tbx1*^{Neo} (120), *Tbx1*^{Neo2} (143), *COET* (148) and *Mesp1Cre* (149). Various homozygous and compound heterozygous mutants were generated by heterozygous mutant mating. Embryos were collected at E8.5 and E9.5, considering the day of observation of a vaginal plug to be E0.5. Mice were genotyped by PCR as described in the original reports.

2.2 Cloning, plasmids and mutagenesis

We have previously described the pCDNA-Tbx1-c-myc expression vector (120). 3X-MEF2-luc reporter construct (150) was kindly provided by Dr. Olson EN; pCDNA3.1-Gata4-c-myc-His and pCDNA3.1-Ils1 were kindly provided by Dr. Schwartz RJ.

The minimal SHF-specific enhancer of the mouse *Mef2c* gene described by Dodou et al. (2) was amplified by PCR and cloned into the pGL3-Promoter Vector (Promega) so generating the Mef2c-Enh-Luc reporter construct. MutMef2c-Enh-Luc reporter construct was generated by substitution of three nucleotides in the conserved TBE of the original

Mef2c-Enh-Luc reporter construct, using the QuikChange II Site-Directed Mutagenesis Kit (Stratagene).

2.3 Cell culture and transfections

EBRTcTbx1 cells were cultured in the absence of feeder cells in Glasgow minimal essential medium (GMEM, Sigma-Aldrich) supplemented with 10% fetal calf serum (Hyclone), 1 mM sodium pyruvate (Invitrogen), 10^{-4} M 2-mercaptoethanol (Sigma-Aldrich), 1x nonessential amino acids (Invitrogen), 1000 U/ml of leukemia inhibitor factor (LIF, Millipore) and 200ng/ml of doxycycline (Sigma-Aldrich) on gelatine-coated dishes, at 37 °C with 5% CO₂. The incomplete removal of doxycycline has been reported to result in insufficient induction of Tet-off system (151). Therefore, the cells to be induced were washed twice with PBS, cultured for more than 3 hours in GMEM without doxycycline, trypsinized and replated onto new dishes. After 24 hours, cells were collected for RNA extraction.

Mouse C2C12 myoblasts (ATCC) were cultured in Dulbecco's modified Eagle's medium (DMEM, Invitrogen) supplemented with 10% fetal bovine serum (Hyclone) at 37 °C with 5% CO₂. To allow cells to differentiate, medium was changed to DMEM medium supplemented with 2% horse serum (Hyclone).

C2C12 cells were transiently transfected using the PolyFect Transfection Reagent (QIAGEN); for each kind of experiment, the number of cells to be plated and the amount of DNA to be transfected were chosen accordingly to the manufacturer's instructions. Cells were collected 24 hours after transfection for RNA or protein extraction.

2.4 Microarray analysis

Total RNA was isolated from E9.5 embryos with nine different genotypes (*Tbx1*^{+/+}, *Tbx1*^{Neo2/+}, *Tbx1*^{Neo/+}, *Tbx1*^{+/-}, *Tbx1*^{Neo2/Neo2}, *Tbx1*^{Neo2/Neo}, *Tbx1*^{Neo2/-}, *Tbx1*^{Neo/Neo} and *Tbx1*^{-/-}) using TRIzol (Invitrogen) according to the manufacturer's instructions. RNAs from three embryos of the same genotype were combined and cleaned using the RNeasy cleanup Kit (QIAGEN); RNA was then checked for quality using an Agilent bioanalyser and degraded samples were eliminated. Quantification was performed using spectrophotometry. Procedures for cRNA preparation and GeneChip processing were performed following standard procedures (<http://www.affymetrix.com>). Biotinylated target cRNAs were hybridized to GeneChip Mouse Genome 430 2.0 arrays following standard procedure (Affimetrix). Three chip sets were run for RNA isolated from wild-type embryos and three for RNA isolated from embryos of each mutant genotype. Statistical comparisons of chip data were performed

using GC-Robust Multichip Analysis (ArrayAssist V2.6.1642.30743, Iobion informatics) with variance correction using two-tailed unpaired t tests against wild-type chips; a probe-set expression was considered altered if it had a P value < 0.05 vs. wild type. Genes with statistically significant differential expression across the allelic series, were further analyzed for their correlation to *Tbx1* dosage, using Pearson's correlation coefficient test. A gene was considered highly correlated (or anti correlated) to *Tbx1* dosage, if it had a correlation coefficient with a P value < 0.05 within a 95% confidence interval.

2.5 T-box binding element (TBE) analysis

Mouse and human genomic sequences for all the 256 differentially expressed genes were obtained from both the Ensembl and UCSC Genome Browser web sites, and were aligned using rVISTA, a set of programs for comparing DNA sequences from two or more species. No direct *Tbx1* binding site has been identified so far; however *Tbx1* can activate, *in vitro*, the *Fgf10* promoter, through a conserved *Tbx5* binding site (120). With the Transfac data base we defined the *Tbx5* consensus DNA sequence (A/G/TG/AGTGNNNA) using a position weight matrix (PWM) based on all published T-box binding element and we looked for evolutionary conserved *Tbx5* binding elements, in the aligned sequences,

using the MATCH software.

2.6 Quantitative Real-Time PCR (qRT-PCR)

Total RNA was extracted from whole E9.5 wt and mutant embryos using TRIzol (Invitrogen), from C2C12 and EBRTcTbx1 cells using the RNeasy Mini Kit (QIAGEN). 1 ug of total RNA was reverse transcribed using SuperScript III (Invitrogen) according to the manufacturer's instructions, in a total volume of 20 ul; the resulting cDNA was diluted 1:10. qRT-PCR was performed using SYBR Green for the detection of fluorescence during amplification. Each amplification reaction contained 25 ul of Platinum SYBR Green qPCR SuperMix-UDG (Invitrogen), 0.2 ug each of forward and reverse primers, and 1 or 2 ul of diluted cDNA. All primers were designed with annealing temperatures of 58-62 °C. PCR conditions were: 50°C for 2 minutes, 95°C for 10 minutes, 40 cycles of 95°C for 15 seconds, 60°C for 1 minute, followed by a dissociation stage of 95°C for 15 seconds and 60°C for 15 seconds. All the genes were amplified on a 7900 HT Fast Real-Time PCR System (Applied Biosystems). At least three separate analysis were carried out for each gene. Melt curve analysis was performed after each run to check for the presence of non-specific PCR products and primer dimers. Ct values were related to copy numbers using standard curves, as described previously

(152); normalization was performed using GAPDH as an internal control as described (152).

2.7 In situ hybridization

Digoxigenin-labeled RNA probes were prepared by standard methods (Roche). *Mef2c* and *Gata4* probes were kindly provided by Dr. Black BL. Embryos were dissected in di-ethylpolycarbonated (DEPC, Sigma Aldrich) treated PBS and fixed over night in 4% paraformaldehyde-PBS (Sigma Aldrich) at 4°C.

For in situ hybridization on cryosections, embryos were cryoprotected with increasing concentrations of sucrose (Sigma Aldrich), treated with a mixture of 1 part 30% sucrose to 1 part O.C.T. for at least 2 hours at 4°C, embed in O.C.T. and cutted to generate 10-12 um sections. After postfixation in 4% paraformaldehyde-PBS, sections were incubated in Triethanolamine Buffer (0,2% acetic acid and 1% triethanolamine, Sigma Aldrich) containing acetic anhydride and washed twice in PBS for 5 minutes. The sections were then prehybridized for 1 h at 70°C in the hybridization mix (50% formamide from Sigma Aldrich, 5x SSC, salmon sperm DNA 40 ug/ml and 25mg/ml yeast tRNA from Invitrogen). The probes were denatured for 5 min at 80°C and added to the hybridization mix (400 ng/ml). The hybridization reaction was carried out over night at

70; prehybridization and hybridization were performed in a box saturated with a 5x SSC – 50% formamide solution to avoid evaporation. After incubation, the sections were washed twice with MABT (50mM maleic acid, pH7.5, 250 mM NaCl and 0,1% Tween-20, Sigma Aldrich), treated with MABT containing 10% sheep serum for 1 hour at room temperature and then incubated with alkaline phosphatase-coupled anti-digoxigenin antibody (Roche) diluted 1:2000 in MABT containing 10% sheep serum, over night at 4°C. The day after, sections were washed with MABT and equilibrated for 5 min in Buffer 3 (Tris-HCl 100mM, NaCl 100mM, and MgCl₂ 50mM, pH 9.5); color development was performed at room temperature (time depending on the amount of transcripts to be detected) in Buffer 3 containing NBT and BCIP (Roche). Staining was stopped by a wash in PBS containing 0,1% Tween-20; sections were rehydrated for 5 minutes in deionized water and then dehydrated through successive baths of EtOH (70, 95, and 100%) and xylol, and mounted in Eukitt resin (O. Kindler GmbH & Co.).

Whole mount in situ hybridization was performed according to the previously published methods (In situ Hybridization. A Practical Approach. Edited by D.G. Wilkinson. IRL Press, Oxford. 1992).

At least three somite staged wt and mutant embryos were analyzed with

each probe.

2.8 Western Blotting

Total proteins were extracted after cell lysis with the RIPA buffer (1% NP40, 0.5% NaDoc, 0.1% SDS in PBS, protease inhibitor (Roche).

Nuclear and cytoplasmic proteic extracts were prepared using the NE-PER Nuclear and Cytoplasmic Extraction Reagents (Thermo Scientific).

The primary antibodies were rabbit-anti-Tbx1 (Zymed, 1:500), goat-anti-Mef2c (Santa Cruz Biotechnology, 1:500), rabbit-anti-Gata4 (Santa Cruz Biotechnology, 1:1000), monoclonal anti-alpha-Tubulin (Sigma-Aldrich, 1:5000) and rabbit-anti-beta-Actin (BioVision 1:5000). The secondary antibodies were: HRP-conjugated anti-rabbit and anti-mouse antibodies (GE Healthcare, 1:10.000), HRP-conjugated anti-goat (Santa Cruz Biotechnology, 1:5000). The HRP-derived signal was detected using the Amersham ECL and ECL Plus Western Blotting Detection Reagents (GE Healthcare).

2.9 Luciferase assays

For luciferase assays, mouse C2C12 myoblasts were plated in 24-wells and transfected with PolyFect Transfection Reagent (QIAGEN) according to the manufacturer's instructions. 3X-MEF2-luc, Mef2c-Enh-Luc and MutMef2c-Enh-Luc reporter constructs (and for single

experiments the pCDNA-Tbx1-c-myc, pCDNA3.1-Gata4-c-myc-His and pCDNA3.1-Ils1 plasmids) were always co-transfected with a pCMV-b-Gal expression vector (Clontech); at 24 hours after transfection, cell extracts were prepared and activities of b-galactosidase and firefly luciferase were measured using the Luciferase Assay System (Promega) and the Beta-Glo Assay System (Promega) respectively, on a GLOMAX 96 microplate luminometer (Promega). Relative luciferase activity (firefly luciferase for reporter and b-galactosidase for normalization of transfection efficiency) was measured following manufacturer's instructions (Promega); to correct for transfection efficiency, the luciferase activity was divided by the b-galactosidase activity in every case. The data represent the means and standard deviations of at least, three independent transfections.

2.10 RNA interference

Gata4 Interference in C2C12 myoblasts was achieved by using a set of four different siRNAs specifically directed against the mouse *Gata4* locus (ON-TARGET *plus* SMART Pool, Thermo Scientific). As negative control we used a pool of siRNAs that virtually targeted no mouse genes (ON-TARGET *plus* Negative Control, Thermo Scientific). Cells were plated in 6-wells and transfected with 50nM/well of siRNAs using

Lipofectamine 2000 (Invitrogen) according to the manufacturer's instructions. *Gata4* mRNA level was measured by qRT-PCR and Gata4 protein level by Western Blotting as described above.

CHAPTER 3

Results

3.1 Microarray analysis of *Tbx1* dosage-dependent gene expression changes *in vivo*

We have previously generated a series of genotypes associated with a nearly continuous variation of *Tbx1* mRNA dosage between 0 and 100% of the wild-type level (Figure 1) by combining two different hypomorphic alleles, *Tbx1*^{Neo2} (143) and *Tbx1*^{Neo} (120) and a null allele, *Tbx1*⁻ (93).

To evaluate *Tbx1* dosage-dependent gene expression changes *in vivo*, we performed a microarray-based transcriptome analysis, across the allelic series, at E9.5.

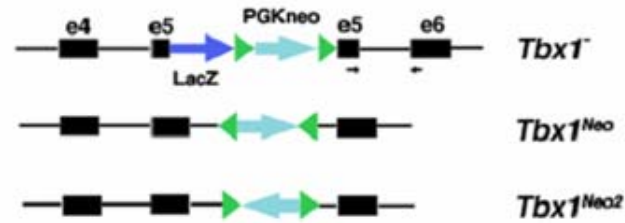
This analysis is aimed at identifying genes with quantitatively changed expression when compared to wild type: differential expression of molecular markers may indicate a direct target of Tbx1, or an indirect target whose altered expression gives clues as to developmental defects in particular tissues or cell populations.

Statistical analysis identified 256 genes differentially expressed across the allelic series and, even if Tbx1 is known to act as a transcriptional activator, we found 120 genes whose expression profile is correlated to

Tbx1 dosage and 136 genes whose expression profile is anti-correlated to it. Among the 256 differentially expressed genes, 52 changed in a manner that was highly correlated (or anti-correlated) to *Tbx1* expression. 35 out of 52 highly correlated genes were upregulated and 17 were downregulated in *Tbx1* mutant embryos (Figure 2A).

Classification of the 256 microarray genes into gene ontology (GO) categories revealed downregulation of apoptosis-related genes; this result is consistent with the role of *Tbx1* in promoting cell proliferation in several tissues. Whereas highly sensitive *Tbx1*-regulated genes account for only 52 out of 256 genes altered in *Tbx1* mutants, the relative ratios between functional classes of genes affected were maintained, suggesting that no single functional class of gene is more sensitive to changes in *Tbx1* dosage (Figure 2B).

(A)



(B)

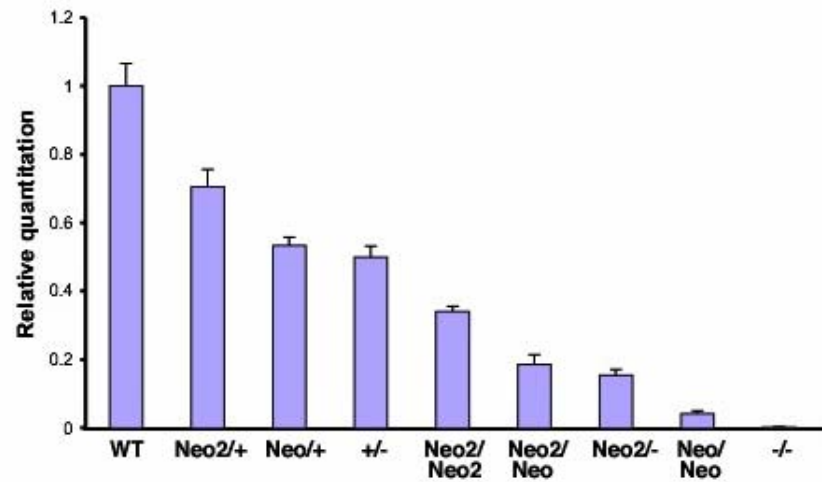


Figure 1. *Tbx1* mRNA dosage in E9.5 embryos with different genotypes. (A) Schematic drawings of the *Tbx1* alleles used in this study. (B) Relative expression level of *Tbx1* associated with the genotypes studied. At least three embryos per genotype were assayed. Error bars indicate standard error.

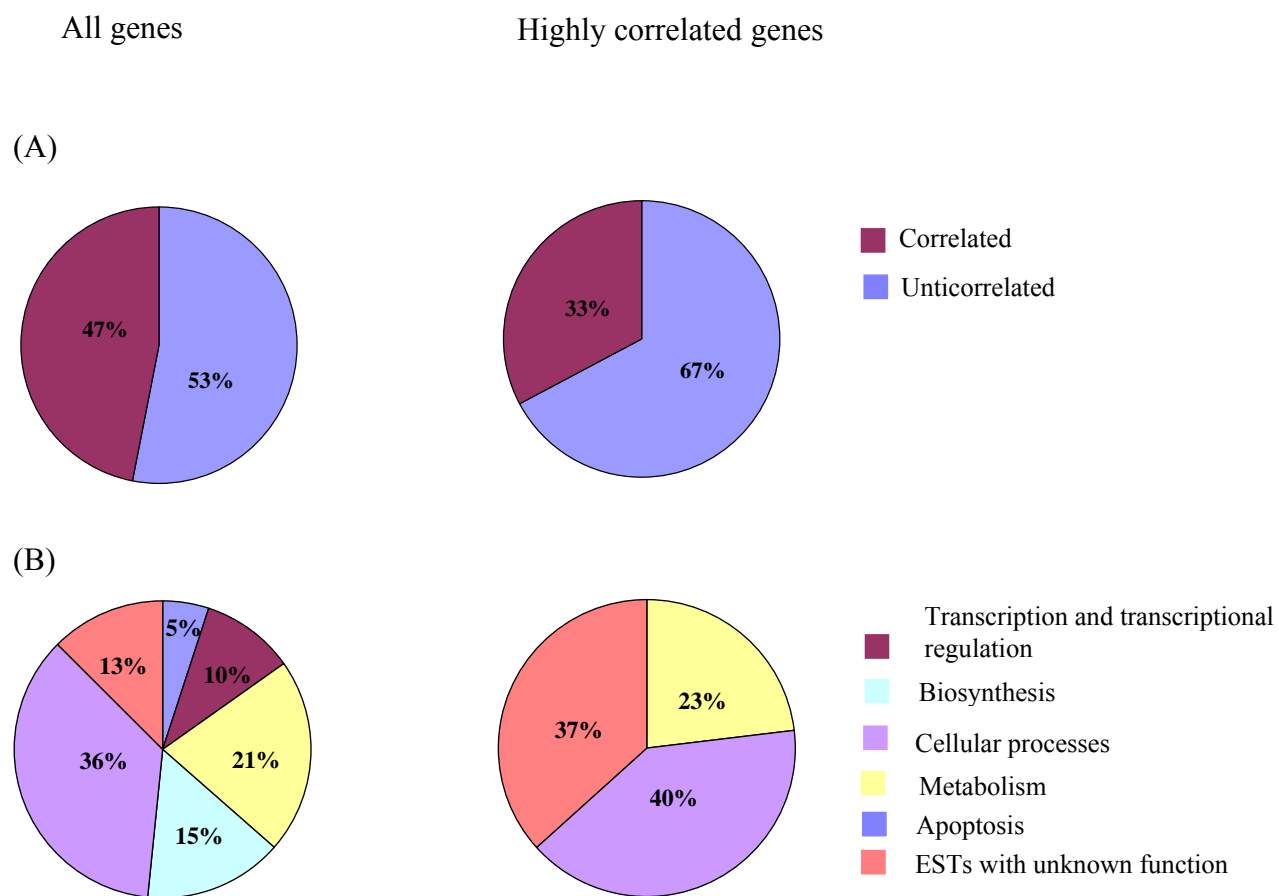


Figure 2. Schematic representation of microarray analysis results. (A) Percentage of correlated and anti-correlated genes. (B) GO classification of differentially expressed genes.

3.2 Conserved T-box binding element analysis

No direct Tbx1 binding sites have been identified so far, anyway Agarwal and colleagues (153) have shown *in vivo* that *Fgf10* requires *Tbx5* for initiation of its expression, whereas Wnt signaling via LEF1 and TCF1 is required to sustain high levels of *Fgf10* expression. This is supported by their in vitro transactivation data, which show powerful activation of the *Fgf10* promoter by TBX5, through an evolutionary conserved T-box binding element (TBE) located in the 5' region of the *Fgf10* gene. We previously showed that Tbx1 can directly activate the *Fgf10* promoter through that TBE in a tissue culture assay (120), raising the intriguing possibility that different T-box transcription factors may share target genes.

So we used the Tbx5 consensus DNA sequence, loosely defined as A/G/TG/AGTGNNA using a position weight matrix (PWM) based on all published T-box binding sites, to look for evolutionary conserved T-box binding elements. The TRANSFAC data base and the rVISTA program were used to align 10kb of upstream human and mouse genomic regions from all 256 differentially expressed genes; we also analyzed the intronic regions of highly correlated genes.

Totally we found one or more potential TBEs in the 10kb upstream region of 90/256 differentially expressed genes, 55 of which were anti-correlated and 35 correlated to *Tbx1* dosage.

25/90 genes with a potential TBE in their upstream region belong to the highly correlated group, which includes 53 genes: so the 47% of the highly correlated genes carries a potential Tbx1 binding site in its 3' upstream region. We also found in some of these genes and in 12 more highly correlated genes, one or more putative TBEs in the intronic regions: so totally, counting both the upstream and the intronic regions, we found that the 70% of the highly correlated genes shows a potential TBE, evolutionary conserved between mouse and human. This 70% includes 25 genes anti-correlated and 11 genes correlated to *Tbx1* dosage.

3.3 Selection of Tbx1 candidate transcriptional targets

We selected a number of genes for further validation, following essentially three main criterions:

- High correlation with *Tbx1* dosage (*Pex2*, *Vps33a*, *Morf4l1*, *Srmm1*, *Hibch*, *Plagl1*, *C1d*, *Commd3*)
- Developmental relevance and known expression pattern (*Mef2c*, *Foxp1*)
- Involvement in signalling pathways (*Fos*, *Tgfbr3*)

3.4 Validation of selected Tbx1 candidate transcriptional targets

By quantitative Real-time PCR (qRT-PCR) of mRNA from *Tbx1* mutant embryos and also from an *in vitro* gain of function model, we confirmed the microarray results on a subset of selected genes, namely *Pex2*, *Vps33a*, *Morf4l1*, *Tgfbr3*, and *Mef2c*.

3.4.1 *Pex2*: peroxin2

Peroxisins are proteins involved in peroxisome biogenesis and are encoded by *PEX* genes. The human *PEX2* (154) gene encodes a 35-kDa peroxisomal integral membrane protein, peroxin 2 (Pex2p) which is a member of the *PEX* zinc finger protein family (155-158). Mutations in the *PEX2* gene are the primary defect in a subset of patients with Zellweger syndrome and related peroxisome biogenesis disorders (neonatal adrenoleucodystrophy, and infantile Refsum disease which is the most mild) that result in abnormal neuronal migration in the central nervous system and severe neurologic dysfunction due to the lack of functional peroxisomes (159). Homozygous *Pex2*-deficient mice survive in utero but die several hours after birth. The mutant animals do not feed and are hypoactive and markedly hypotonic. The *Pex2*-deficient mice lack normal peroxisomes but do assemble empty peroxisome membrane ghosts. They display abnormal peroxisomal biochemical parameters,

including accumulations of very long chain fatty acids in plasma and deficient erythrocyte plasmalogens. Abnormal lipid storage is evident in the adrenal cortex, with characteristic lamellar–lipid inclusions. In the central nervous system of newborn mutant mice, there is disordered lamination in the cerebral cortex and an increased cell density in the underlying white matter, indicating an abnormality of neuronal migration (160).

3.4.2 *Vps33a: vacuolar protein sorting 33A*

Hermansky–Pudlak syndrome (HPS) is a disorder of organelle biogenesis in which oculocutaneous albinism, bleeding, and in most cases pulmonary fibrosis result from defects of melanosomes, platelet-dense granules, and lysosomes (161-164). Somewhat similar disorders, Chediak–Higashi and Griscelli syndromes, are additionally associated with severe immunodeficiency (162, 163). Important clues to the pathogenesis of these disorders have come from the mouse, in which more than 16 loci have been associated with mutant phenotypes similar to those of human HPS, Chediak–Higashi syndrome, and Griscelli syndrome (165, 166). Several of these genes have been identified and in a number of cases have been shown to result in homologous disorders in mice and humans (162-164). Although the functions of many of the

corresponding gene products remain unknown, several are involved in various aspects of trafficking proteins to nascent organelles, particularly melanosomes, lysosomes, and cytoplasmic granules. In the yeast, have been implicated in biogenesis of the cytoplasmic vacuole, which resembles in its function the lysosome of higher organisms, more than 65 proteins including the products of more than 40 vacuolar protein-sorting (*vps*) loci required for trafficking newly synthesized proteins from the Golgi to the vacuole (167, 168). It seems likely that at least as many proteins are associated with organellar biogenesis in mammals.

A subset of these genes, the four *class C vps* genes, which mutations exhibit the most severe disruption of vacuolar morphology, is necessary for the delivery of endocytic and biosynthetic cargo in yeast, and also in *Drosophila*. Correspondently, in humans have been cloned and characterized four genes corresponding to *class C VPS* mutants (*VPS18*, *VPS11*, *VPS16*, and *VPS33* with two isoforms *a* and *b*), that on the basis of phenotype could be HPS genes (169, 170). Suzuki and colleagues (171) have mapped and positionally cloned the mouse buff (*bf*) locus, which is characterized by recessive coat-color hypopigmentation and mild platelet-storage pool deficiency; they find that mouse *bf* results from a missense substitution in *Vps33a*, a homologue of yeast *vps33* and

human *VPS33a*. The *bf* mutation results in defective melanosome morphology and melanogenesis both *in vivo* and *in vitro*. Expression of wild-type *Vps33a* in transfected mouse *bf*-mutant melanocytes complements this aberrant phenotype, whereas expression of *bf*-mutant *Vps33a* does not. These results establish murine *bf* as a murine homologue to the yeast *vps33* mutant and suggest *VPS33A* as a candidate gene for some cases of human HPS.

3.4.3 *Morf4l1*: mortality factor 4 like 1

The human *MRG/MORF* family of transcription factor-like genes which includes *MORF4*, *MORF*-related gene on chromosome 15 (*MRG15* also known as *MORF4L1*), and *MORF*-related gene on the X-chromosome (*MRGX*), since its initial discovery, has been linked to cell proliferation, transcriptional regulation, and DNA damage repair.

In the earliest studies, MRG15 was shown to associate with at least two complexes of nuclear proteins, MRG15-associated factors 1 and 2 (MAF1 and MAF2). MAF1 is composed of MRG15, retinoblastoma (Rb), and PAM14 (172); Rb can, in fact, associate with both MRG15 and MRGX. The association with MRG15 activates the *Bmyb* promoter in both EJ and HeLa cells (173), while the association with MRGX activates the *B-myb* promoter in HeLa while repressing it in EJ cells (174). This

implies a potential mechanism of the MRG family's effect on cellular proliferation. MAF2 contained MRG15 bound to hMOF, a MYST family HAT.¹⁹ Further, it was demonstrated that MRG family proteins are components of mSin3A/Pf1/HDAC complexes. The chromodomain of MRG15 is bound by the plant homeodomain zinc finger protein Pf1, which acts as an adaptor between the two transcriptional repressors mSin3A and the transducin-like enhancer of split (TLE). Additionally, MRG15 alone or MORF4 or MRGX fused with the Gal4 DNA binding domain can bind the mSin3A–TLE corepressor complex and induce transcriptional repression (175). Finally, MRG15 was identified in the TIP60 HAT complex implicated in transcriptional activation in addition to DNA repair and apoptosis (176, 177). Further underscoring the importance of these two genes, knockdown or deletion of either gene in mice results in a similar phenotype including DNA repair defects and embryonic lethality (178); in particular with the majority of the embryos succumbing between E14.5 and birth (179). The null embryos are approximately 74% the size of their wild-type littermates with most of their tissues proportionately smaller. In addition to their small size, the embryos appear pale, suggesting possible circulation, vascularization, and/or hematopoiesis defects. Of those that survived to birth, all died

soon thereafter and examination revealed severe abnormalities in multiple organ systems. The null lungs contained reduced alveolar space and likely failed to inflate following birth. The hearts of the neonates were grossly defective, with ventricular and atrial hypertrophy, enlarged cardiomyocytes, and myocardial fiber disarray. Additionally, the neonates exhibited congestion in multiple organs, but of the liver, lung, and spleen in particular. The skin of the neonates was thinner and less keratinized than the wild-type control with diminished cell number and BrdUpositive staining in the basal cell layer (179).

Pena et al. (180) studied the growth properties of mouse embryonic fibroblasts (MEFs) from E13.5 embryos, founding correspondence with what predicted from the gross histology of the embryos. In particular, the *Mrg15*^{-/-} MEFs show a significantly reduced growth curve than MEFs cultured from wild-type littermates. A colony size distribution assay also revealed a smaller percentage of null MEFs in colonies of greater than four cells with a concomitant increase in null MEFs in single-cell colonies, implying an inability to divide. Finally, null MEFs tended to adopt the large, flattened morphology characteristic of senescent cells at an earlier passage than the wild-type controls.

Some rescue was achieved, however, when MRG15 was reintroduced by adenoviral infection, indicating that the observed growth defects were directly linked to *Mrg15* deficiency (178). To better understand the mechanism of diminished cell cycle progression, Pena and colleagues (180) also examined the tumor suppressor p21, p53, and p19^{ARF} expression. While the upstream regulators of p21, p53, and p19^{ARF} showed no change in expression, p21 expression was significantly increased in the *MRG15* null MEFs as compared to the wild-type.

3.4.4 *Tgfb3: transforming growth factor, beta receptor III*

The transforming growth factor b (TGFb) superfamily is composed of homodimeric polypeptide growth factors, including TGFb isoforms, bone morphogenetic proteins, growth and differentiation factors, activins and inhibins (181). The TGFb signaling pathway has essential roles in regulating many cellular responses including proliferation, differentiation, migration and apoptosis (182-186). There are three TGFb isoforms, TGFb1, TGFb2 and TGFb3, which are encoded by distinct genes and expressed in both a tissue-specific and a developmentally regulated manner. TGFb exerts its biological function through binding to three high-affinity cell-surface receptors, the TGFb type I, type II and type III receptors (TbRI or ALK-5, TbRII and TbRIII or betaglycan,

respectively). TbRI and TbRII contain serine/threonine protein kinases in their cytoplasmic domains. Upon ligand binding, TbRII recruits and phosphorylates TbRI, activating its kinase activity to initiate intracellular signaling. TbRI signals by directly phosphorylating Smad2 and Smad3, which form a complex with the common mediator Smad4, translocate to nucleus and regulate gene transcription (187, 188). While Smad-dependent pathways represent a major mechanism for TGFb signaling, crosstalk and signaling through Smad-independent pathways, including the mitogen-activated protein kinase (MAPK) and phosphatidylinositol 3-kinase (PI3K)/Akt pathways has been reported (189-195).

TbRIII is the most abundant TGFb receptor and is traditionally thought to function as a co-receptor, binding TGFb and presenting it to TbRII (196). This is particularly important for the TGFb2 isoform, which cannot bind TbRII independently. In addition, several studies support essential, non-redundant roles for TbRIII in mediating TGFb sensitivity in intestinal goblet cells (197), in the mesenchymal transformation of chick embryonic heart development (198) and for mouse embryonic development (199). It has been reported the frequent loss of TbRIII expression in human breast, prostate and ovarian cancers, with loss of expression correlating with disease progression and re-expression studies

establishing a direct role for T β RIII in regulating cancer cell migration and invasion *in vitro*, and angiogenesis and metastasis *in vivo*.

T β RIII has a short cytoplasmic domain without kinase activity; while this cytoplasmic domain is not essential for mediating the presentation role, it does contribute to T β RIII/TGF β -mediated inhibition of proliferation (200, 201). In L6 myoblasts, T β RIII expression enhanced TGF β 1-mediated growth inhibition, with this effect mediated, in part, by the T β RIII cytoplasmic domain. The effects of T β RIII were not due to altered ligand presentation or to differences in Smad2 phosphorylation. Instead, T β RIII specifically increased Smad3 phosphorylation, both basal and TGF β -stimulated Smad3 nuclear localization and Smad3-dependent activation of reporter genes independent of its cytoplasmic domain. Conversely, SB431542, a T β RI inhibitor, as well as dominant-negative Smad3 specifically and significantly abrogated the effects of T β RIII on TGF β 1-mediated inhibition of proliferation. T β RIII also specifically increased p38 phosphorylation, and SB203580, a p38 kinase inhibitor, specifically and significantly abrogated the effects of T β RIII/TGF β 1-mediated inhibition of proliferation in L6 myoblasts and in primary human epithelial cells. Importantly, treatment with the T β RI and p38 inhibitors together had additive effects on abrogating T β RIII/TGF β 1-

mediated inhibition of proliferation. In a reciprocal manner, short hairpin RNA-mediated knockdown of endogenous TbRIII in various human epithelial cells, attenuated TGFb1-mediated inhibition of proliferation. Taken together, these data demonstrate that TbRIII contributes to and enhances TGFb-mediated growth inhibition through both TbRI/Smad3-dependent and p38 mitogen activated protein kinase pathways (200, 201).

3.4.5 *Mef2c: myocyte enhancer factor 2C*

Mef2c belongs to the MEF2 (myocyte-specific enhancer-binding factor 2) subfamily of MADS (named for MCMI, which regulates mating type-specific genes in yeast, *Agamous* and *Deficiens*, which have a homeotic function in plants, and Serum Response Factor, which mediates serum-inducible transcription) transcription factors (202). The MADS domain is a 56-amino acid motif that mediates DNA binding, homo- and heterodimerization, and interaction with basic helix-loop-helix proteins (202-209). The four MEF2 family members (MEF2A, MEF2B, MEF2C, MEF2D) are highly homologous within the MADS domain and an adjacent 26-amino acid region, known as the MEF2 domain, but they are divergent in their carboxyl termini. Additional complexity of this family of regulators arises from alternative splicing of MEF2 transcripts,

yielding isoforms with common DNA-binding domains and unique carboxyl terminal regions.

MEF2 genes are expressed in cardiac, skeletal, and vascular smooth muscle cells, endothelial cells, several types of hematopoietic cells and discrete neurons of the central nervous system (210-214). Accordingly, several lines of evidence have implicated members of this family in transcriptional regulation of muscle-specific genes and of genes regulated by extracellular signals (215).

Members of MEF2 transcription factor family play key roles in cardiac myogenesis. *Mef2c* in particular is among the earliest markers of the cardiac lineage with its expression detectable in mesodermal cells that give rise to the primitive heart tube, at about E7.5, shortly after the expression of the *Nkx2.5* and *Gata* genes (210, 214, 216-222). By E8.5, *Mef2c* (together with *Mef2a* and *Mef2d*) transcripts are detected in the myocardium and interestingly at the time of cardiac looping, they are present in the left ventricle and atria but are much more robustly expressed in the right ventricle, outflow tract and pharyngeal mesoderm. By E9.0, *Mef2c* is expressed in rostral myotomes, where its expression lags by about a day behind that of *Myf5* and several hours behind that of *myogenin* (210). Its expression is observed in muscle-forming regions

within the limbs at E11.5 and within muscle fibers throughout the embryo at later stages. *Mef2c* is also expressed in endothelial cells, surrounding mesenchyme and smooth muscle cells (SMCs) of the developing vasculature of the embryo (210, 223). In the absence of *Mef2c*, the endothelial cell plexus is not stabilized and SMCs do not differentiate suggesting that it plays multiple roles in vascular development, being required for endothelial cell interactions and in mesenchymal cells surrounding the endothelial network, for their responsiveness to endothelial cell signaling, their migration or their differentiation. The apparent failure of endothelial cells to interact properly to form a vascular plexus in *Mef2c* mutant embryos, could also reflect an underlying defect in cell adhesion.

After E12.5, *Mef2c* transcripts are detected at high levels in specific regions of the brain too (206, 224, 225).

In agreement with the microarray results, *Pex2* and *Morf4l* showed down-regulated expression in *Tbx1*^{-/-} embryos at E9.5, while *Vps33a* and *Mef2c* were up-regulated (Figure 3).

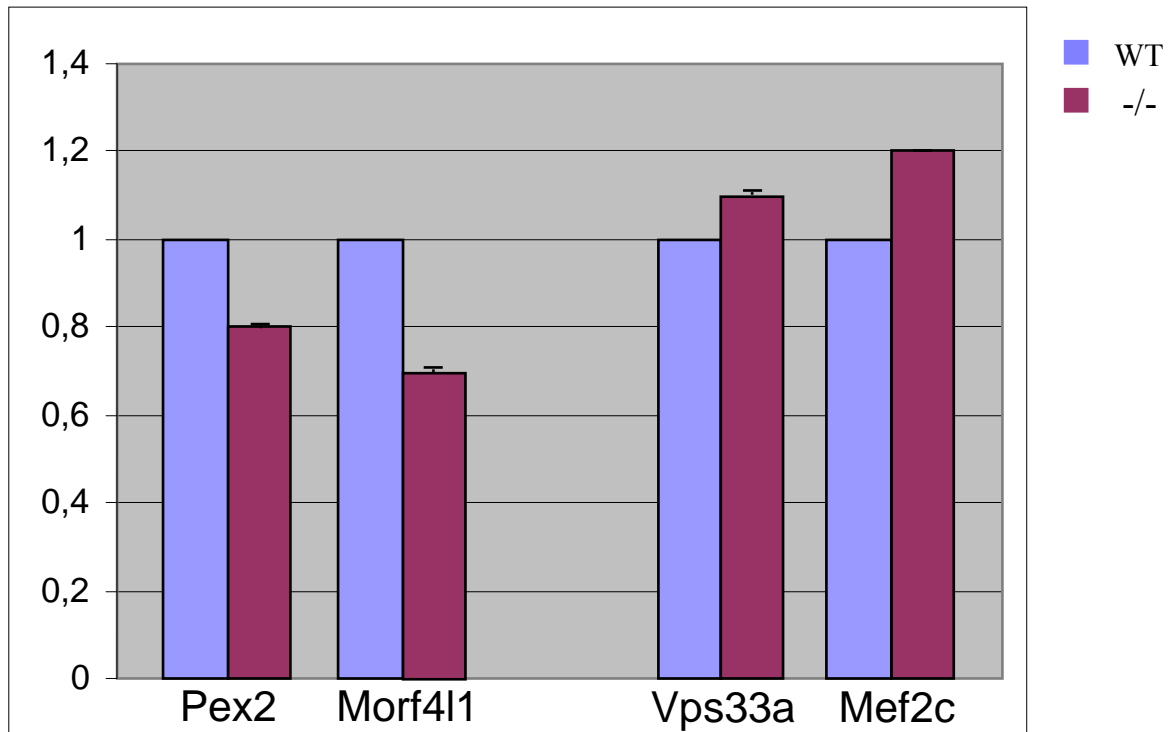


Figure 3. qRT-PCR on mRNA from E9.5 wt and *Tbx1* null mutant embryos. *Pex2* and *Morf4l1* are down-regulated in *Tbx1* null mutants, while *Vps33a* and *Mef2c* are up-regulated.

To confirm the microarray results, we also used an in vitro gain-of-function model, a *Tbx1*-expressing tetracycline (Tc) inducible mouse embryonic stem cell line, previously established in our laboratory using the ROSA-TET system described by Masui et al. (226). Tc-regulated transgene expression systems, known as Tet-off and Tet-on systems, have been widely applied to a variety of biological materials, including mammalian cells (227, 228). The Tet-off system is based on a Tc-regulatable transactivator (tTA), which induces transcription in the absence of Tc or its analog doxycycline (Dox) through binding to the hCMV-1 promoter. This promoter is composed of a Tc-responsive element (TRE) followed by a minimal promoter of the human cytomegalovirus (hCMV) immediate early gene. The tTA protein is a fusion protein composed of the TRE-binding domain of Tc repressor protein and the herpes simplex virus VP16 activation domain (229). Alternatively, the Tet-on system uses a reverse Tc-regulated transactivator (rtTA) which binds TRE and induces transcription of the transgene in the presence of Dox (230). The ROSA-TET system allows researchers to establish ES cell lines carrying a Tc-regulatable transgene at the *ROSA26* locus that is regarded as a locus from which proteins can be expressed ubiquitously at a moderate level. This system is based on a

knock-in step of a construct carrying both loxP and its mutant sequences (loxPV) into the *ROSA26* locus, followed by a subsequent exchange step that introduces a cDNA to be Tc-regulated to the locus, using the recombinase-mediated cassette exchange reaction (Figure 4).

In our laboratory, an exchange vector carrying the *Tbx1* cDNA was co-transfected along with a Cre-expression vector into EBRTcH3 cells which had been derived from EB3 cells by the knock-in step, to establish an ES cell line (named EBRTcTbx1) expressing *Tbx1* under the control of the *ROSA26* promoter in a Tc-dependent manner (Figure 5A). In Tc-medium, tTA binds to the hCMV-1 promoter, inducing expression of *Tbx1*-IRES-Venus.

By qRT-PCR on mRNA from cells cultured for 24 hours in the absence of doxycycline, we observed a *Tbx1* mRNA level increased of about 45 folds, confirming the efficiency of the system (Figure 5B).

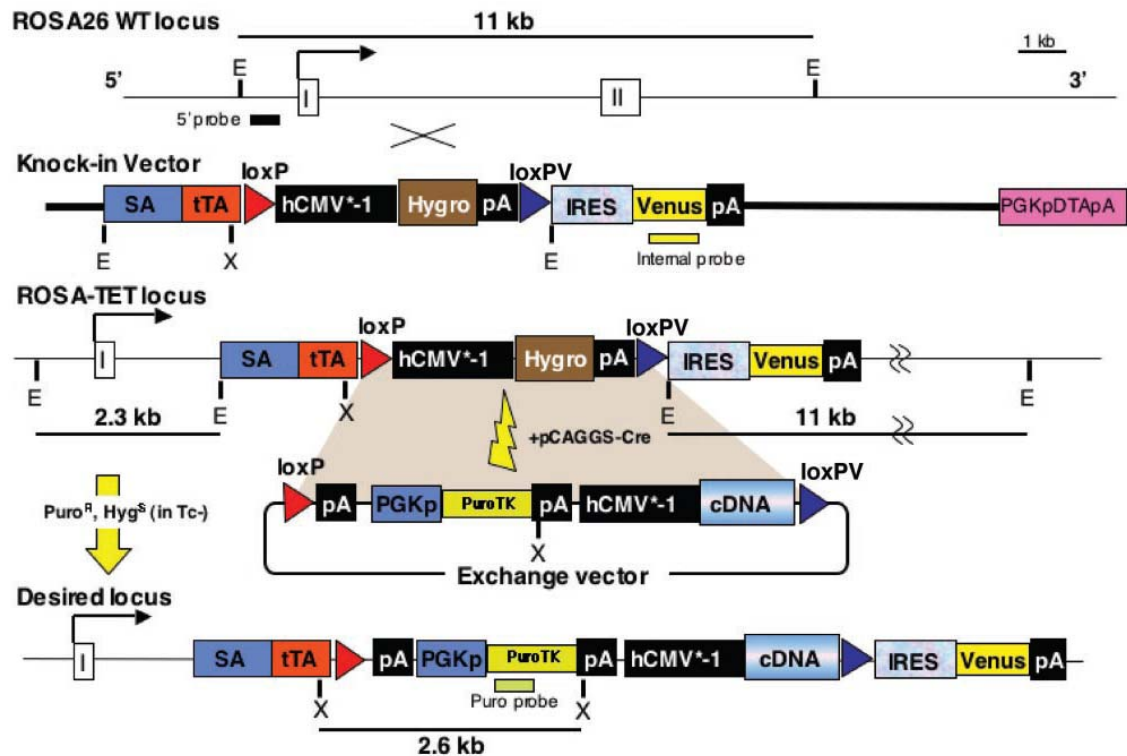


Figure 4. Experimental strategy to generate the *ROSA-TET* locus and the desired locus.

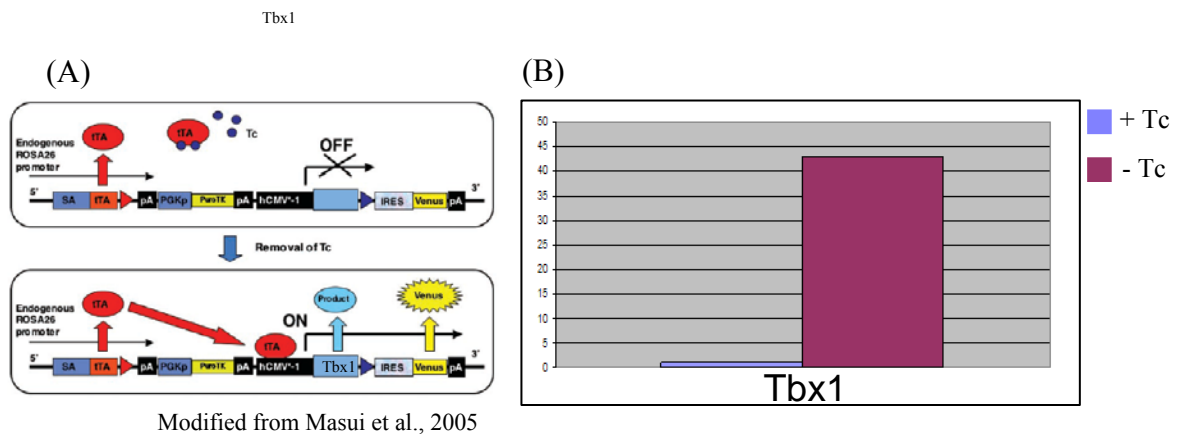


Figure 5. Induction of expression in the ROSA-TET system (A) Schematic representation of the induction of Tbx1-IRES-Venus expression. (B) qRT-PCR on mRNA from EBRTcTbx1 cells grown in ES medium with and without Tc.

In these conditions *Mef2c*, *Tgfbr3* and *Vps33a* were down-regulated, while *Morf4l1* and *Pex2* showed an increased expression (Figure 6).

Totally the *in vivo* loss-of-function and *in vitro* gain-of-function systems allowed us to confirm the microarray results on a half of selected genes; however we decided to focus our attention on understanding the mechanism by which *Tbx1* regulates *Mef2c* expression, for several reasons. First, *Mef2c* seems to have a key role in the transcriptional pathways controlling myoblast differentiation in the second heart field; second, *Tbx1* is strongly expressed in that tissue and it is required for mesodermal cell proliferation. Finally, our microarray results showed a negative regulation of *Mef2c* by *Tbx1*: taken together these data suggested a putative model in which *Tbx1* can exert its anti-differentiative role on SHF mesodermal cells, through a mechanism involving *Mef2c* transcriptional repression.

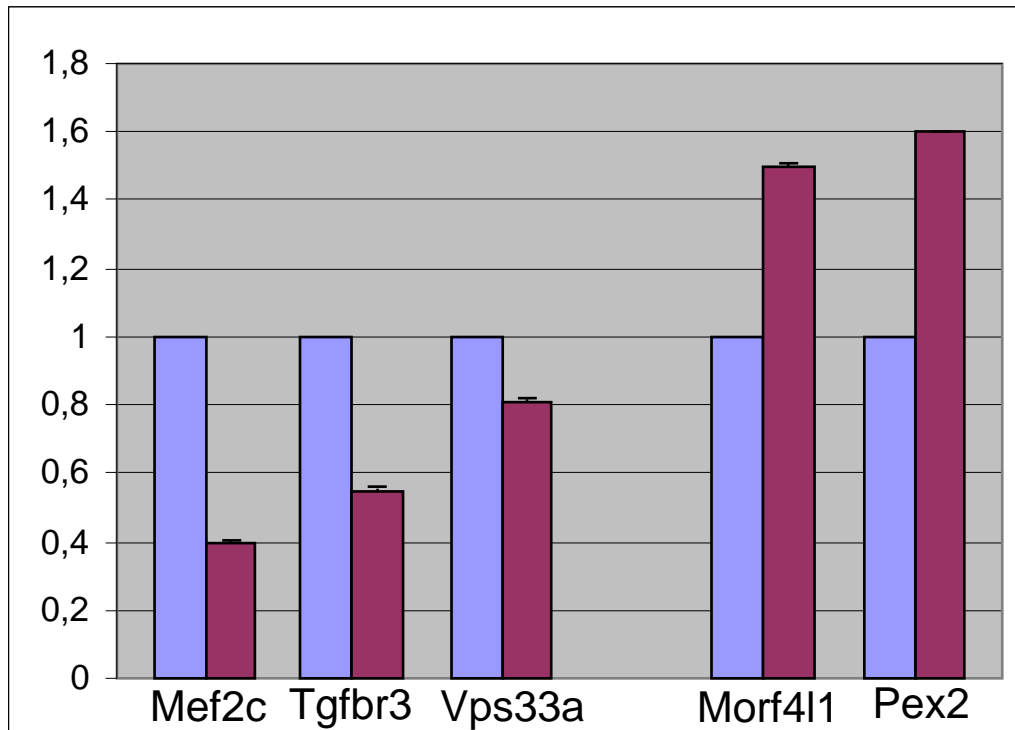


Figure 6. qRT-PCR on mRNA from EBRTcTbx1 cells. *Mef2c*, *Tgfbr3* and *Vps33a* are down-regulated in *Tbx1* over-expressing cells, while *Pex2* and *Morf4l1* are up-regulated.

3.5 *Mef2c* is specifically overexpressed in the second heart field of *Tbx1*^{-/-} mutant embryos

In situ hybridization (ISH) served as an independent method of validating the *Mef2c* microarray results, enabling assessment of qualitative gene expression changes in *Tbx1* null mutant embryos. Interestingly, ISH on embryo cryosections at E9.5 revealed upregulation of *Mef2c* in the second heart field of *Tbx1*^{-/-} mutants compared to wt littermates (Figure 7).

3.6 *Mef2c* expression is *Tbx1* dosage-dependent in transfected C2C12 myoblasts

In order to confirm the microarray results for *Mef2c*, we also used an *in vitro* gain of function model, represented by C2C12 myoblasts. By qRT-PCR on mRNA from C2C12 cells transfected with different amount of a *Tbx1* expressing vector (pCDNATbx1-c-myc), we confirmed that *Mef2c* expression is *Tbx1* dosage-dependent (Figure 8).

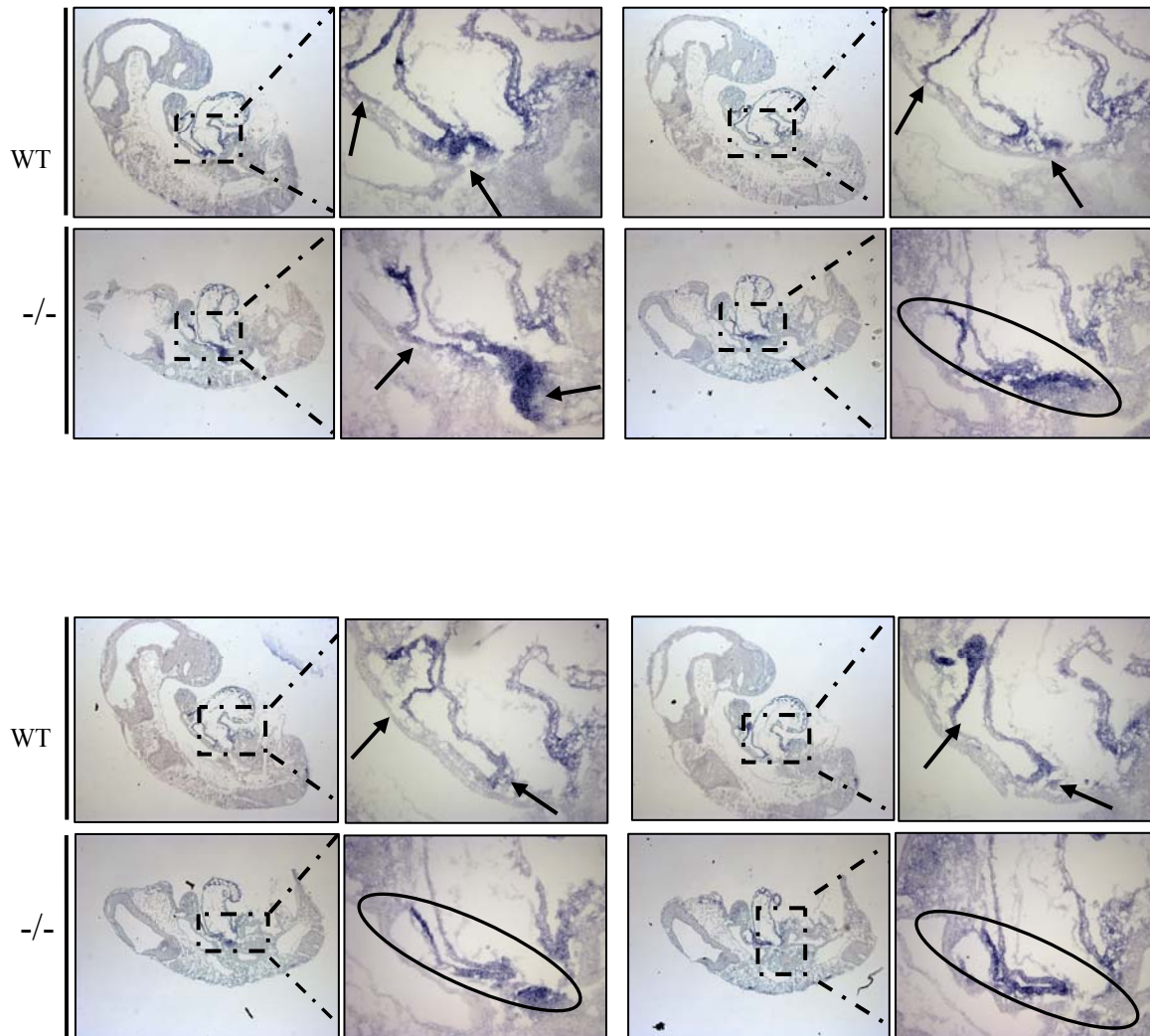


Figure 7. In situ hybridization on cryosection of E9.5 wt and *Tbx1* null mutant embryos with a digoxigenin-labeled *Mef2c* antisense probe. *Mef2c* is specifically up-reguated in the SHF of *Tbx1* null mutants.

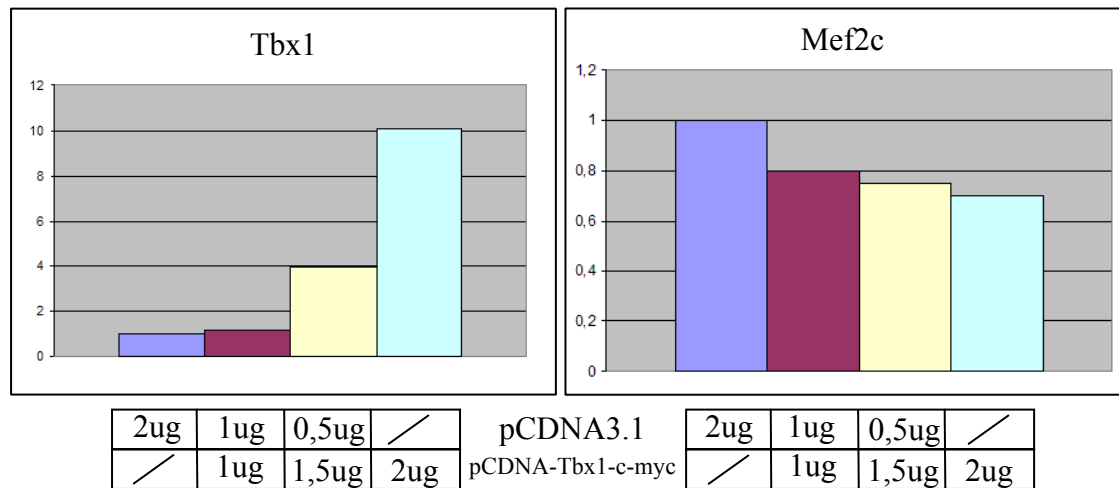


Figure 8. qRT-PCR on mRNA from transfected C2C12 myoblasts. *Mef2c* expression is *Tbx1*-dosage dependent.

3.7 Mef2c protein level is affected by Tbx1 dosage in transfected C2C12 myoblasts

To demonstrate that *Mef2c* negative regulation by Tbx1, also affects Mef2c protein level, we performed a Western Blotting analysis on total protein extracts from transfected C2C12 myoblasts.

We found a low protein level reduction (Figure 9), but we were able to confirm that result in multiple experiments (data not shown).

In addition, we performed luciferase assays on transfected C2C12 cells, using a minimal MEF2-luciferase reporter construct (3X-MEF2-luc), in which firefly luciferase expression is driven by a thymidine kinase promoter with three upstream tandem copies of a high-affinity MEF2 binding site from the *desmin* gene, termed *desMEF2* (150, 231).

Hui Li and Yassemi Capetanakil (232) showed that Mef2c (and also other members of MEF transcription factor family) was able to bind that site, so triggering the *desmin* gene muscle-specific transcription in concert with bHLH myogenic regulator family. Since it has been demonstrated that *Mef2c* is a direct transcriptional target of Isl1 and Gata4 factors in the SHF, during mouse embryonic development (2), we performed luciferase assays on C2C12 cells transfected with the reporter construct

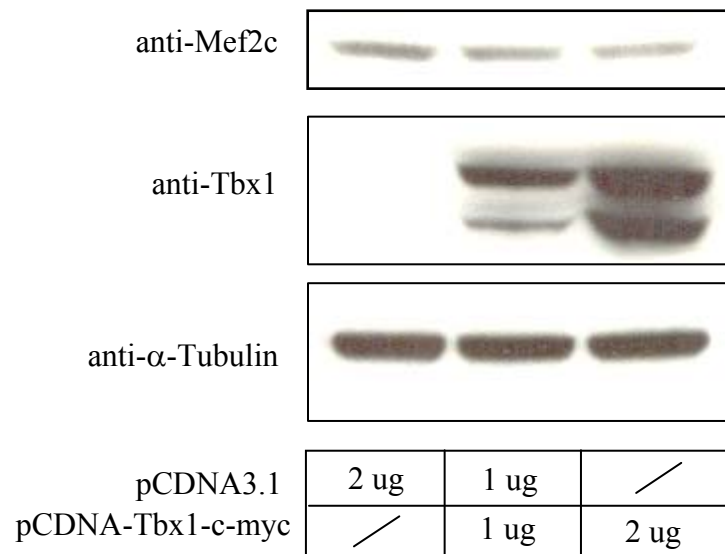


Figure 9. Western Blotting analysis on transfected C2C12 myoblasts. Tbx1 dosage affects Mef2c protein level.

together with different amounts of a Gata4 or Isl1 expressing vector in order to test the functionality of the system. As expected, our experiments showed an increased luciferase activity in the presence of Gata4 or Isl1 (Figures 10A and 10B); we also performed luciferase assays on C2C12 myoblasts transfected with different amounts of a Tbx1 expressing vector, but unfortunately, we were not able to appreciate a decreased luciferase activity as result of a lower Mef2c protein level due to Tbx1 over-expression (Figure 10A).

A possible explanation for a such as result was that probably in our experiment, the basal luciferase activity was too low to appreciate a decrease in the presence of Tbx1; so we decided to perform luciferase assays on C2C12 cells transfected with both Gata4 (or Isl1) and Tbx1 expression vectors.

Our results showed that Tbx1 was able to interfere with Gata4-dependent luciferase activity enhancement (Figure 10C), but not with the Isl1-dependent one (Figure 10D), suggesting that *Tbx1* could regulated Mef2c expression through a mechanism requiring Gata4 activity.

It has been shown by Liao et al. that Gata4 is overexpressed in *Tbx1*^{-/-} mutants; since *Mef2c* is regulated by Gata4 (2), one can argue that

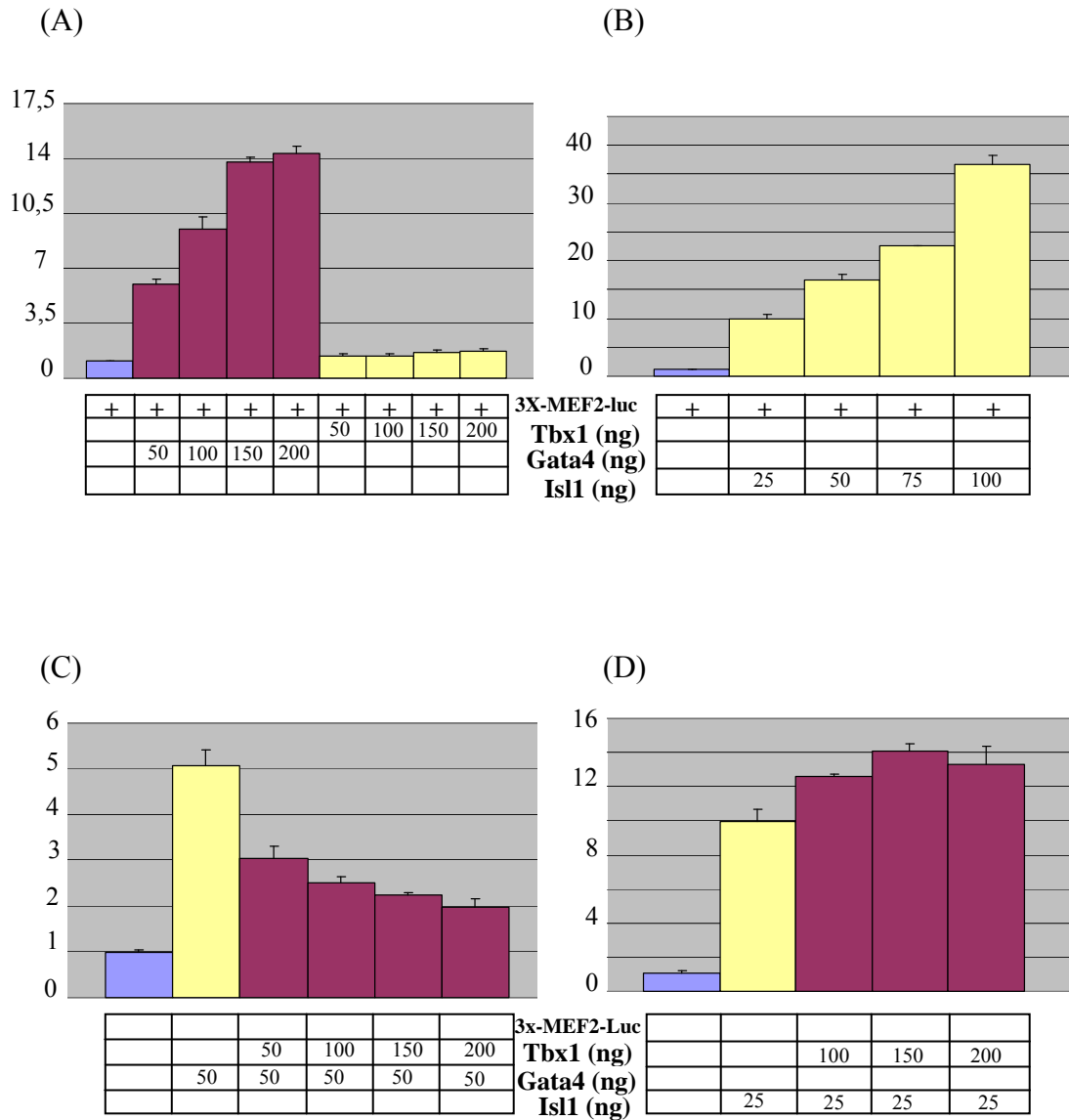


Figure 10. Luciferase assays on transfected C2C12 myoblasts. (A, B) Mef2c protein activity is sensitive to Gata4 and Isl1 dosage, but not to Tbx1 dosage. (C,D) Tbx1 interferes with Gata4- but not with Isl1-dependent activity of Mef2c protein.

reduced Mef2c protein level observed in our experiments is just the result of a Gata4 negative regulation by Tbx1; this hypothesis seems unlikely since we performed our luciferase assays on cells transfected with a Gata4 expression vector carrying the Gata4 cDNA without the regulatory regions that could be, *in vivo*, targeted by Tbx1. Theoretically, the Tbx1 negative effect on endogenous *Gata4* could contribute to the reduced Mef2c protein level observed in Gata4/Tbx1 transfected cells, but this effect seems to be negligible, since we did not observe any significant decreased Mef2c protein level in Tbx1 and Isl1/Tbx1 overexpressing cells. So it seems to be more likely the hypothesis of a Tbx1 mechanism of action affecting Gata4 protein activity rather than *Gata4* gene transcription.

3.8 Conserved T-box binding element analysis of *Mef2c* locus

Our first analysis for conserved TBEs was not able to find any potential Tbx1 binding site in the 10kb upstream region of *Mef2c* locus; both our *in vivo* and *in vitro* results, however, suggest a possible negative regulation of *Mef2c* by Tbx1. So, as part of the effort to understand the mechanism by which Tbx1 regulates its expression, we decided to extend our analysis also to the intronic regions of *Mef2c* locus. Using the TRANSFAC data base and the rVISTA program, we found 91 potential

Tbx1 binding sites evolutionary conserved between human and mouse; this result is not surprising since all the regulatory regions of *Mef2c* gene, so far identified, reside in its intronic regions.

In particular, by generating a *Mef2c-lacZ* transgenic mouse, Dodou and colleagues identified a minimal intronic enhancer that specifically directs *Mef2c* expression in the second heart field (2). They looked for cardiac-specific transcription factor binding sites and found that this conserved regulatory region carries three conserved candidate binding sites for the Gata family of transcription factors and two conserved perfect consensus elements for the LIM-homeodomain transcription factor Isl1. In addition, they identified two candidate E boxes, representing potential binding sites for Hand factors, and a putative Nke binding site for Nk class factors such as Nkx2.5. However, among all the sites in the enhancer, robust binding by putative transcriptional regulators, was only detected for two of the Gata elements and for both the Isl sites.

The cardiac Gata transcription factors, Gata4/5/6, are expressed more broadly than the second heart field restricted pattern of the *Mef2c-lacZ* transgene described in Dodou study (216, 219-221). The broader expression pattern of the Gata factors suggests that additional regulators must be required to restrict enhancer function to the second heart field.

Indeed, they also showed that the *Mef2c* enhancer is directly bound by Isl1. As is the case for the Gata factors, Isl1 expression within the embryo is broader than the pattern directed by the *Mef2c* enhancer they described, but expression of Isl1 within cardiogenic lineages appears to be limited to the anterior heart field (114). Thus, their data suggest a model in which *Mef2c* anterior heart field-specific expression is dependent on the combined activities of Isl1 and Gata4; interestingly, one of the putative Tbx1 binding sites we identified, also resides in the conserved SHF-specific enhancer (Figure 11). This observation agrees with our previous results suggesting that Tbx1 can negatively regulate *Mef2c* expression by interfering somehow with Gata4 activity, may be by preventing binding to its sites in the enhancer. On the other hand, these data also open the question of whether the *Mef2c* regulatory mechanism involves a direct Tbx1 binding to the SHF-specific enhancer.

3.9 *Mef2c* regulation by Tbx1 seems to be mediated by Gata4

To test if Tbx1 could regulate *Mef2c* expression through the SHF-specific enhancer described by Dodou et al., we cloned it upstream of a luciferase gene, which expression was driven by a minimal SV40 promoter, so generating the Mef2c-Enh-Luc reporter construct.

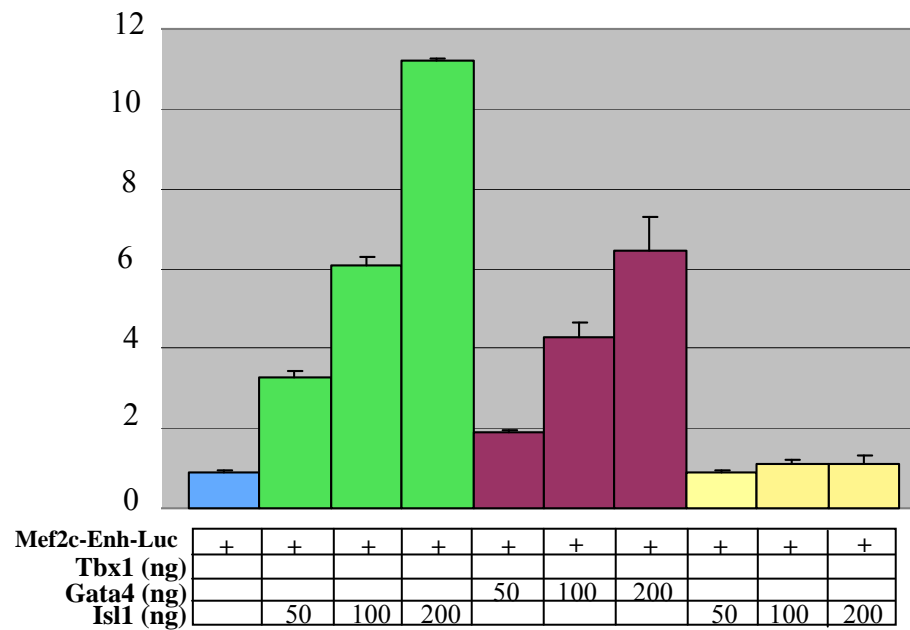
Luciferase assays were performed on C2C12 transfected with different amount of a Tbx1 expression vector; as control we used Gata4- and Isl1-overexpressing cells. As expected, we found an increased luciferase activity in Gata4 or Isl1 transfected C2C12 cells, compared to the control empty-vector transfected cells (Figure 12A).

Unfortunately we were not able to appreciate any significant difference, in luciferase activity between Tbx1-overexpressing and control C2C12 myoblasts, probably because, also in this case, basal luciferase activity was too low to appreciate a decrease in the presence of Tbx1 (Figure 12A). However, our previous results suggested a putative regulatory mechanism of *Mef2c* expression by Tbx1 that involves Gata4; thus, to both confirm this hypothesis and increase basal luciferase activity, assays were performed on C2C12 cells transfected with Tbx1 and Gata4 expression vectors at the same time. As additional control, we performed

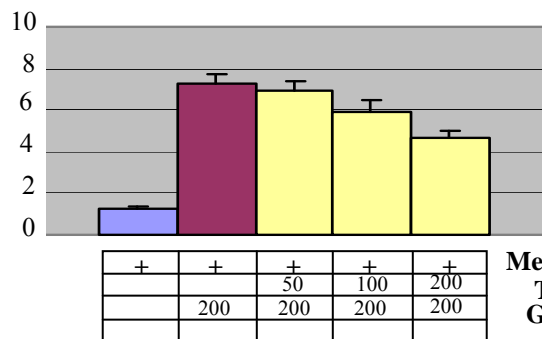
luciferase assays on C2C12 myoblasts transfected with both Tbx1 and Isl1 expression vectors.

Our results showed again that Tbx1 was able to interfere with Gata4-dependent luciferase activity enhancement (Figure 12B), but not with the Isl1-dependent one (Figure 12C), supporting the hypothesis that *Mef2c* regulation by Tbx1 could be mediated by Gata4 activity, and opening the question of whether this regulatory mechanism actually requires Tbx1 direct binding to the *Mef2c* SHF-specific enhancer.

(A)



(B)



(C)

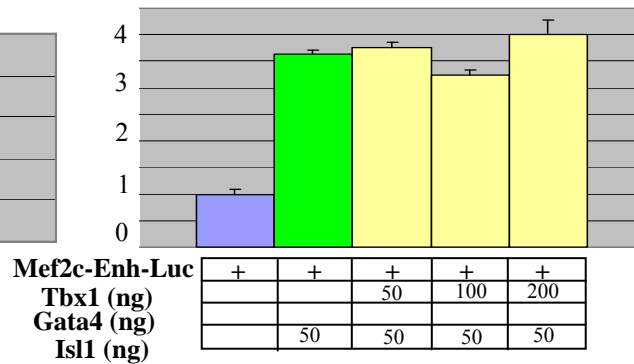


Figure 12. Luciferase assays on transfected C2C12 myoblasts. (A) Gata4 and Isl1 activate the *Mef2c* SHF-specific enhancer, while Tbx1 doesn't repress it. Tbx1 interferes with the Gata4- but not Isl1-dependent activation of the *Mef2c* SHF specific enhancer.

3.10 *Mef2c* regulation by Tbx1 does not require a direct binding to the SHF-specific enhancer

In order to understand if *Mef2c* regulation requires direct binding of Tbx1 to the conserved TBE in the SHF-specific enhancer of *Mef2c* locus, we mutagenized three out of ten base pairs within its sequence.

Luciferase assays were performed on C2C12 cells transfected with the mutant (and wt as control) Mef2c-Enh-Luc reporter in the presence of both Gata4 and Tbx1, and we found that, also in this case Tbx1 was able to interfere with Gata4-dependent *Mef2c* activation (Figure 13).

Taken together these results suggest that *Mef2c* regulation by Tbx1 could be mediated by Gata4; this mechanism doesn't require a direct Tbx1 binding to the SHF-specific enhancer, so it is likely that Tbx1 can somehow interfere with Gata4-dependent *Mef2c* activation.

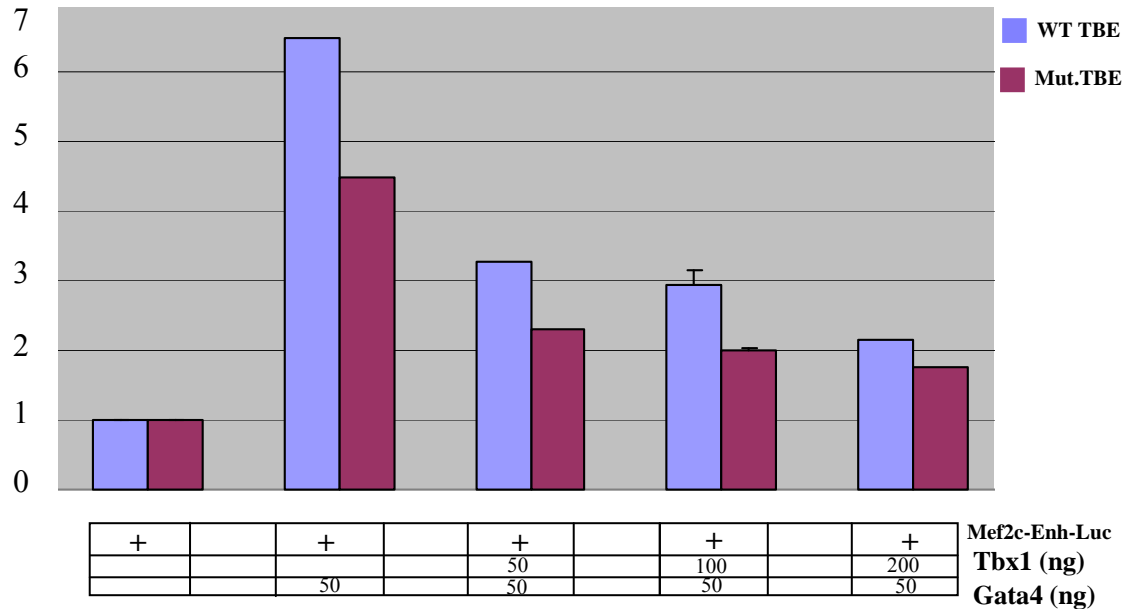


Figure 13. Luciferase assays on transfected C2C12 myoblasts. Gata4-dependent regulation of *Mef2c* expression by Tbx1 doesn't require its direct binding to the TBE in the SHF-specific enhancer of *Mef2c* locus.

3.11 *Tbx1* dosage does not affect *Mef2c* expression in the absence of *Gata4* in transfected C1C12 myoblasts

To test if *Tbx1* regulates *Mef2c* transcription through a mechanism involving *Gata4*, we decided to evaluate *Tbx1* dosage-dependent *Mef2c* expression in the absence of *Gata4*. Since C2C12 myoblasts express endogenous *Gata4*, we used siRNAs specifically directed against the *Gata4* locus in order to compare *Mef2c* expression level in *Tbx1* overexpressing myoblasts, where also *Gata4* was knocked down, to cells where only *Gata4* was downregulated by RNA interference. If *Tbx1* and *Gata4* independently regulate *Mef2c*, we expected an increased downregulation of the gene when at the same time, *Tbx1* was overexpressed and *Gata4* knocked down, since both *Tbx1* over-expression and *Gata4* downregulation result in a lower *Mef2c* level. On the other hand, if *Tbx1* regulates *Mef2c* expression through a mechanism involving *Gata4*, cells where *Tbx1* was overexpressed and *Gata4* downregulated, had to show a *Mef2c* dosage comparable to that of cells where only *Gata4* was knocked down, since in the absence of *Gata4* (or with a small residual protein level) which supposedly is the mediator of the regulatory mechanism, there is no more effect of *Tbx1* overexpression on *Mef2c* level. After transfection of C2C12 myoblasts with (50 nM) *Gata4*-specific siRNAs,

Gata4 mRNA and protein levels were measured by qRT-PCR and Western Blotting respectively (Figures 14A and B). In these conditions we had a downregulation of about 80% of the wild type level for both Gata4 mRNA (Figure 14A) and protein (Figure 14B), resulting in a *Mef2c* downregulation of about 20% of the wild type level (Figure 15 A). Interestingly we found no significant difference in *Mef2c* level between cells where at the same time, *Gata4* was knocked down and *Tbx1* over-expressed, compared to C2C12 myoblasts where only *Gata4* was downregulated (Figures 15A, B and C). This result strongly supports our hypothesis of a Gata4-mediated *Mef2c* regulation by Tbx1.

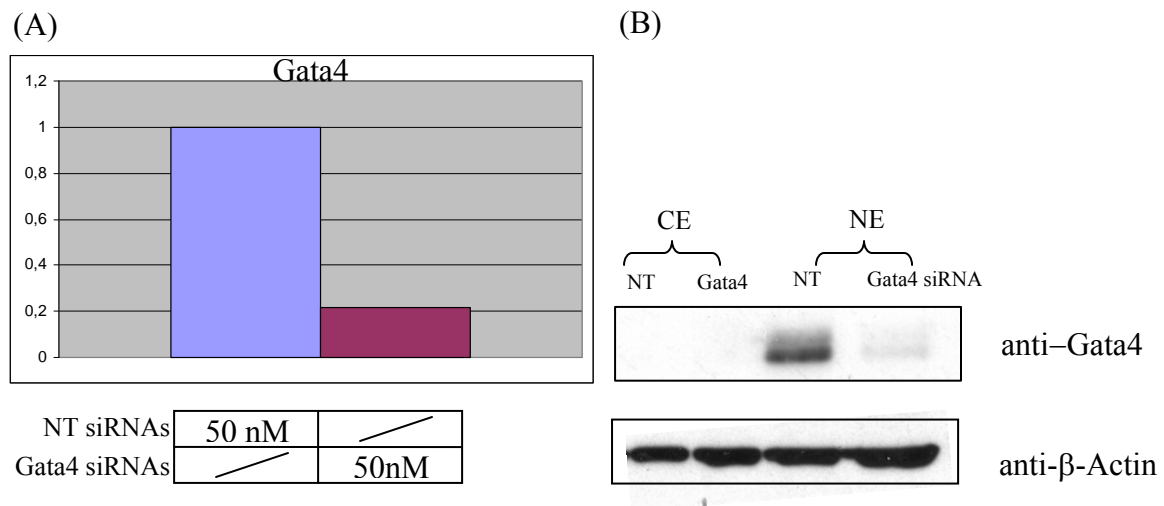


Figure 14. Endogenous *Gata4* RNA interference in C2C12 myoblasts. (A) qRT-PCR and (B) Western Blotting analysis on C2C12 myoblast transfected with *Gata4*siRNAs and non-targeting (NT) siRNAs. CE and NE: cytoplasmic and nuclear extracts respectively.

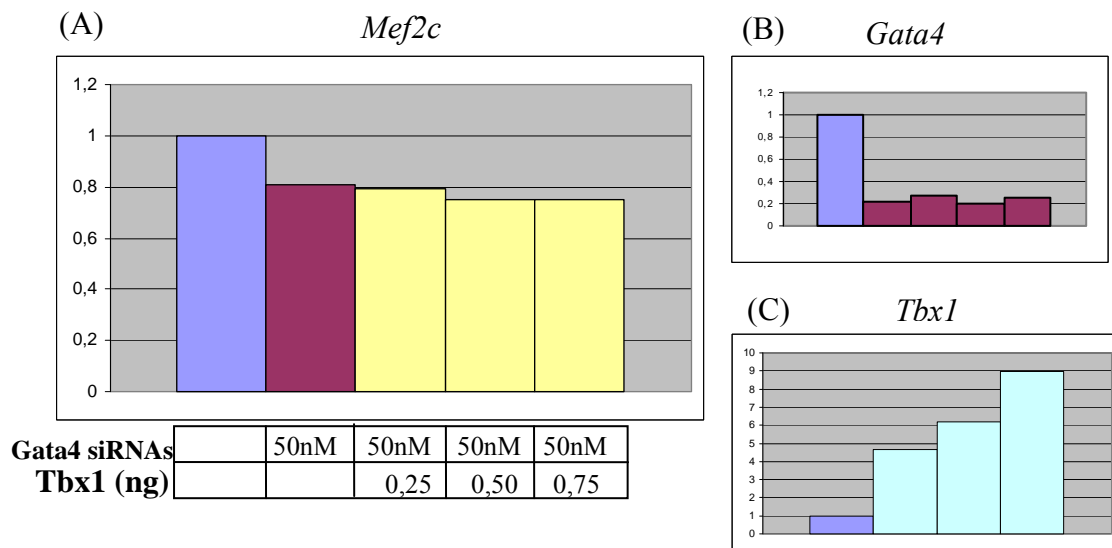


Figure 15. qRT-PCR on mRNA from transfected C2C12 myoblasts. (A) In the absence of Gata4, Tbx1 is not still able to regulate *Mef2c* expression. (B) *Gata4* and (C) *Tbx1* mRNA dosage in transfected C2C12 where *Mef2c* expression level was measured.

3.12 *Mef2c* is negatively regulated by *Tbx1* in skeletal muscle cells *in vivo*

If *Mef2c* expression is *Tbx1* dosage-dependent *in vivo*, we expected to observe a *Mef2c* downregulation in *Tbx1* gain-of-function mutants. To this aim, whole mount *in situ* hybridization was performed on COET;*Mesp1*^{Cre/+} embryos at E9.5 (148); the COET (for Conditional over-expression of *Tbx1*) transgene expresses *Tbx1* mRNA in response to Cre recombination. *Mesp1* is initially expressed in epiblast cells sorting through the primitive streak and is quickly downregulated after E7 (149), i.e. before *Tbx1* is turned on. The progeny of *Mesp1*-expressing cells contributes heavily to the cranial mesoderm (149). *Mesp1Cre*-induced recombination, as visualized by crosses with the R26R reporter (233), is restricted to mesodermally derived tissues and was not detected in endodermal or ectodermal cells. So *Mesp1Cre* drives *Tbx1* expression in all its mesodermal domains of the pharynx, head mesenchyme and splanchnic mesoderm (Figure 16).

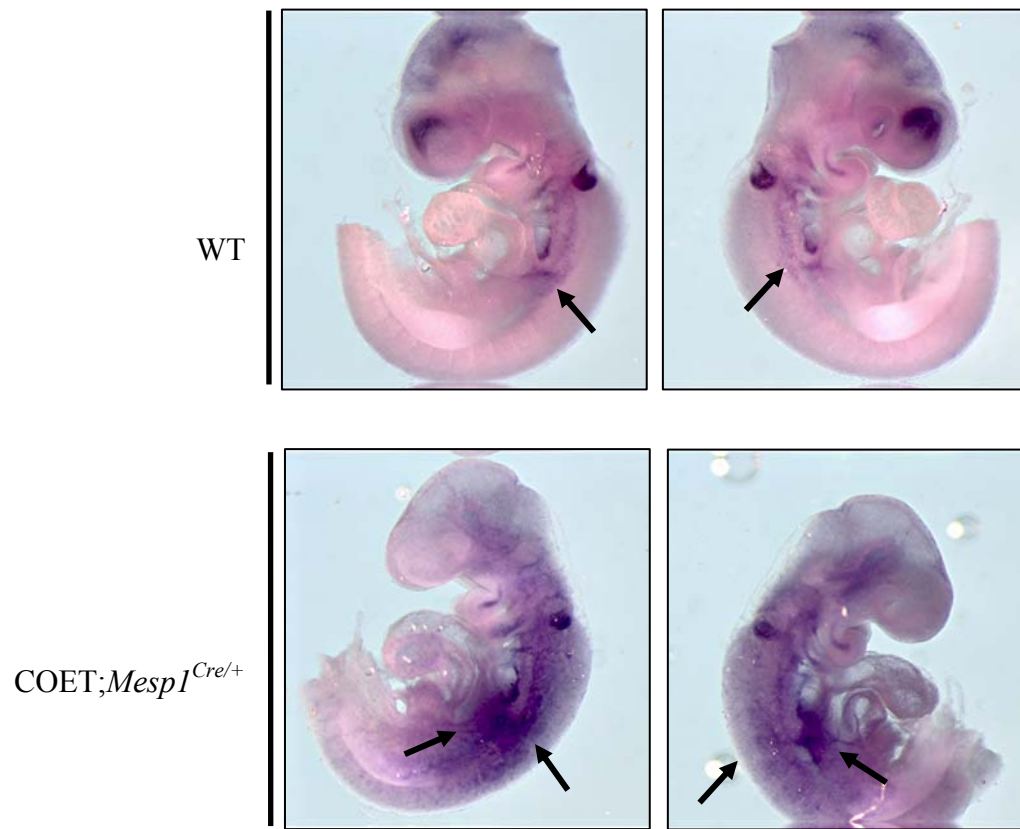


Figure 16. Whole mount in situ hybridization on E9.5 wt and COET;*Mesp1*^{Cre/+} mutant embryos with a digoxigenin-labeled *Tbx1* antisense probe. *Tbx1* is over-expressed in all its mesodermal domains.

A single mix of probe and hybridization solution was used to examine E9.5 wild type and mutant embryos in adjacent wells of a six well dish, in order to keep experimental conditions as closely similar as possible between the two groups of embryos.

According with our previous data, whole mount ISH showed a *Mef2c* down-regulation in the SHF of COET;*Mesp1*^{Cre/+} mutants compared to control embryos (Figure 17).

It has been show that of the four vertebrate *Mef2* genes, *Mef2c* is the earliest to be expressed in skeletal muscle (210); in particular *Mef2c* expression, in the mouse should be dectectable, even if very low, by E9.0 in the myotomal compartment within rostral somites, and expand throughout all of skeletal muscle as development progresses (210). In our previous in situ hybridization experiments, we were not able to appreciate *Mef2c* expression in somite compartment of wt embryos at E9.5; here instead we found a strong *Mef2c* expression in somites of control embryos and, interestingly this expression was dramatically reduced in COET;*Mesp1*^{Cre/+} (Figure 18), suggesting that Tbx1 is able to repress *Mef2c* also in skeletal muscle cells.

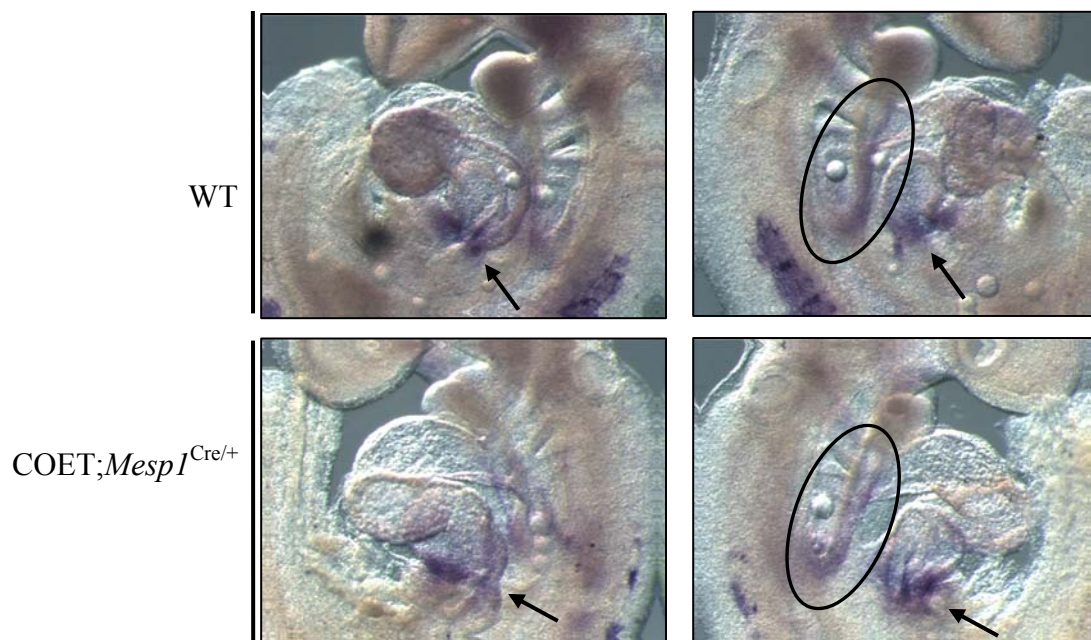


Figure 17. Whole mount in situ hybridization on E9.5 wt and COET;*Mesp1*^{Cre/+} mutant embryos with a digoxigenin-labeled *Mef2c* antisense probe. *Mef2c* is down-regulated in the SHF and inflow tract of COET;*Mesp1*^{Cre/+} mutants.

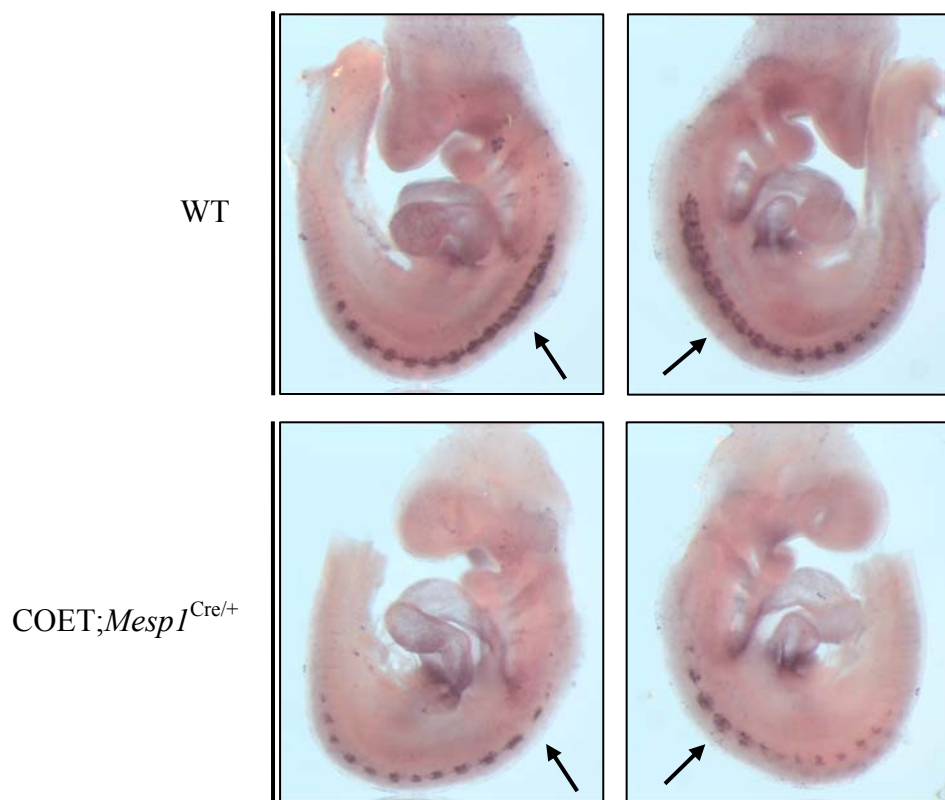


Figure 18. Whole mount in situ hybridization on E9.5 wt and COET;*Mesp1*^{Cre/+} mutant embryos with a digoxigenin-labeled *Mef2c* antisense probe. *Mef2c* is down-regulated in the SHF and in somites (arrows) of COET;*Mesp1*^{Cre/+} mutants.

These results open the question of whether *Mef2c* can be regulated by Tbx1, through a Gata4-dependent mechanism, also in skeletal muscle cells.

We analyzed *Gata4* expression at E8.5 and E9.5 by whole mount in situ hybridization on control and COET;*Mesp1*^{Cre/+} mutant embryos. Liao et al. (234) previously described a *Gata4* ectopic expression in the SHF of *Tbx1*^{-/-} embryos at E9.0-E9.5. So, as expected, we found, a marked *Gata4* downregulation in COET;*Mesp1*^{Cre/+} mutant hearts compared to control embryos (Figure 19), suggesting that at least partially, *Mef2c* downregulation reflects *Gata4* repression by Tbx1.

Gata4 seems to be not expressed in skeletal muscle cells, so an outstanding question is how Tbx1 can negatively regulates *Mef2c* expression in somites. Even if Tbx1 doesn't bind the putative TBE in the SHF-specific enhancer of *Mef2c* gene, we cannot exclude that it can directly bind other regulatory regions, so repressing *Mef2c* transcription in skeletal muscle cells, likely in a tissue-specific manner. Alternatively, regulation of *Mef2c* by Tbx1 could require involvement of an intermediate, a skeletal muscle-specific transcription factor which is a direct transcriptional target of Tbx1 or whose activity is somehow

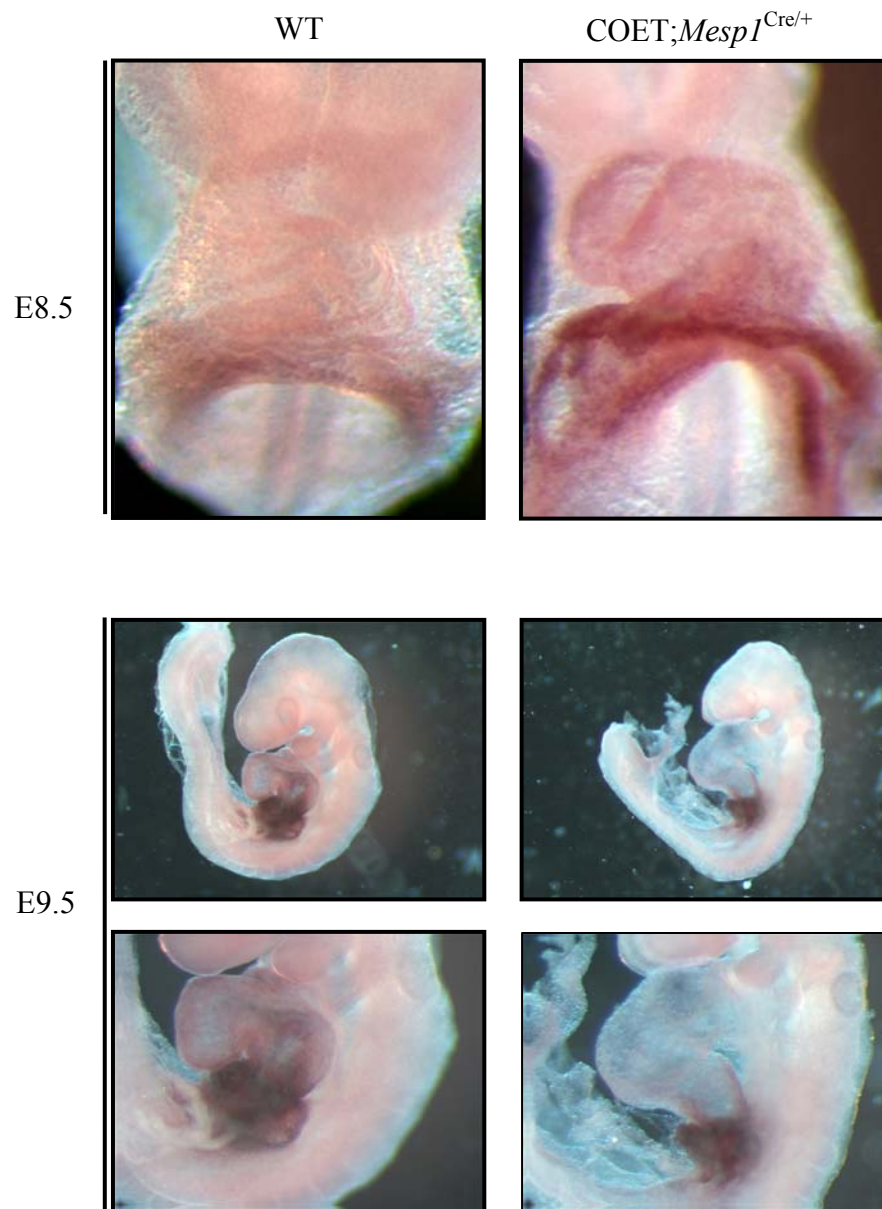


Figure 19. Whole mount in situ hybridization on E8.5 and E9.5 wt and COET;*Mesp1*^{Cre/+} mutant embryos with a digoxigenin-labeled *Gata4* antisense probe. *Gata4* is down-regulated in the SHF of COET;*Mesp1*^{Cre/+} mutants.

affected by Tbx1. Good candidates to this role, corresponding to the Gata4 one in the cardiac lineage, are basic helix-loop-helix (bHLH) proteins of MyoD family (235). These transcription factors are required for expression of skeletal muscle-specific genes (235-237), including *Mef2c* (235) and seem to be repressed by Tbx1 in our in vitro assays (data not shown).

3.13 *Mef2c* is negatively regulate by Tbx1 during *in vitro* C2C12 myoblast differentiation

C2C12 myoblasts can easily differentiate, *in vitro*, by switching of culture conditions from standard medium supplemented with 10% fetal bovine serum (FBS) to medium supplemented with 2% horse serum (238). Typically cells form myotubes 3-5 days after culturing in differentiation media; however we observed an increased expression of myogenic markers like *MyoD* and *myogenin* (data not shown) already at day 2 of differentiation.

By qRT-PCR, we also found, as expected, that *Mef2c* expression increases during in vitro C2C12 myoblast differentiation (Figure 20A) and interestingly his process is inhibited by Tbx1 (Figure 20B). These

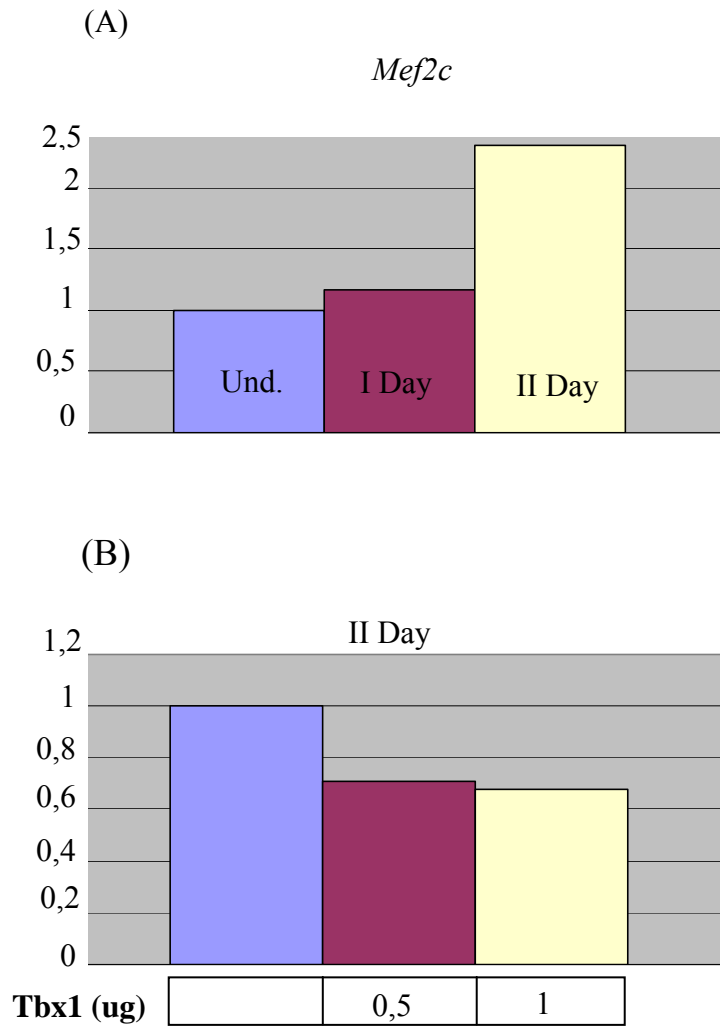


Figure 20. qRT-PCR on mRNA from differentiating C2C12 myoblasts. (A) *Mef2c* over-expression during C2C12 myoblast differentiation. (B) Tbx1 inhibits *Mef2c* over-expression during C212 myoblast differentiation.

data, together with the observation of a reduced *Mef2c* expression in somite compartment of *Tbx1*-gain-of-function mutants, suggest that *Tbx1* may also inhibit, *in vivo*, skeletal muscle cell differentiation through a mechanism involving *Mef2c* transcriptional repression.

CHAPTER 4

Discussion

22q11DS causes a wide range of congenital abnormalities, and in humans is predominantly associated with hemizigosity for approximately 3 Mb of DNA, encoding about 40 genes (1). Chromosome engineering, transgenic complementation, and gene targeting experiments revealed that haploinsufficiency of the T-box transcription factor *Tbx1* produces a partial phenocopy of the syndrome; *Tbx1*^{-/-} embryos have a more severe spectrum of defects, such as persistent truncus arteriosus, absence of the thymus and parathyroid glands, and craniofacial dysmorphism, all observed in 22q11DS patients (91-93). *Tbx1* acts as transcriptional regulator, and thus identification of its downstream targets, will be vital in elucidating the developmental pathways affected in 22q11DS. The identification of transcription factor targets represents a considerable challenge with several techniques having been developed, but no single methodology representing the one of choice. Here, we have described a microarray-based transcriptome analysis to evaluate gene expression changes *in vivo*, using a novel dosage gradient approach. Pharyngeal and heart development is very sensitive to *Tbx1* dosage, as we have shown by

generation of a panel of mutants expressing a nearly continuous variation of *Tbx1* mRNA level between 0 and 100% of the wild-type level (239).

Microarray analysis at E9.5, identified 256 genes differentially expressed across the allelic series (120 down-regulated and 136 up-regulated); of these, 52 changed in a manner that was highly correlated (or anti-correlated) to *Tbx1* expression. It is likely that genes highly sensitive to perturbations in *Tbx1* level are linked to fundamental disease-associated processes, whereas those that are only moderately affected by *Tbx1* haploinsufficiency perhaps have roles in modulating the severity of the 22q11DS-associated defects. Modifier genes might therefore be involved in modulating *Tbx1* expression from the remaining wild-type allele in response to haploinsufficiency or may act as genetic amplifiers to enhance expression of specific *Tbx1* targets.

Fgf8 and *Fgf10* expression is downregulated in *Tbx1*^{-/-} mice (103, 120); but neither gene was expressed above threshold levels in our experiments.

We also noted some inconsistencies between our microarray data and a few previous reports about expression changes of *Tbx1*-regulated genes (234); many of these are down- or up-regulated in a tissue-specific manner, while our microarray analysis was performed on mRNA from total embryos. A possible explanation of why our analysis failed to detect

expression changes of previously reported genes is that *Tbx1* target genes may also be expressed in non *Tbx1*-expressing tissues at E9.5; so the differential regulation of such targets will be diluted using the methods employed here, despite for example dissection of the pharyngeal apparatus containing regions.

We have confirmed the microarray data on a subset of selected genes using quantitative real-time PCR of mRNA from mutant embryos and also from *in vitro* gain of function models; in addition bioinformatic analysis of the 10 kb immediately upstream and intronic regions revealed, in all the confirmed genes, potential conserved Tbx1 binding sites.

4.1 *Pex2* and *Vps33a*: cytoplasmic organelle biogenesis and brain abnormalities

Behavioral and psychiatric disorders are a prominent part of the 22q11DS phenotype. In children, these disorders include cognitive defects, anxiety, attention deficit disorder, and problems of social interaction that are increasingly recognized to meet the criteria of autistic spectrum disorder (240, 241), a neurodevelopmental disorder. In adults, high rates of psychotic disorders, especially schizophrenia, have been reported (241-244).

Df1/+ mice which recapitulate many of the cardiovascular defects associated with 22q11DS (88), also display abnormal behavior, including impaired sensorimotor gating, as measured by prepulse inhibition (PPI) of the startle response (90), a behavioral abnormality that is associated with several psychiatric and behavioral disorders including schizophrenia and schizotypal personality (245), 22q11DS (246), and Asperger syndrome (247). We previously demonstrated that PPI deficits in *Df1/-* mice are caused by haploinsufficiency of two genes, *Tbx1* and *Gnb1l* (248): mutation of either gene is sufficient to cause reduced PPI. In addition, we reported that psychiatric disorders, in particular Asperger syndrome, can occur in association with inactivating mutations of *TBX1*, rather than with a 22q11 chromosomal deletion, consistent with our mouse studies (248). *Tbx1* and *Gnb1l* are apparently unrelated and have distinct expression patterns in brain, suggesting that they are unlikely to function in the same genetic pathway. Future studies into the functions of these two genes in brain should clarify the genetic pathways affected by their mutation and, potentially, may lead to the identification of drug targets aimed at prevention and or treatment of the psychiatric symptoms in 22q11DS patients.

Tbx1 expression is very low in preterm embryonic brain, whereas levels increase steadily from birth to 3 months; in addition it seems to be limited to the vasculature in term embryos and in adult mice (248).

Interestingly, among the confirmed genes, there are two genes involved in cytoplasmic organelle biogenesis and whose mutations are associated with defects in the developing and postnatal brain: *Pex2* (154) and *Vps33a* (169, 170).

In particular, peroxisome biogenesis disorders, of which Zellweger syndrome is the most severe, result in severe neurological dysfunction associated with abnormal CNS neuronal migrations due to the lack of functional peroxisomes (159, 249, 250). The *Pex2*^{-/-} mouse model for Zellweger syndrome has enabled researchers to evaluate the role of peroxisomes in the development and functioning of the nervous system. These studies have shown that, in addition to disturbances in neuronal migration in developing cerebral cortex and cerebellum, defects in neuronal differentiation, proliferation and survival may also contribute to the CNS malformations (160, 251).

The peroxisome is a ubiquitous cellular organelle that participates in a wide variety of metabolic reactions. In Zellweger syndrome, infants have neonatal hypotonia and seizures associated with CNS neuronal migration

defects. In the postnatal period, severe hepatic dysfunction ensues, with development of fatty liver, cholestasis and cirrhosis. CNS degeneration continues, with abnormalities in myelination and astrocyte proliferation. The majority of peroxisomal reactions involve lipids, including β -oxidation and α -oxidation of fatty acids, and synthesis of bile acids, ether phospholipids, docosahexaenoic acid and isoprene compounds. In the CNS, peroxisomes are generally more abundant in differentiating neurons than in mature neurons and are seen at sites such as axon terminals and dendrites, where they are rare in the mature nervous system (159, 249, 250). These findings suggest that peroxisomes are important for neuronal cellular enlargement and formation of processes. However, the effect on the developing nervous system of the various peroxisomal lipid deficiencies as well as potential toxic accumulations (very long-chain fatty acids, bile acid, intermediates) has not been established.

Vps33a, is a member of the Sec1 and Class C multi-protein complex that regulates vesicle trafficking to specialized lysosome-related organelles. Mutations in Vps33a cause Hermansky–Pudlak Syndrome (HPS)-like-symptoms in the *bf* mouse mutant (171). As Sec1 signaling pathways have been implicated in pre-synaptic function, Chintala and colleagues (252) examined in detail brain size, cerebellar cell number and the

behavioral phenotype of *bf* mutants. Young *bf* mice exhibited significant impairments in several behavioral tests and this defect was augmented in older mice confirming a progressive impairment of motor functions with age. In addition, general examination of brain sections, did not reveal any size difference in the cerebellum of young *bf* mice when compared to their age-matched heterozygous controls; in contrast old *bf* mice, revealed a strong reduction of cerebellar size mostly attributable to progressive loss of Purkinje cells (252).

Our data suggest a putative positive regulation of *Pex2* and a putative negative regulation of *Vps33a* by *Tbx1*; even if these genes belong to the *Tbx1* dosage-highly correlated group, further analysis is required to establish if they are direct transcriptional targets of *Tbx1* or if *Tbx1* modulates expression of *Pex2* and/or *Vps33a* transcriptional regulators. Mutations in both *Pex2* and *Vps33a* are associated mainly with postnatal brain defects and, interestingly, *Tbx1* expression in brain increases postnatally (248, 253); so it could be interesting to evaluate if *Tbx1* mutants exhibit defects in organelle biogenesis, a study that has not been performed so far, and if these defects could cause CNS abnormalities that account for some of 22q11DS neurobehavioral phenotypes.

4.2 *Morf4l1* and *TgfrbIII*: positive regulation of cell proliferation

Our microarray results also revealed differential expression of two genes involved in regulation of cell proliferation: *Morf4l1* (180) and *TgfrbIII* (181). As expected, by qRT-PCR we found a *Morf4l1* (also known as *Mrg15*) downregulation in *Tbx1* null mutant embryos while its expression was increased in *Tbx1*-overexpressing cells, suggesting a putative positive regulation of *Tbx1* on transcription of this gene. Deletion of *Mrg15* in mice results in death between E14.5 and birth (178); null embryos exhibit defects in multiple organs, including heart and are approximately 74% the size of their wild-type littermates with most of their tissues proportionately smaller, suggesting a role of *Mrg15* in sustainment of cellular proliferation (178). In particular *Mrg15*^{-/-} MEFs show a significantly increased expression of cell cycle inhibitor p21 (180). By qRT-PCR we found a *p21* upregulation in *Tbx1* null embryos at E9.5 (data not shown) suggesting a putative model in which *Tbx1* can exert its well demonstrated pro-proliferative role through a mechanism involving p21 (and may be other cell cycle negative regulators) repression: demonstration of *p21* overexpression in other tissues than skin of *Mrg15*^{-/-} would suggest a role for *Morf4l1* as intermediate in this process.

On the other hand, by qRT-PCR on mRNA from Tbx1-overexpressing cells, we confirmed the microarray-based data of a putative negative regulation of *TgfrbIII* by Tbx1. Binding of transforming growth factors beta (TGFb) to their receptors (TbRs) in vivo, is involved in signal transduction of many cellular responses including proliferation, differentiation, migration and apoptosis (182-186). TbRIII is the most abundant TGFb receptor and is traditionally thought to function as a co-receptor, binding TGFb and presenting it to TbRII (196). However it has been demonstrated that TbRIII has an additional role, since it contributes to and enhances TGFb-mediated cellular proliferation inhibition through both TbRI/Smad3-dependent and p38 mitogen activated protein kinase pathways (200), suggesting that Tbx1 can stimulate cell proliferation through a mechanism involving *TgfrbIII* repression.

While it is possible that these two genes represent direct transcriptional targets of Tbx1, additional approaches will be required to address this question; anyway negative regulation of *TgfrbIII* by Tbx1 together with its positive role on *Morf4II*, strongly support our previous data indicating a positive effect of Tbx1 on cellular proliferation in several tissues.

4.3 *Mef2c*: negative regulation of cardiac and skeletal muscle cell differentiation

Our microarray-based transcriptome analysis, also revealed differential *Mef2c* expression across the *Tbx1* allelic series; interestingly this gene was anti-correlated to *Tbx1* dosage. We were able to confirm that result by using loss- and gain-of function models, both *in vivo* and *in vitro*.

Particularly, qRT-PCR on mRNA from E9.5 embryos showed a *Mef2c* over-expression in *Tbx1*^{-/-} mutants compared to their wt littermates; by in situ hybridization at the same stage, we were able to appreciate a SHF-specific up-regulation of *Mef2c* in *Tbx1* null mutant embryos. We also observed a *Tbx1*-dosage dependent *Mef2c* expression in two independent in vitro gain-of-function models: a Tc-inducible *Tbx1*-overexpressing mouse ES cell line and a *Tbx1* expression vector-transfected myoblast cell line (C2C12); in *Tbx1*-overexpressing C2C12 cells, we also observed a diminished *Mef2c* protein level. Finally whole mount in situ hybridization at E9.5, on COET;*Mesp1*^{Cre/+} mutants which over-express *Tbx1* in all its mesodermal domains of the pharynx, head mesenchyme and splanchnic mesoderm, revealed a strong *Mef2c* down-regulation in somite compartment (in addition to the SHF) compared to control embryos.

Taken together these results strongly supported the hypothesis that *Tbx1* could regulate *Mef2c* expression in vivo, in both cardiac and skeletal muscle cells. But what about the regulatory mechanism?

Mef2 genes are expressed in cardiac, smooth, and skeletal muscles, vasculature, as well as in a restricted set of other tissues (206, 210, 211). In particular, targeted inactivation of the *Mef2c* gene in mice, resulted in profound cardiac and vascular defects and embryonic lethality at E9.5 (214, 254, 255). In *Mef2c* knockout mice, endothelial cells were initially present but failed to organize correctly, suggesting an endothelial cell differentiation defect.

Mef2c is among the earliest markers of the cardiac lineage with transcripts evident in the developing heart beginning at about E7.5, shortly after the expression of the *Nkx2.5* and *Gata* genes (210, 216-218, 220-222); of the four vertebrate *Mef2* genes, it is the earliest to be expressed in skeletal muscle too. However despite the early expression of *Mef2c* in cardiac and skeletal muscle lineages, its activity (and activity of other *Mef2* genes) is not required for myoblast specification; instead, it appears to play a key role in differentiation. This notion is strongly supported by work in *Drosophila*, in which inactivation of the single *Mef2* gene, results in a complete loss of muscle differentiation in all three

muscle lineages, with no apparent defect in myoblast specification (256-258).

A common theme that has emerged through the analysis of muscle gene transcription is the modularity of *cis*-regulatory elements, in which multiple independent regulatory regions, are required to generate the complete spatio-temporal expression pattern of a gene through development (259). Accordingly, the proposed model for *Mef2c* gene regulation, is based on the independent regulation of multiple, tissue-specific, enhancers. In particular De Val et al. identified a transcriptional enhancer from the mouse *Mef2c* gene sufficient to direct its expression to the vascular endothelium in transgenic embryos. This enhancer is active in endothelial cells within the developing vascular system from very early stages in vasculogenesis, and remains robustly active in the vascular endothelium during embryogenesis and in adulthood. This *Mef2c* endothelial cell enhancer contains four perfect consensus sites for Ets family of winged helix transcription factors; these sites are efficiently bound by Ets-1 protein *in vitro* and are required for enhancer function in transgenic embryos (223). They also identified additional, separate, modular enhancers from *Mef2c* that independently direct its expression to smooth muscle and to neural crest (unpublished observations).

Skeletal muscle development is controlled by the MyoD family of myogenic bHLH proteins and MEF2 family of transcription factors, which interact to establish a unique transcriptional code for activation of skeletal muscle-specific genes (260, 261). Members of the MyoD family (MyoD, myogenin, Myf5 and MRF4) are expressed exclusively in the skeletal muscle lineage and can each activate the complete muscle differentiation program in transfected fibroblasts (262-265).

Dodou et al. (235) have isolated an enhancer region from the mouse *Mef2c* gene that is sufficient to direct its expression to skeletal muscle during murine development; furthermore, they have defined *cis*-acting sequences within the skeletal muscle enhancer of *Mef2c* that are essential for its expression *in vivo*. Among these *cis*-acting elements is an E box that is bound by myogenic bHLH proteins with extremely high affinity and is absolutely required for expression *in vivo*. The data they presented support a direct link between myogenic specification and differentiation, by demonstrating that myogenic bHLH proteins directly activate the expression of *Mef2c* in skeletal muscle *in vivo*.

Additionally, as mentioned before, Dodou et al. (2) also identified a *Mef2c* SHF-specific enhancer carrying evolutionarily conserved binding sites for Gata4 and Isl1 transcription factors; these sites are completely

required for enhancer function *in vivo*. Finally von Both et al. (266) demonstrated that *Mef2c* expression in the SHF is also dependent on forkhead transcription factor Foxh1 and identified a Foxh1-Nkx2.5 binding site within the *Mef2c* gene, that is regulated by TGFb signalling in a Smad-dependent manner.

The evolution of multiple independent enhancers provides a potential mechanism for regulatory diversity by allowing gene expression to be controlled in a very fine-tuned manner in each lineage where *Mef2c* is expressed. Another emerging theme is dependence of these tissue-specific enhancer, for their functionality, on the combined activities of different transcription factor families.

Accordingly, our results suggest that *Mef2c* could be regulated by Tbx1 through different mechanisms between the cardiac and skeletal muscle lineages. In particular, our *in vitro* data, support the hypothesis of a *Mef2c* negative regulation by Tbx1 that is Gata4-dependent. We observed, in fact that Tbx1 was able to repress the SHF-enhancer described by Dodou et al. (2), only in the presence of Gata4; this repression does not require a Tbx1 direct binding to the conserved TBE we identified in the same enhancer.

In addition, we observed, by qRT-PCR on mRNA from transfected C2C12 myoblasts, that when the 80% of endogenous *Gata4* is knocked-down by RNA interference, *Tbx1* over-expression does not still affect endogenous *Mef2c* gene expression, so confirming our hypothesis.

However, we and other observed that *Gata4* is negatively regulated, *in vivo*, by *Tbx1*; in particular Liao et al. (234) described a *Gata4* ectopic expression in the SHF of *Tbx1*^{-/-} embryos at E9.0-E9.5. At the same stages, we observed a marked *Gata4* downregulation in COET;*Mespl*^{Cre/+} gain-of-function mutant hearts compared to control embryos, suggesting that at least partially, *Mef2c* down-regulation reflects *Gata4* repression by *Tbx1*.

Gata4, however, is not expressed in skeletal muscle, opening the question of how *Mef2c* is regulated by *Tbx1* in that tissue.

Even if, we did not identify any putative *Tbx1* binding site in the skeletal muscle-specific enhancer described by Dodou et al. (235), we cannot exclude the existence of other regulatory regions that specifically drive *Mef2c* expression in skeletal muscle cells and that are directly bound by *Tbx1* *in vivo*. In addition, we can also hypothesize a regulatory mechanism similar to that evoked for cardiac lineage, requiring involvement of an intermediate transcription factor.

Our unpublished data, show a *MyoD* and *myogenin* down-regulation in Tbx1 over-expressing C2C12 myoblasts, suggesting that these bHLH proteins could have, in skeletal muscle cells, a role similar to that hypothesized for Gata4, in cardiac lineage.

Whatever the regulatory mechanism can be, what is the functional meaning of *Mef2c* repression by Tbx1?

We have recently shown that *Tbx1* is expressed in cardiac progenitor cells (CPCs) that, in clonal assays, can give rise to the three heart lineages expressing endothelial, smooth muscle and cardiomyocyte markers (147). In these multipotent cells, Tbx1 stimulates proliferation, explaining why *Tbx1*^{-/-} embryos have reduced proliferation in the SHF. In this population, Tbx1 is expressed while cells are undifferentiated and it disappears with the onset of muscle markers; loss of *Tbx1* is associated with premature differentiation, while its ectopic expression in the OFT results in suppression of differentiation. Because Tbx1 can regulate *Fgf8* expression in the mesodermal region that includes the SHF (97, 103, 120, 143, 267), some of its mitogenic activity could be mediated by the FGF signaling. On the other hand, Tbx1 seems to inhibit differentiation by regulating, directly or indirectly, proteasome-mediated degradation of the

myogenic transcription factor Srf which, in turn, activates the muscle transcription program.

So Tbx1 could exert its, *in vivo*, anti-differentiative role in the SHF population of heart progenitors, also repressing *Mef2c* expression.

And even if we observed a *Gata4* negative regulation by Tbx1, that can account for some of *in vivo* *Mef2c* down-regulation, our data suggest that the mechanism by which Tbx1 regulates *Mef2c* somehow affects Gata4 protein activity. So it is possible that regulation of proteasome-mediated degradation observed for Srf, is a general mechanism; co-immunoprecipitation experiments will tell us if Tbx1 can bind, *in vivo*, Gata4 protein and reduce its stability.

As said above, we also found a *Mef2c*-downregulation in somite compartment of *Tbx1*-gain-of function mutant embryos and our *in vitro* experiments showed that *Mef2c* over-expression during C2C12 myoblast differentiation is inhibited by Tbx1, suggesting that Tbx1 can negatively regulates *Mef2c* expression in skeletal muscle cells too. Additional experiments will clarify if Tbx1 directly binds skeletal muscle-specific regulatory regions of *Mef2c* locus, or, also in this case, Tbx1 interferes with the activity of *Mef2c* direct regulators, for example the myogenic proteins of MyoD family.

Finally our data beg the question of whether the function of *Tbx1* in regulating the balance between proliferation and differentiation, may also apply to other tissues where *Tbx1* is expressed. Indeed, *Tbx1* loss of function in mice, and, to a lesser extent, *TBX1* haploinsufficiency in DiGeorge syndrome patients, is associated with hypoplasia or aplasia of several organs and tissues. Thus, it is tempting to speculate that dysregulation of the balance between proliferation and differentiation of different types of progenitor cells or stem cells may be a basic pathogenic mechanism for the loss of function phenotype.

CHAPTER 5

Appendix

5.1 Towards a human model of DiGeorge Syndrome (DGS)

Syndromes associated with segmental aneuploidies are caused by gene dosage imbalance. There may be one or more critical genes within the aneuploid segment, that encode different classes of proteins, but the common characteristic is that the processes in which they are involved (developmental or otherwise) are sensitive to their concentration. In most if not all cases, the mechanisms underlying dosage sensitivity are unknown. A complicating issue is that mouse modelling of these syndromes, while technically feasible in many cases, is hindered by different sensitivity to dosage of a particular gene product across species. This problem translates into the finding that similar gene dosage reduction in mice and humans (e.g. heterozygous deletion), leads to different phenotypes in the two species. Heterozygous multigene deletion of region corresponding to 22q11 in the mouse as well as *Tbx1*^{+/-} animals, presented with a less severe phenotype than the majority of 22q11.2DS patients or *TBX1* mutant patients, with the caveat that mild patients may escape clinical diagnosis. Most intriguingly, the great phenotypic variability observed in human patients could not be modelled

in mice, although different phenotypic penetrance, but not expressivity, has been reported as a function of strain or genotype at interacting loci (89, 91, 103, 268, 269).

So, murine models of congenital and acquired disease are invaluable yet often do not faithfully mirror human pathophysiology; for cases where murine and human physiology differ, however, human Embryonic Stem cell (hESc) culture represents an essential complement to research with animal models.

ES cells, derived from the inner cell mass of mammalian blastocysts, have the ability to grow indefinitely while maintaining pluripotency (270, 271), and allow investigators to explore early stages of human embryonic development through *in vitro* differentiation, which recapitulates aspects of normal gastrulation and tissue formation. So *in vitro* differentiating genetically modified ES cells, are particularly attractive for the study of congenital disorders, offering the unprecedented opportunity to study in detail disease initiation and progression during development, moreover enabling generation of customized cellular therapies by *in vitro* gene correction in autologous cells. Use of human embryos, however, faces ethical controversies that hinder the applications of human ES cells; in addition it is difficult to generate patient-or-disease specific ES cells,

which are required for their effective application. One strategy for producing autologous, patient-derived pluripotent stem cells is somatic nuclear transfer (NT); in a proof of principle experiment, NT-ES cells generated from mice with genetic immunodeficiency were used to combine gene and cell therapy to repair the genetic defect (272). To date, NT has not proven successful in the human, and given the paucity of human oocytes, is destined to have limited utility; in contrast, introducing a set of transcription factors linked to pluripotency can directly reprogram human somatic cells to produce induced pluripotent stem (iPS) cells, a method that has been achieved by several groups worldwide (273-276).

Reprogramming somatic cells taken from patients with specific diseases, can truly turn back time in patient's history, allowing the unique opportunity to study disease development in the specific context of each individual. Since successful generation of disease-specific pluripotent stem cell lines by reprogramming of patient skin or blood samples (277-283), has been recently reported, we tried to reprogram adult fibroblasts from a DiGeorge syndrome patient, by transduction of a set of five genes encoding the transcription factors OCT4, SOX2, C-MYC, KLF4 and NANOG, as described by Lowry et al. (274). To date we obtained a promising clone, that we are still characterizing; however, our

preliminary results, open the possibility to obtain DGS-specific pluripotent stem cells as the starting materials for generating an *in vitro* model of the human disease, improving our understanding of its initiation and progression during development as well as our knowledge of *Tbx1* role in its pathogenesis.

5.2 Materials and Methods

5.2.1 Cell culture

Retroviral pMX vectors encoding *OCT4*, *SOX2*, *C-MYC*, *NANOG*, *KLF4*, and GFP (Addgene) were transfected into Phoenix Ampho Cells (Orbigen) by using Fugene (Roche). Viral supernatants were harvested 3 days later, combined, and used to infect DiGeorge syndrome fibroblasts (GM07215, Coriell Institute) in DMEM with 10% FBS (Foundation), nonessential amino acids, L-glutamine, and penicillin–streptomycin (Invitrogen). A second round of infection was performed at day 3, and the transfection efficiency of each virus as extrapolated from that of GFP in the viral mix was 15–20%, suggesting that nearly 100% of cells received at least one virus. Four days later, cells were passaged onto irradiated murine embryonic fibroblasts (MEFs). Reprogrammed cells and hES cells (H9) were cultured on irradiated MEFs as described (284, 285) in DMEM F12 supplemented with L-glutamine, nonessential amino acids,

penicillin–streptomycin, knockout serum replacement (Invitrogen), and 4 ng/ml basic FGF. For early passages, iPS cells were propagated manually, whereas subsequent passaging was performed with collagenase treatment as described (284, 285).

5.2.2 Genomic DNA analysis

Genomic DNA was isolated by using the DNeasy kit (Qiagen) and analyzed for retroviral integration events by PCR with specific primers (273).

5.2.3 Expression analysis

Total RNA was isolated by using the RNeasy Mini Kit (QIAGEN) and reverse-transcribed with the ImProm-II Reverse Transcription System (Promega) with oligo dT primers. cDNAs was analyzed by PCR with specific primers (273).

5.2.4 Alkaline Phosphatase Staining, Immunofluorescence and DAPI staining

Alkaline phosphatase staining was performed using the Alkaline Phosphatase Substrate Kit III (Vector Laboratories) according to the manufacturer's instructions.

For immunofluorescence, cells were fixed with PBS containing 2% paraformaldehyde (EMS) for 1 hour at room temperature. After washing

with PBS, the cells were treated with PBS containing 2% FBS (Foundation), 0,1% sodium azide (Sigma-Aldrich), for 30 minutes at room temperature. For OCT3/4 staining cells were permeabilized with cold 90% methanol (Sigma Aldrich) for 30 minutes at 4°C. Primary antibodies included: monoclonal Oct-4 (Santa Cruz Biotechnology, 1:200), monoclonal SSEA-4 (Santa Cruz Biotechnology, 1:200), IgG_{2b} (Santa Cruz Biotechnology, 1:200) and IgG₃ (Santa Cruz Biotechnology, 1:200). Primary antibodies were diluted in PBS containing 2% FBS (Foundation), 0,1% sodium azide (Sigma-Aldrich) and 0,1% Triton-100 (Sigma Aldrich). Secondary antibodies used were: goat anti-mouse IgG-FITC (Santa Cruz Biotechnology, 1:1000) and Alexa Fluor 488 goat anti-mouse IgG (Invitrogen, 1:1000). Secondary antibodies were diluted in PBS containing 2% FBS (Foundation), 0,5% sodium azide (Sigma-Aldrich) and 0,1% Triton-100 (Sigma Aldrich).

For DAPI (4'-6-Diamidino-2-phenylindole) staining, OCT3/4 and SSEA-4 labeled cells, were washed with PBS containing 2% FBS (Foundation), 0,1% sodium azide (Sigma-Aldrich) and 0,1% Triton-100 (Sigma Aldrich) and treated with PBS containing 1ug/ml DAPI (Invitrogen) for 1 minute at room temperature.

5.2.5 Fluorescence-activated cell sorting analysis

For Fluorescence-activated cell sorting (FACS) analysis, 2.5×10^6 cells were resuspended in 0.5 ml of PBS containing 2% FBS (Foundation) and 0,1% sodium azide (Sigma-Aldrich) and divided into five 0.1 ml aliquots (aliquot 1: negative control, aliquot 2: CD-29 labeling to exclude the MEF feeder cell population, aliquot 3: OCT3/4 labeling, aliquot 4 SSEA-4 labeling, aliquot 5: OCT3/4 and SSEA-4 double labeling). Aliquot 1 was labeled with IgG1 antibody (Alexa 488, AbD Serotec); aliquot 2 was labeled with CD-29 antibody (Alexa 488, AbD Serotec); aliquot 3 was labeled with SSEA-4 (R&D Systems) and IgG1 antibodies; aliquot 5 was labelled with CD-29 and SSEA-4 antibodies (0.01 ml of each antibody, for 30 minutes at 4°C.)

Cells were then fixed with PBS containing 2% paraformaldehyde (EMS) for 30 minutes at room temperature and permeabilized with PBS containing 0,1% Bovine Serum Albumin (Sigma Aldrich) and 0,1% Saponine (Sigma Aldrich). After centrifugation, each aliquot was resuspended in about 0.05 ml of permeabilization buffer and 0.01 ml of the following antibodies were added: IgG1 (PE, BD Biosciences for aliquots 1, 2 and 4), Oct-4 (PE, BD Biosciences for aliquots 3 and 5). Cells from each aliquot were also stained with PBS containing 1ug/ml

DAPI (Invitrogen), transferred to FACS tubes using cell strainers (BD Biosciences) and stored at least 1 hour at 4°C. FACS analysis was performed using a LSR II (BD Biosciences).

5.3 Results and discussion

5.3.1 Generation of human induced Pluripotent Stem (hiPS) cells from DGS fibroblasts

Human foreskin fibroblasts donated from a single newborn DGS patient (referred as DGSF), were reprogrammed to an ES-like state, by retroviral transduction of a set of five genes encoding the transcription factors NANOG, OCT3/4, SOX2, C-MYC and KLF4 as described by Lowry et al. (274).

After virus generation in Phoenix-A packaging cells using pMX vectors encoding the five factors, fibroblasts were infected twice over 3 days and replated four days later onto a feeder layer of irradiated murine embryonic fibroblasts (MEFs); a GFP-expressing pMX virus was added to monitor infection efficiency. Control cells infected with empty pMX virus and the GFP-bearing virus in a 5:1 ratio did not change the morphology of the cells, which continued to grow as a monolayer. In contrast, in those fibroblasts cultures that were infected with viruses carrying the five defined factors and GFP, colonies formed about two

weeks after infection; these “early” colonies, however, didn’t show a hESc-like morphology, with characteristic refractive edges and three-dimensional growth. At three weeks after infection, a new colony emerged in the infected fibroblast cultures that adopted a tightly packed morphology, reminiscent of hESc colonies. Since, as described, it could have been reprogrammed to an ES-like state, this “late” appearing colony was picked from the original plate and expanded. Since the original clone (namely clone #18), after few passages, started to adopt a heterogeneous morphology, we derived from it three more subclones (namely #18.1, 18.6, 18.9). Colonies from these three subclones were cultured in hESc media (with knockout serum replacer and basic FGF) on irradiated MEFs and were propagated with standard protocols using collagenase (Amit et al. 2006 *Methods Mol Biol*; Akutsu et al. 2006 *Methods Enzymol*); since after several passages in culture, these colonies were still showing an hESc-like morphology (Figure 21) we decided subsequently, to analyze them in more detail to understand whether faithfully reprogramming to the ES-like state, had indeed occurred.

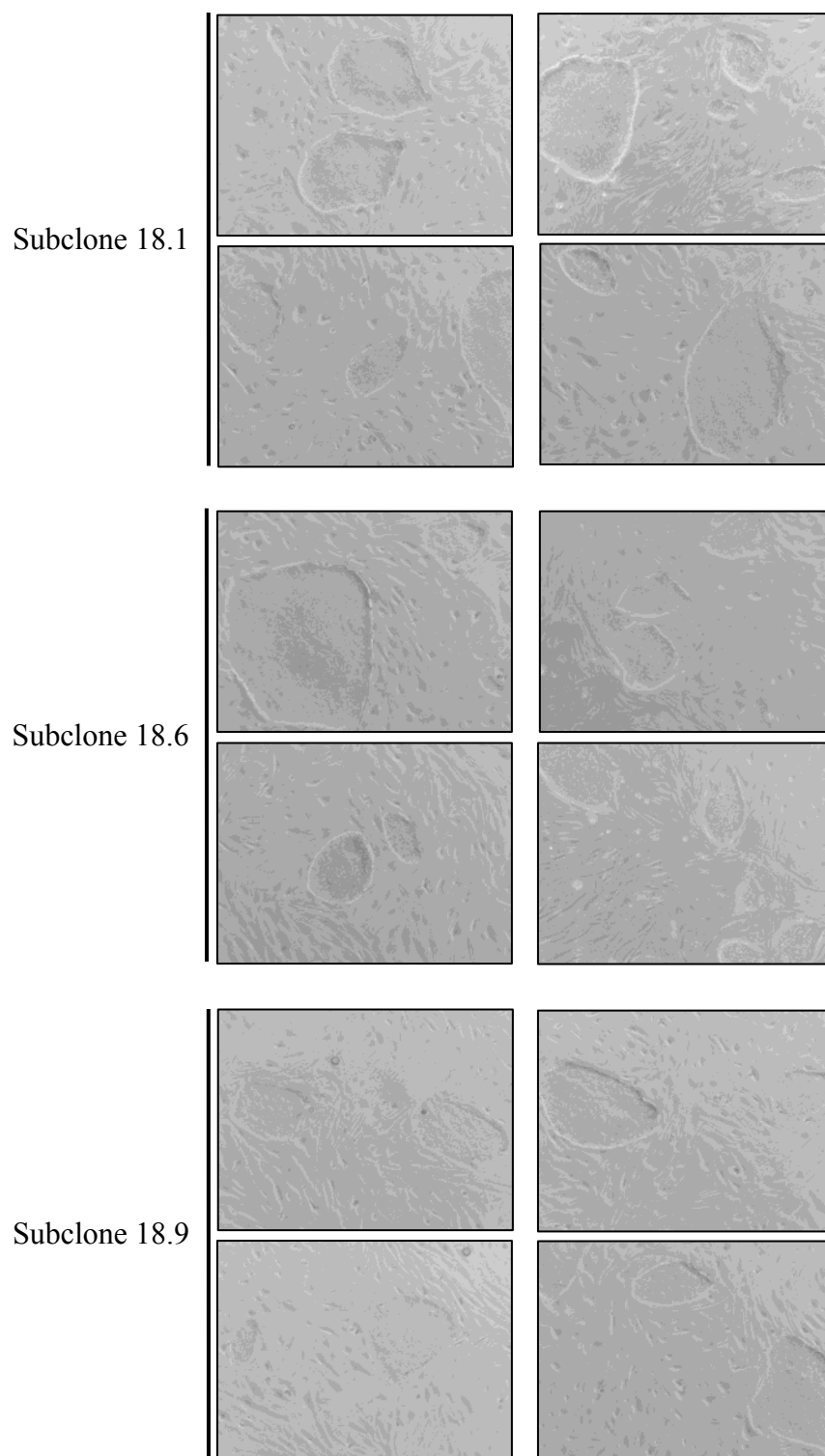


Figure 21. Morphology of colonies from subclones 18.1, 18.6 and 18.9.

5.3.2 Characterization of hiPS cells generated from DGS fibroblasts

5.3.2.I Alkaline Phosphatase staining

Alkaline Phosphatase (AP or TRA-2-49/6E) is a hydrolase responsible for dephosphorylating molecules such as nucleotides, proteins, and alkaloids, under alkaline conditions. It is a stem cell membrane marker and high levels of expression of this enzyme are typically associated with the undifferentiated state of pluripotent cells (286).

Colonies from our original clone and all tested subclones showed positive staining for alkaline phosphatase (Figure 22), suggesting that they could effectively be the result of efficient reprogramming of DGS fibroblasts to an ES-like status.

5.3.2.II Genotype analysis

PCR on genomic DNA revealed integration of all the five retroviruses used for DGS fibroblast reprogramming in all tested subclones (Figure 23).

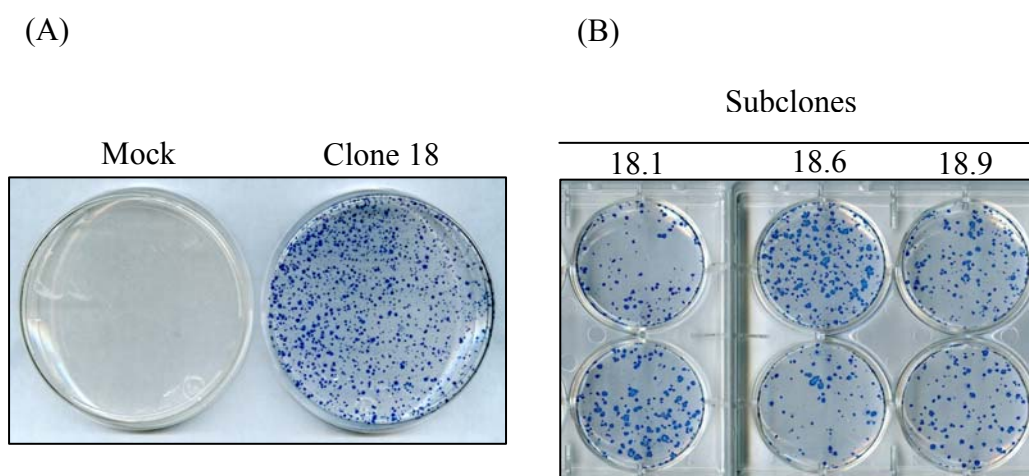


Figure 22. AP staining of (A) the original clone and (B) subclones 18.1, 18.6 and 18.9.

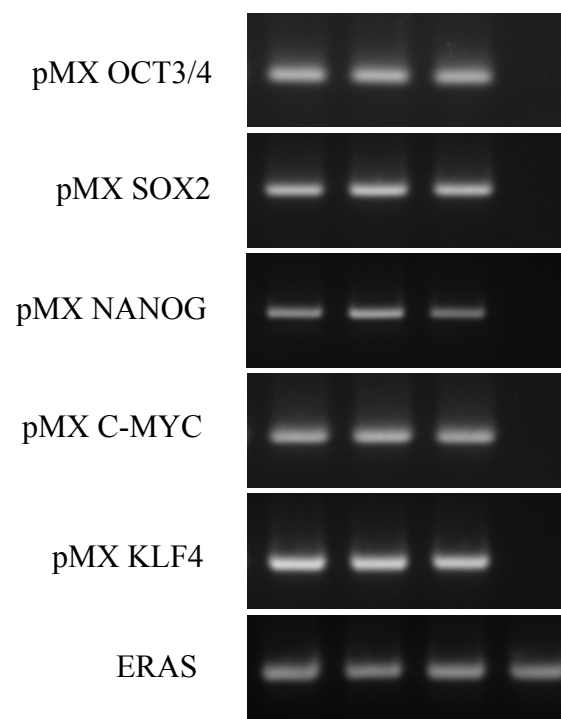


Figure 23. Genomic PCR revealing integration of all the five retroviruses in subclones 18.1, 18.6 and 18.9.

5.3.2.III ES cell marker expression analysis

RT-PCR showed that our original clone and all subclones express the endogenous counterparts of the defined factors using for reprogramming (endogenous *OCT3/4*, *SOX2*, *NANOG*, *C-MYC* and *KLF4*) as well as many un-differentiated ES cell-marker genes (286) such as *reduced expression 1 (REX1)*, *developmental pluripotency-associated 2 (DPPA2)*, *DPPA4*, *DPPA5* *growth and differentiation factor 3 (GDF3)*, *fibroblast growth factor4 (Fgf4)*, *msh homeobox 1 (MSX1)* and *telomerase reverse transcriptase (TERT)* at levels equivalent to those in the hES cell line H9 (Figure 24).

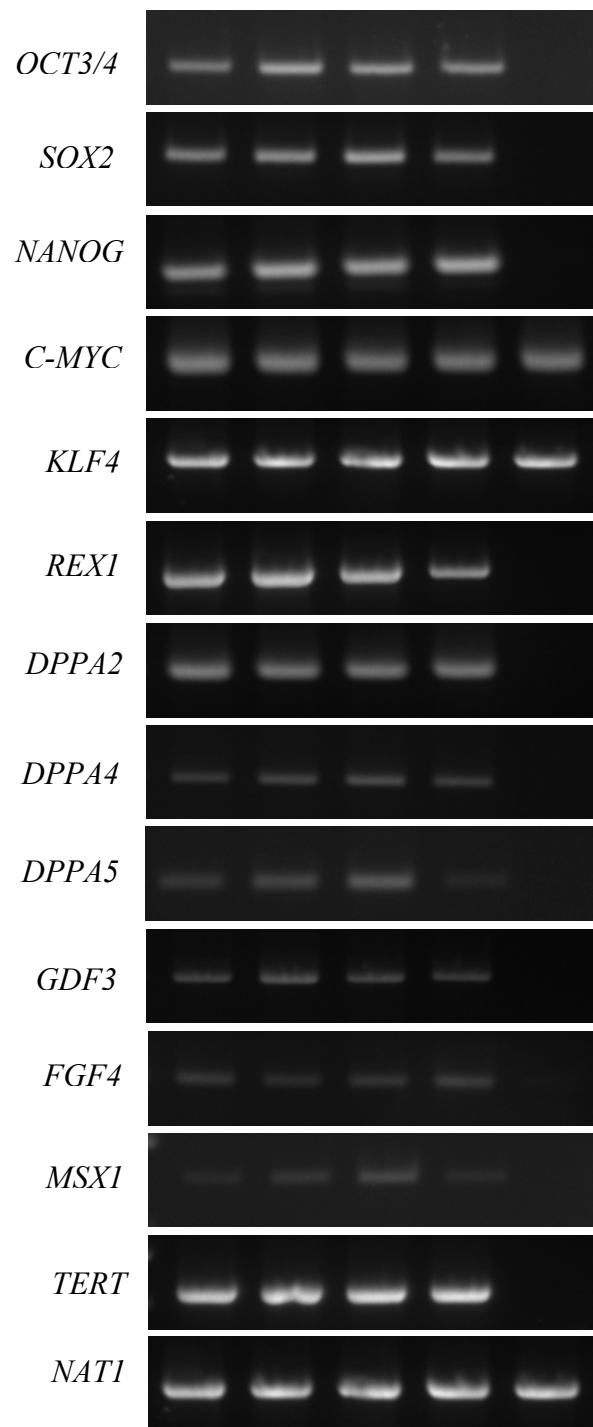


Figure 24. RT-PCR showing expression of endogenous *OCT3/4*, *SOX2*, *NANOG*, *C-MYC*, *KLF4* and several human embryonic stem cell marker genes.

5.3.2.IV OCT3/4 expression analysis

Since a critical level of Oct3/4 is required to maintain the pluripotency and self-renewal of ES cells (287, 288), we also tested our subclones for OCT3/4 protein expression, by immunofluorescence. As confirmed by DAPI staining, in each colony, all cell nuclei were strongly positive for OCT3/4 (Figure 25).

5.3.2.V SSEA-4 surface antigen expression analysis

Another approach to defining and characterizing stem cells, perhaps the most versatile, is that based upon the surface antigen phenotype of the cells (286). The extracellular markers that have been used to characterize hES cells are primarily carbohydrate epitopes on proteoglycans or sphingolipids, such as stage-specific embryonic antigen (SSEA)-3 and -4 (286, 289, 290).

Also several glycoproteins are specifically expressed by hES cells including Thy1, the major histocompatibility complex (MHC) class 1 antigens (HLA), a series of tumor related antigens, notably the keratin sulfate proteoglycans TRA-1-60, TRA-1-81, and GCTM2 (291, 292). As a starting point, we tested our subclones for SSEA-4 expression, by immunofluorescence, and found that all of them stained homogeneously positive for this surface antigen (Figure 26).

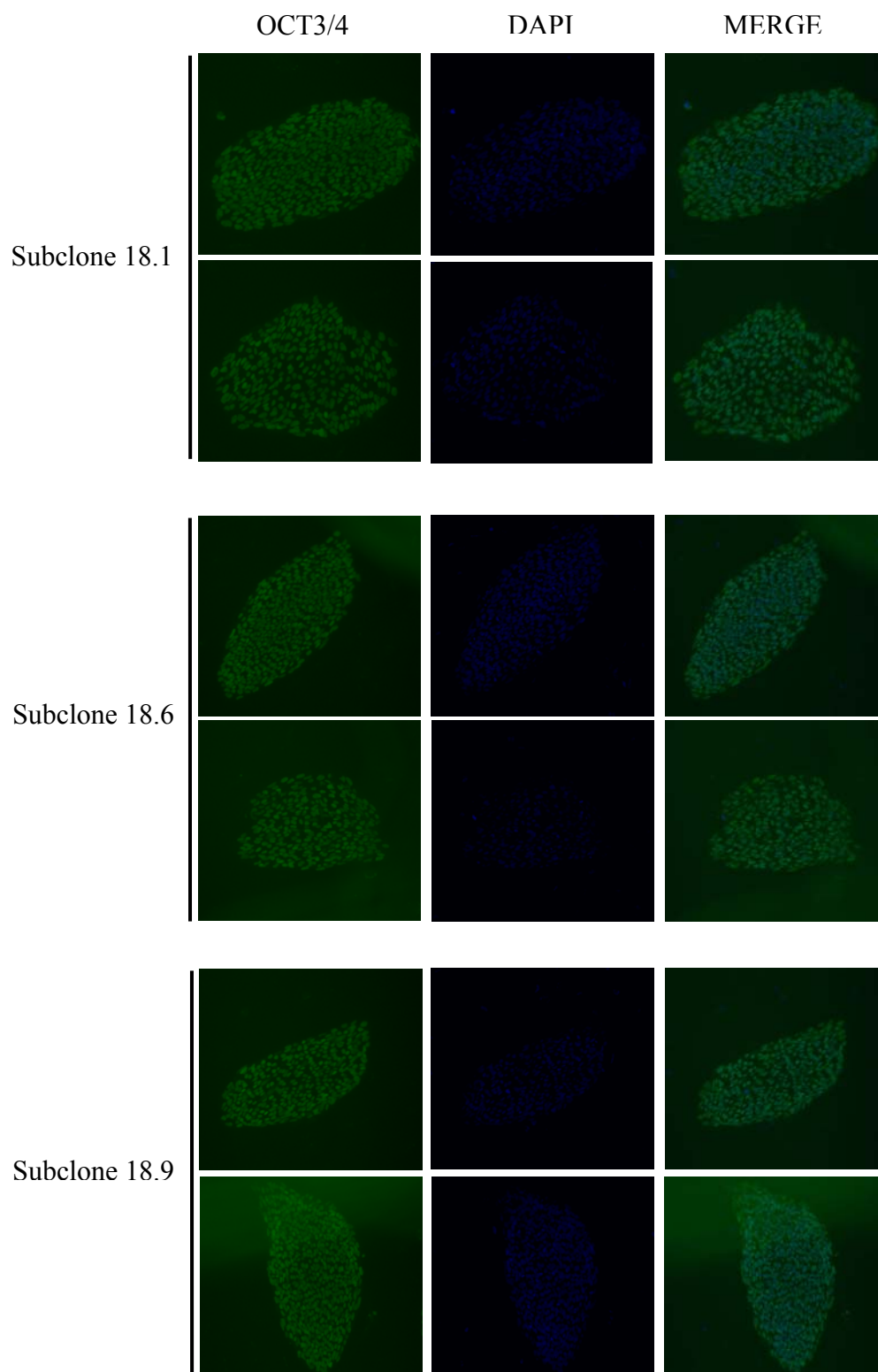


Figure 25. Immunofluorescence analysis revealing OCT3/4 expression in subclones 18.1, 18.6 and 18.9.

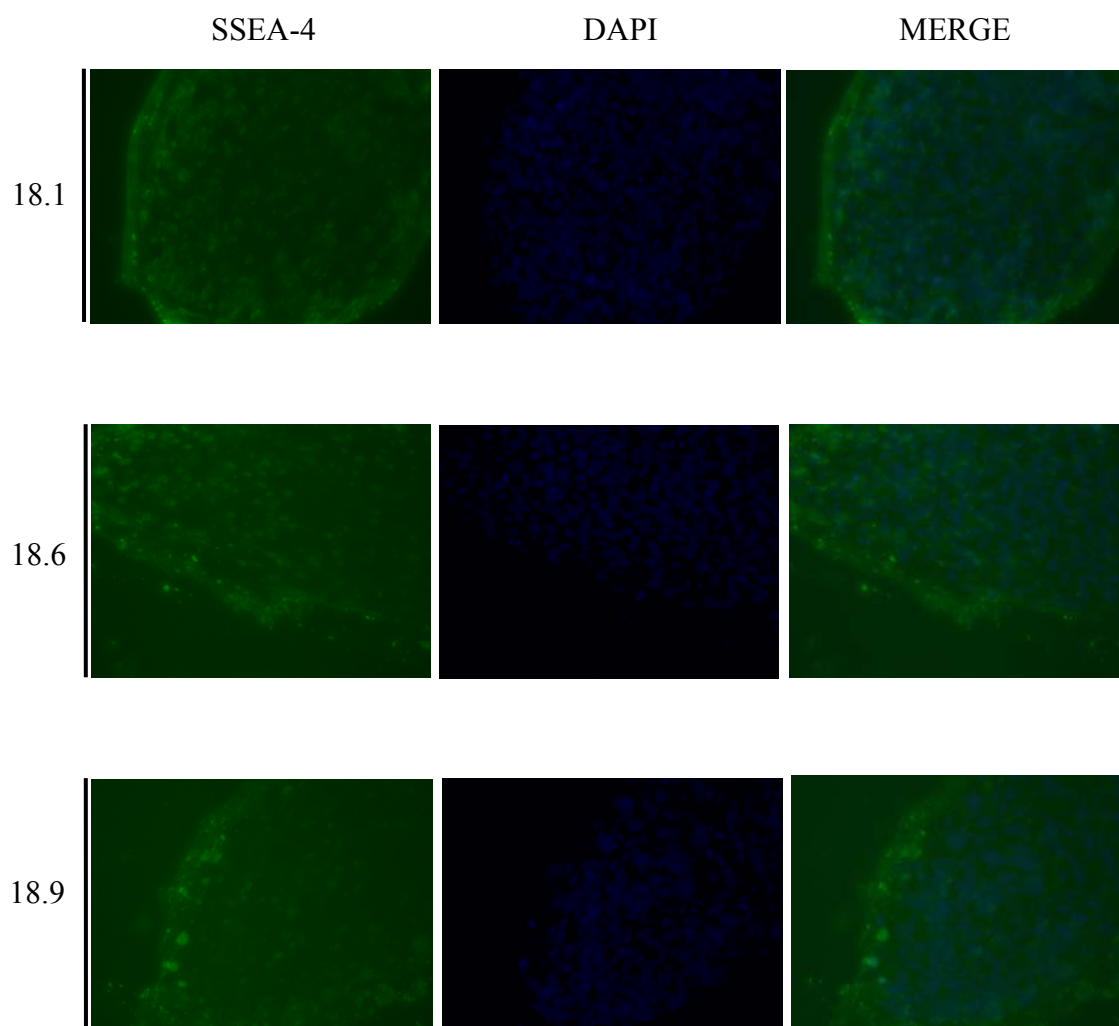


Figure 26. Immunofluorescence analysis revealing SSEA-4 expression in subclones 18.1.18.6 and 18.9.

5.3.2.VI Fluorescence-activated cell sorting analysis

To quantitatively evaluate OCT3/4 and SSEA-4 expression observed in our subclones, we also performed a fluorescence-activated cell sorting (FACS) analysis. In a homogeneous hES cell population, typically the 80% of cells express at the same time OCT3/4 and SSEA-4 (data not shown). We found a 82% of double positive cells in our subclone 18.1, a 93% in subclone 18.6 and a 97% in subclone 18.9 respectively (Figure 27).

To demonstrate the pluripotency of our subclones, we need to confirm their ability to both form teratomas in immunodeficient (SCID) mice and differentiate *in vitro* in multiple lineages.

To exclude the possibility that our hiPS cells are simply a contaminant from laboratory hES cell cultures, DNA fingerprinting will be used to accurately identify their origin. In addition karyotypic analysis will be required to show that gross chromosomal abnormalities were not generated as a result of reprogramming, so suggesting that large genomic rearrangements are not required for reprogramming to occur.

And even if multiple iPS cell lines made from a single patient should be genetically identical, it remains possible that these will display functional differences as a result of epigenetic drift between clones; so several

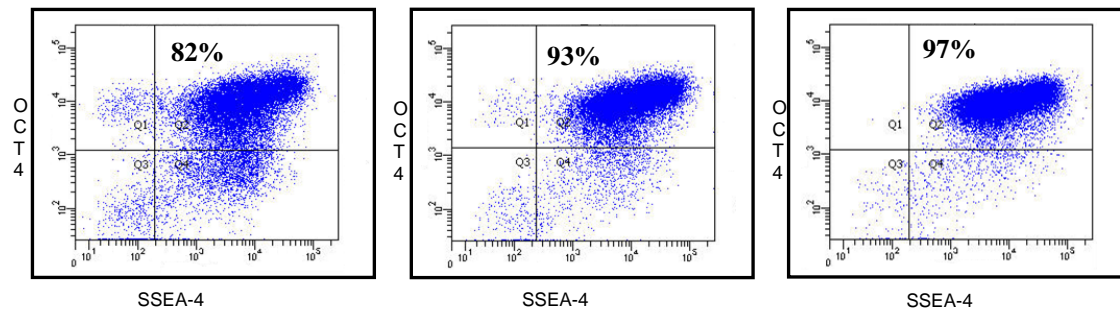


Figure 27. FACS analysis showing the percentage of OCT3/4-SSEA-4 double positive cells in subclones 18.1, 18.6 and 18.9.

clones should be studied from the same patient, requiring us to obtain additional iPS cell lines from the same patient fibroblast donor.

5.3.3 Human induced Pluripotent Stem cells and disease modeling

Many transgenic murine models of congenital and acquired diseases do not faithfully mirror the respective human pathophysiology; differences in tissue composition, anatomy, and physiology between animals and humans, all may underlie these observations. Another challenge in using murine disease models can arise from the differences in colinearity of the human and mouse genomes and the lack of conservation of gene order; so the same genetic abnormalities often do not produce identical phenotypical defects in the two species. Further, only a relatively small subset of age-regulated gene expression changes, is conserved from mouse to man. Lastly, the inbred genetic background of mice can also influence the phenotype resulting from the disease-associated mutations. Humans are of mixed genetic background, and this complexity results in phenotypical variations of genetically defined diseases. So although animal models continue to produce key insights into disease mechanisms, these systems have limitations that could be potentially overcome by human cellular models of disease.

For cases where murine and human physiology differ, so disease-specific pluripotent cells capable of differentiation into the various tissues affected in each condition, could undoubtedly provide new insights into disease pathophysiology by permitting analysis in a human system, under controlled conditions *in vitro*, using a large number of genetically-modifiable cells, and in a manner specific to the genetic lesions in each, whether known or not.

Our preliminary results open the possibility to generate induced pluripotent stem cells as starting material to develop a human model of DiGeorge syndrome.

The establishment of disease models through patient-specific reprogramming involves two steps: first, derivation of hiPS cells from somatic cells of a patient and second, differentiating the established hiPS clones into cell types affected by the patient's disease.

Successfully generation of disease-specific Pluripotent Stem cell lines by reprogramming of patient skin or blood samples (277-283) has been described; however, so far, only a handful of reports have observed a disease phenotype *in vitro* (279, 282, 293, 294).

During mouse cardiogenesis, the major lineages of the mature heart, cardiomyocytes, smooth muscle cells, and endothelial cells arise from a

common, multipotent cardiovascular progenitor expressing the transcription factors *Isl1* and *Nkx2.5* (295-297).

We have recently reported that *Tbx1* marks these multipotent cells, supports their proliferation and inhibits their differentiation (147). Interestingly, Moretti et al. have (298) recently shown that *Isl1*⁺ multipotent cardiovascular progenitors, can be generated from mouse iPS cells and spontaneously differentiate in all three cardiovascular progenitors *in vivo*.

They also reported the identification of human iPS-derived *ISL1*⁺ progenitors with similar developmental potential; it will be interesting to test if *TBX1* is expressed in cardiac progenitor cells also in humans.

Most disease phenotypes are only observed in lineage-committed or differentiated cells and not in the ES cells or iPS cells, so pertinent information on the pathogenesis of a disease may only be obtained from hiPS cells that have been differentiated *in vitro* to disease-relevant cell types. In addition, the specificity of a particular disease phenotype should be checked by direct or indirect correction of the genetic lesion.

Since *Tbx1* regulates the balance between proliferation and differentiation in cardiac progenitor cells, it will be interesting to apply the protocol described by Moretti et al. (298) to the hiPS cells derived

from DGS fibroblasts to observe a possible disease phenotype; and if this will be the case, the rescue of the observed phenotype by TBX1 transduction, will allow us to better understand the molecular mechanism underlying TBX1 function on a cellular level.

Hypoplasia or aplasia of several organs and tissues is observed in TBX1 mutant patients. Since hiPS cells can differentiate *in vitro*, in multiple lineages, availability of an *in vitro* cellular model of DGS, will help us in understanding whether dysregulation of the balance between proliferation and differentiation of different types of progenitors cells or stem cells, may be a key molecular mechanism underlying the disease pathogenesis.

CHAPTER 6

Bibliography

1. Stalmans, I., Lambrechts, D., De Smet, F., Jansen, S., Wang, J., Maity, S., Kneer, P., von der Ohe, M., Swillen, A., Maes, C. *et al.* (2003) VEGF: a modifier of the del22q11 (DiGeorge) syndrome? *Nature medicine*, **9**, 173-82.
2. Dodou, E., Verzi, M.P., Anderson, J.P., Xu, S.M. and Black, B.L. (2004) Mef2c is a direct transcriptional target of ISL1 and GATA factors in the anterior heart field during mouse embryonic development. *Development (Cambridge, England)*, **131**, 3931-42.
3. Kispert, A. and Hermann, B.G. (1993) The Brachyury gene encodes a novel DNA binding protein. *The EMBO journal*, **12**, 4898-9.
4. Papapetrou, C., Edwards, Y.H. and Sowden, J.C. (1997) The T transcription factor functions as a dimer and exhibits a common human polymorphism Gly-177-Asp in the conserved DNA-binding domain. *FEBS letters*, **409**, 201-6.
5. Bruneau, B.G., Nemer, G., Schmitt, J.P., Charron, F., Robitaille, L., Caron, S., Conner, D.A., Gessler, M., Nemer, M., Seidman, C.E. *et al.* (2001) A murine model of Holt-Oram syndrome defines roles of the T-box transcription factor Tbx5 in cardiogenesis and disease. *Cell*, **106**, 709-21.
6. Hsueh, Y.P., Wang, T.F., Yang, F.C. and Sheng, M. (2000) Nuclear translocation and transcription regulation by the membrane-associated guanylate kinase CASK/LIN-2. *Nature*, **404**, 298-302.
7. Lamolet, B., Pulichino, A.M., Lamonerie, T., Gauthier, Y., Brue, T., Enjalbert, A. and Drouin, J. (2001) A pituitary cell-restricted T box factor, Tpit, activates POMC transcription in cooperation with Pitx homeoproteins. *Cell*, **104**, 849-59.
8. Paxton, C., Zhao, H., Chin, Y., Langner, K. and Reecy, J. (2002) Murine Tbx2 contains domains that activate and repress gene transcription. *Gene*, **283**, 117-24.
9. Sinha, S., Abraham, S., Gronostajski, R.M. and Campbell, C.E. (2000) Differential DNA binding and transcription modulation by three T-box proteins, T, TBX1 and TBX2. *Gene*, **258**, 15-29.
10. Stennard, F.A., Costa, M.W., Elliott, D.A., Rankin, S., Haast, S.J., Lai, D., McDonald, L.P., Niederreither, K., Dolle, P., Bruneau, B.G. *et al.* (2003) Cardiac T-box factor Tbx20 directly interacts with Nkx2-

- 5, GATA4, and GATA5 in regulation of gene expression in the developing heart. *Developmental biology*, **262**, 206-24.
11. Ghosh, T.K., Packham, E.A., Bonser, A.J., Robinson, T.E., Cross, S.J. and Brook, J.D. (2001) Characterization of the TBX5 binding site and analysis of mutations that cause Holt-Oram syndrome. *Human molecular genetics*, **10**, 1983-94.
12. Lingbeek, M.E., Jacobs, J.J. and van Lohuizen, M. (2002) The T-box repressors TBX2 and TBX3 specifically regulate the tumor suppressor gene p14ARF via a variant T-site in the initiator. *The Journal of biological chemistry*, **277**, 26120-7.
13. Conlon, F.L., Fairclough, L., Price, B.M., Casey, E.S. and Smith, J.C. (2001) Determinants of T box protein specificity. *Development (Cambridge, England)*, **128**, 3749-58.
14. Kispert, A., Koschorz, B. and Herrmann, B.G. (1995) The T protein encoded by Brachyury is a tissue-specific transcription factor. *The EMBO journal*, **14**, 4763-72.
15. Zaragoza, M.V., Lewis, L.E., Sun, G., Wang, E., Li, L., Said-Salman, I., Feucht, L. and Huang, T. (2004) Identification of the TBX5 transactivating domain and the nuclear localization signal. *Gene*, **330**, 9-18.
16. Carreira, S., Dexter, T.J., Yavuzer, U., Easty, D.J. and Goding, C.R. (1998) Brachyury-related transcription factor Tbx2 and repression of the melanocyte-specific TRP-1 promoter. *Molecular and cellular biology*, **18**, 5099-108.
17. Habets, P.E., Moorman, A.F., Clout, D.E., van Roon, M.A., Lingbeek, M., van Lohuizen, M., Campione, M. and Christoffels, V.M. (2002) Cooperative action of Tbx2 and Nkx2.5 inhibits ANF expression in the atrioventricular canal: implications for cardiac chamber formation. *Genes & development*, **16**, 1234-46.
18. Stennard, F.A., Costa, M.W., Lai, D., Biben, C., Furtado, M.B., Solloway, M.J., McCulley, D.J., Leimena, C., Preis, J.I., Dunwoodie, S.L. *et al.* (2005) Murine T-box transcription factor Tbx20 acts as a repressor during heart development, and is essential for adult heart integrity, function and adaptation. *Development (Cambridge, England)*, **132**, 2451-62.
19. Singh, M.K., Christoffels, V.M., Dias, J.M., Trowe, M.O., Petry, M., Schuster-Gossler, K., Burger, A., Ericson, J. and Kispert, A. (2005) Tbx20 is essential for cardiac chamber differentiation and repression of Tbx2. *Development (Cambridge, England)*, **132**, 2697-707.

20. Kusch, T., Storck, T., Walldorf, U. and Reuter, R. (2002) Brachyury proteins regulate target genes through modular binding sites in a cooperative fashion. *Genes & development*, **16**, 518-29.
21. Fan, C., Liu, M. and Wang, Q. (2003) Functional analysis of TBX5 missense mutations associated with Holt-Oram syndrome. *The Journal of biological chemistry*, **278**, 8780-5.
22. Garg, V., Kathiriyai, I.S., Barnes, R., Schluterman, M.K., King, I.N., Butler, C.A., Rothrock, C.R., Eapen, R.S., Hirayama-Yamada, K., Joo, K. *et al.* (2003) GATA4 mutations cause human congenital heart defects and reveal an interaction with TBX5. *Nature*, **424**, 443-7.
23. Krause, A., Zacharias, W., Camarata, T., Linkhart, B., Law, E., Lischke, A., Miljan, E. and Simon, H.G. (2004) Tbx5 and Tbx4 transcription factors interact with a new chicken PDZ-LIM protein in limb and heart development. *Developmental biology*, **273**, 106-20.
24. Naiche, L.A., Harrelson, Z., Kelly, R.G. and Papaioannou, V.E. (2005) T-box genes in vertebrate development. *Annual review of genetics*, **39**, 219-39.
25. Packham, E.A. and Brook, J.D. (2003) T-box genes in human disorders. *Human molecular genetics*, **12 Spec No 1**, R37-44.
26. Bamshad, M., Krakowiak, P.A., Watkins, W.S., Root, S., Carey, J.C. and Jorde, L.B. (1995) A gene for ulnar-mammary syndrome maps to 12q23-q24.1. *Human molecular genetics*, **4**, 1973-7.
27. Bamshad, M., Lin, R.C., Law, D.J., Watkins, W.C., Krakowiak, P.A., Moore, M.E., Franceschini, P., Lala, R., Holmes, L.B., Gebuhr, T.C. *et al.* (1997) Mutations in human TBX3 alter limb, apocrine and genital development in ulnar-mammary syndrome. *Nature genetics*, **16**, 311-5.
28. Bamshad, M., Le, T., Watkins, W.S., Dixon, M.E., Kramer, B.E., Roeder, A.D., Carey, J.C., Root, S., Schinzel, A., Van Maldergem, L. *et al.* (1999) The spectrum of mutations in TBX3: Genotype/Phenotype relationship in ulnar-mammary syndrome. *American journal of human genetics*, **64**, 1550-62.
29. Pallister, P.D., Herrmann, J. and Opitz, J.M. (1976) Studies of malformation syndromes in man XXXII: a pleiotropic dominant mutation affecting skeletal, sexual and apocrine-mammary development. *Birth defects original article series*, **12**, 247-54.
30. Franceschini, P., Vardeu, M.P., Dalforno, L., Signorile, F., Franceschini, D., Lala, R. and Matarazzo, P. (1992) Possible relationship between ulnar-mammary syndrome and split hand with

- aplasia of the ulna syndrome. *American journal of medical genetics*, **44**, 807-12.
31. Schinzel, A., Illig, R. and Prader, A. (1987) The ulnar-mammary syndrome: an autosomal dominant pleiotropic gene. *Clinical genetics*, **32**, 160-8.
 32. Bollag, R.J., Siegfried, Z., Cebra-Thomas, J.A., Garvey, N., Davison, E.M. and Silver, L.M. (1994) An ancient family of embryonically expressed mouse genes sharing a conserved protein motif with the T locus. *Nature genetics*, **7**, 383-9.
 33. Chapman, D.L., Garvey, N., Hancock, S., Alexiou, M., Agulnik, S.I., Gibson-Brown, J.J., Cebra-Thomas, J., Bollag, R.J., Silver, L.M. and Papaioannou, V.E. (1996) Expression of the T-box family genes, Tbx1-Tbx5, during early mouse development. *Dev Dyn*, **206**, 379-90.
 34. Cunha, G.R. (1994) Role of mesenchymal-epithelial interactions in normal and abnormal development of the mammary gland and prostate. *Cancer*, **74**, 1030-44.
 35. Peters, H. and Balling, R. (1999) Teeth. Where and how to make them. *Trends Genet*, **15**, 59-65.
 36. Haraguchi, R., Suzuki, K., Murakami, R., Sakai, M., Kamikawa, M., Kengaku, M., Sekine, K., Kawano, H., Kato, S., Ueno, N. *et al.* (2000) Molecular analysis of external genitalia formation: the role of fibroblast growth factor (Fgf) genes during genital tubercle formation. *Development (Cambridge, England)*, **127**, 2471-9.
 37. Newbury-Ecob, R.A., Leanage, R., Raeburn, J.A. and Young, I.D. (1996) Holt-Oram syndrome: a clinical genetic study. *Journal of medical genetics*, **33**, 300-7.
 38. Basson, C.T., Bachinsky, D.R., Lin, R.C., Levi, T., Elkins, J.A., Soultz, J., Grayzel, D., Kroumpouzou, E., Traill, T.A., Leblanc-Straceski, J. *et al.* (1997) Mutations in human TBX5 [corrected] cause limb and cardiac malformation in Holt-Oram syndrome. *Nature genetics*, **15**, 30-5.
 39. Basson, C.T., Huang, T., Lin, R.C., Bachinsky, D.R., Weremowicz, S., Vaglio, A., Bruzzzone, R., Quadrelli, R., Lerone, M., Romeo, G. *et al.* (1999) Different TBX5 interactions in heart and limb defined by Holt-Oram syndrome mutations. *Proceedings of the National Academy of Sciences of the United States of America*, **96**, 2919-24.
 40. Cross, S.J., Ching, Y.H., Li, Q.Y., Armstrong-Buisseret, L., Spranger, S., Lyonnet, S., Bonnet, D., Penttinen, M., Jonveaux, P., Leheup, B. *et al.* (2000) The mutation spectrum in Holt-Oram syndrome. *Journal of medical genetics*, **37**, 785-7.

41. Li, Q.Y., Newbury-Ecob, R.A., Terrett, J.A., Wilson, D.I., Curtis, A.R., Yi, C.H., Gebuhr, T., Bullen, P.J., Robson, S.C., Strachan, T. *et al.* (1997) Holt-Oram syndrome is caused by mutations in TBX5, a member of the Brachyury (T) gene family. *Nature genetics*, **15**, 21-9.
42. Yang, J., Hu, D., Xia, J., Yang, Y., Ying, B., Hu, J. and Zhou, X. (2000) Three novel TBX5 mutations in Chinese patients with Holt-Oram syndrome. *American journal of medical genetics*, **92**, 237-40.
43. Akrami, S.M., Winter, R.M., Brook, J.D. and Armour, J.A. (2001) Detection of a large TBX5 deletion in a family with Holt-Oram syndrome. *Journal of medical genetics*, **38**, E44.
44. Liu, J., Lin, C., Gleiberman, A., Ohgi, K.A., Herman, T., Huang, H.P., Tsai, M.J. and Rosenfeld, M.G. (2001) Tbx19, a tissue-selective regulator of POMC gene expression. *Proceedings of the National Academy of Sciences of the United States of America*, **98**, 8674-9.
45. Yi, C.H., Terrett, J.A., Li, Q.Y., Ellington, K., Packham, E.A., Armstrong-Buisseret, L., McClure, P., Slingsby, T. and Brook, J.D. (1999) Identification, mapping, and phylogenomic analysis of four new human members of the T-box gene family: EOMES, TBX6, TBX18, and TBX19. *Genomics*, **55**, 10-20.
46. Pulichino, A.M., Vallette-Kasic, S., Couture, C., Gauthier, Y., Brue, T., David, M., Malpuech, G., Deal, C., Van Vliet, G., De Vroede, M. *et al.* (2003) Human and mouse TPIT gene mutations cause early onset pituitary ACTH deficiency. *Genes & development*, **17**, 711-6.
47. Schutte, B.C. and Murray, J.C. (1999) The many faces and factors of orofacial clefts. *Human molecular genetics*, **8**, 1853-9.
48. Wilkie, A.O. and Morriss-Kay, G.M. (2001) Genetics of craniofacial development and malformation. *Nature reviews*, **2**, 458-68.
49. Moore, G.E., Ivens, A., Chambers, J., Farrall, M., Williamson, R., Page, D.C., Bjornsson, A., Arnason, A. and Jensson, O. (1987) Linkage of an X-chromosome cleft palate gene. *Nature*, **326**, 91-2.
50. Gorski, S.M., Adams, K.J., Birch, P.H., Friedman, J.M. and Goodfellow, P.J. (1992) The gene responsible for X-linked cleft palate (CPX) in a British Columbia native kindred is localized between PGK1 and DXYS1. *American journal of human genetics*, **50**, 1129-36.
51. Stanier, P., Forbes, S.A., Arnason, A., Bjornsson, A., Sveinbjornsdottir, E., Williamson, R. and Moore, G. (1993) The localization of a gene causing X-linked cleft palate and ankyloglossia (CPX) in an Icelandic kindred is between DXS326 and DXYS1X. *Genomics*, **17**, 549-55.

52. Gorski, S.M., Adams, K.J., Birch, P.H., Chodirker, B.N., Greenberg, C.R. and Goodfellow, P.J. (1994) Linkage analysis of X-linked cleft palate and ankyloglossia in Manitoba Mennonite and British Columbia Native kindreds. *Human genetics*, **94**, 141-8.
53. Laugier-Anfossi, F. and Villard, L. (2000) Molecular characterization of a new human T-box gene (TBX22) located in xq21.1 encoding a protein containing a truncated T-domain. *Gene*, **255**, 289-96.
54. Ruvinsky, I., Silver, L.M. and Gibson-Brown, J.J. (2000) Phylogenetic analysis of T-Box genes demonstrates the importance of amphioxus for understanding evolution of the vertebrate genome. *Genetics*, **156**, 1249-57.
55. Braybrook, C., Doudney, K., Marciano, A.C., Arnason, A., Bjornsson, A., Patton, M.A., Goodfellow, P.J., Moore, G.E. and Stanier, P. (2001) The T-box transcription factor gene TBX22 is mutated in X-linked cleft palate and ankyloglossia. *Nature genetics*, **29**, 179-83.
56. Braybrook, C., Warry, G., Howell, G., Mandryko, V., Arnason, A., Bjornsson, A., Ross, M.T., Moore, G.E. and Stanier, P. (2001) Physical and transcriptional mapping of the X-linked cleft palate and ankyloglossia (CPX) critical region. *Human genetics*, **108**, 537-45.
57. Braybrook, C., Warry, G., Howell, G., Arnason, A., Bjornsson, A., Moore, G.E., Ross, M.T. and Stanier, P. (2001) Identification and characterization of KLHL4, a novel human homologue of the Drosophila Kelch gene that maps within the X-linked cleft palate and Ankyloglossia (CPX) critical region. *Genomics*, **72**, 128-36.
58. Braybrook, C., Lisgo, S., Doudney, K., Henderson, D., Marciano, A.C., Strachan, T., Patton, M.A., Villard, L., Moore, G.E., Stanier, P. *et al.* (2002) Craniofacial expression of human and murine TBX22 correlates with the cleft palate and ankyloglossia phenotype observed in CPX patients. *Human molecular genetics*, **11**, 2793-804.
59. Scott, J.E. and Taor, W.S. (1979) The "small patella" syndrome. *The Journal of bone and joint surgery*, **61-B**, 172-5.
60. Vanek, J. (1981) [Ischiopatellar dysplasia (Scott and Taor's syndrome of the small patella)]. *Rofo*, **135**, 354-6.
61. Morin, P., Vielpeau, C., Fournier, L. and Denizet, D. (1985) [The coxopodopatellar syndrome]. *Journal de radiologie*, **66**, 441-6.
62. Dellestable, F., Pere, P., Blum, A., Regent, D. and Gaucher, A. (1996) The 'small-patella' syndrome. Hereditary osteodysplasia of the knee, pelvis and foot. *The Journal of bone and joint surgery*, **78**, 63-5.
63. Poznanski, A.K. (1997) Comments on the ischio-pubic-patellar syndrome. *Pediatric radiology*, **27**, 428-9.

64. Bongers, E.M., Van Bokhoven, H., Van Thienen, M.N., Kooyman, M.A., Van Beersum, S.E., Boetes, C., Knoers, N.V. and Hamel, B.C. (2001) The small patella syndrome: description of five cases from three families and examination of possible allelism with familial patella aplasia-hypoplasia and nail-patella syndrome. *Journal of medical genetics*, **38**, 209-14.
65. Sandhaus, Y.S., Ben-Ami, T., Chechick, A. and Goodman, R.M. (1987) A new patella syndrome. *Clinical genetics*, **31**, 143-7.
66. Kozlowski, K. and Nelson, J. (1995) Small patella syndrome. *American journal of medical genetics*, **57**, 558-61.
67. Azouz, E.M. and Kozlowski, K. (1997) Small patella syndrome: a bone dysplasia to recognize and differentiate from the nail-patella syndrome. *Pediatric radiology*, **27**, 432-5.
68. Habboub, H.K. and Thneibat, W.A. (1997) Ischio-pubic-patellar hypoplasia: is it a new syndrome? *Pediatric radiology*, **27**, 430-1.
69. Bongers, E.M., Duijf, P.H., van Beersum, S.E., Schoots, J., Van Kampen, A., Burckhardt, A., Hamel, B.C., Losan, F., Hoefsloot, L.H., Yntema, H.G. *et al.* (2004) Mutations in the human TBX4 gene cause small patella syndrome. *American journal of human genetics*, **74**, 1239-48.
70. Lausch, E., Hermanns, P., Farin, H.F., Alanay, Y., Unger, S., Nikkel, S., Steinwender, C., Scherer, G., Spranger, J., Zabel, B. *et al.* (2008) TBX15 mutations cause craniofacial dysmorphism, hypoplasia of scapula and pelvis, and short stature in Cousin syndrome. *American journal of human genetics*, **83**, 649-55.
71. Candille, S.I., Van Raamsdonk, C.D., Chen, C., Kuijper, S., Chen-Tsai, Y., Russ, A., Meijlink, F. and Barsh, G.S. (2004) Dorsoventral patterning of the mouse coat by Tbx15. *PLoS biology*, **2**, E3.
72. Curry, G.A. (1959) Genetical and development studies on droopy-eared mice. *Journal of embryology and experimental morphology*, **7**, 39-65.
73. Kuijper, S., Beverdam, A., Kroon, C., Brouwer, A., Candille, S., Barsh, G. and Meijlink, F. (2005) Genetics of shoulder girdle formation: roles of Tbx15 and aristaless-like genes. *Development (Cambridge, England)*, **132**, 1601-10.
74. Singh, M.K., Petry, M., Haenig, B., Lescher, B., Leitges, M. and Kispert, A. (2005) The T-box transcription factor Tbx15 is required for skeletal development. *Mechanisms of development*, **122**, 131-44.
75. Cai, C.L., Zhou, W., Yang, L., Bu, L., Qyang, Y., Zhang, X., Li, X., Rosenfeld, M.G., Chen, J. and Evans, S. (2005) T-box genes

- coordinate regional rates of proliferation and regional specification during cardiogenesis. *Development (Cambridge, England)*, **132**, 2475-87.
76. Kirk, E.P., Sunde, M., Costa, M.W., Rankin, S.A., Wolstein, O., Castro, M.L., Butler, T.L., Hyun, C., Guo, G., Otway, R. *et al.* (2007) Mutations in cardiac T-box factor gene TBX20 are associated with diverse cardiac pathologies, including defects of septation and valvulogenesis and cardiomyopathy. *American journal of human genetics*, **81**, 280-91.
 77. Campbell, C., Goodrich, K., Casey, G. and Beatty, B. (1995) Cloning and mapping of a human gene (TBX2) sharing a highly conserved protein motif with the Drosophila omb gene. *Genomics*, **28**, 255-60.
 78. Barlund, M., Monni, O., Kononen, J., Cornelison, R., Torhorst, J., Sauter, G., Kallioniemi, O.-P. and Kallioniemi, A. (2000) Multiple genes at 17q23 undergo amplification and overexpression in breast cancer. *Cancer research*, **60**, 5340-4.
 79. Jacobs, J.J., Keblusek, P., Robanus-Maandag, E., Kristel, P., Lingbeek, M., Nederlof, P.M., van Welsem, T., van de Vijver, M.J., Koh, E.Y., Daley, G.Q. *et al.* (2000) Senescence bypass screen identifies TBX2, which represses Cdkn2a (p19(ARF)) and is amplified in a subset of human breast cancers. *Nature genetics*, **26**, 291-9.
 80. Shaikh, T.H., Kurahashi, H., Saitta, S.C., O'Hare, A.M., Hu, P., Roe, B.A., Driscoll, D.A., McDonald-McGinn, D.M., Zackai, E.H., Budarf, M.L. *et al.* (2000) Chromosome 22-specific low copy repeats and the 22q11.2 deletion syndrome: genomic organization and deletion endpoint analysis. *Human molecular genetics*, **9**, 489-501.
 81. Edelman, L., Pandita, R.K. and Morrow, B.E. (1999) Low-copy repeats mediate the common 3-Mb deletion in patients with velo-cardio-facial syndrome. *American journal of human genetics*, **64**, 1076-86.
 82. McDermid, H.E. and Morrow, B.E. (2002) Genomic disorders on 22q11. *American journal of human genetics*, **70**, 1077-88.
 83. Emanuel, B.S. and Shaikh, T.H. (2001) Segmental duplications: an 'expanding' role in genomic instability and disease. *Nature reviews*, **2**, 791-800.
 84. Shaffer, L.G. and Lupski, J.R. (2000) Molecular mechanisms for constitutional chromosomal rearrangements in humans. *Annual review of genetics*, **34**, 297-329.

85. Saitta, S.C., Harris, S.E., Gaeth, A.P., Driscoll, D.A., McDonald-McGinn, D.M., Maisenbacher, M.K., Yersak, J.M., Chakraborty, P.K., Hacker, A.M., Zackai, E.H. *et al.* (2004) Aberrant interchromosomal exchanges are the predominant cause of the 22q11.2 deletion. *Human molecular genetics*, **13**, 417-28.
86. Bassett, J.H. and Thakker, R.V. (1995) Molecular genetics of disorders of calcium homeostasis. *Bailliere's clinical endocrinology and metabolism*, **9**, 581-608.
87. Scuccimarri, R. and Rodd, C. (1998) Thyroid abnormalities as a feature of DiGeorge syndrome: a patient report and review of the literature. *J Pediatr Endocrinol Metab*, **11**, 273-6.
88. Lindsay, E.A., Botta, A., Jurecic, V., Carattini-Rivera, S., Cheah, Y.C., Rosenblatt, H.M., Bradley, A. and Baldini, A. (1999) Congenital heart disease in mice deficient for the DiGeorge syndrome region. *Nature*, **401**, 379-83.
89. Taddei, I., Morishima, M., Huynh, T. and Lindsay, E.A. (2001) Genetic factors are major determinants of phenotypic variability in a mouse model of the DiGeorge/del22q11 syndromes. *Proceedings of the National Academy of Sciences of the United States of America*, **98**, 11428-31.
90. Paylor, R., McIlwain, K.L., McAninch, R., Nellis, A., Yuva-Paylor, L.A., Baldini, A. and Lindsay, E.A. (2001) Mice deleted for the DiGeorge/velocardiofacial syndrome region show abnormal sensorimotor gating and learning and memory impairments. *Human molecular genetics*, **10**, 2645-50.
91. Jerome, L.A. and Papaioannou, V.E. (2001) DiGeorge syndrome phenotype in mice mutant for the T-box gene, *Tbx1*. *Nature genetics*, **27**, 286-91.
92. Merscher, S., Funke, B., Epstein, J.A., Heyer, J., Puech, A., Lu, M.M., Xavier, R.J., Demay, M.B., Russell, R.G., Factor, S. *et al.* (2001) TBX1 is responsible for cardiovascular defects in velo-cardio-facial/DiGeorge syndrome. *Cell*, **104**, 619-29.
93. Lindsay, E.A., Vitelli, F., Su, H., Morishima, M., Huynh, T., Pramparo, T., Jurecic, V., Ogunrinu, G., Sutherland, H.F., Scambler, P.J. *et al.* (2001) *Tbx1* haploinsufficiency in the DiGeorge syndrome region causes aortic arch defects in mice. *Nature*, **410**, 97-101.
94. Gong, W., Gottlieb, S., Collins, J., Blescia, A., Dietz, H., Goldmuntz, E., McDonald-McGinn, D.M., Zackai, E.H., Emanuel, B.S., Driscoll, D.A. *et al.* (2001) Mutation analysis of TBX1 in non-deleted patients

- with features of DGS/VCFS or isolated cardiovascular defects. *Journal of medical genetics*, **38**, E45.
95. Yagi, H., Furutani, Y., Hamada, H., Sasaki, T., Asakawa, S., Minoshima, S., Ichida, F., Joo, K., Kimura, M., Imamura, S. *et al.* (2003) Role of TBX1 in human del22q11.2 syndrome. *Lancet*, **362**, 1366-73.
 96. Kelly, R.G., Jerome-Majewska, L.A. and Papaioannou, V.E. (2004) The del22q11.2 candidate gene Tbx1 regulates branchiomeric myogenesis. *Human molecular genetics*, **13**, 2829-40.
 97. Vitelli, F., Morishima, M., Taddei, I., Lindsay, E.A. and Baldini, A. (2002) Tbx1 mutation causes multiple cardiovascular defects and disrupts neural crest and cranial nerve migratory pathways. *Human molecular genetics*, **11**, 915-22.
 98. Srivastava, D. and Olson, E.N. (2000) A genetic blueprint for cardiac development. *Nature*, **407**, 221-6.
 99. Driscoll, D.A., Spinner, N.B., Budarf, M.L., McDonald-McGinn, D.M., Zackai, E.H., Goldberg, R.B., Shprintzen, R.J., Saal, H.M., Zonana, J., Jones, M.C. *et al.* (1992) Deletions and microdeletions of 22q11.2 in velo-cardio-facial syndrome. *American journal of medical genetics*, **44**, 261-8.
 100. Scambler, P.J., Kelly, D., Lindsay, E., Williamson, R., Goldberg, R., Shprintzen, R., Wilson, D.I., Goodship, J.A., Cross, I.E. and Burn, J. (1992) Velo-cardio-facial syndrome associated with chromosome 22 deletions encompassing the DiGeorge locus. *Lancet*, **339**, 1138-9.
 101. Hogan, B.L. and Kolodziej, P.A. (2002) Organogenesis: molecular mechanisms of tubulogenesis. *Nature reviews*, **3**, 513-23.
 102. Garg, V., Yamagishi, C., Hu, T., Kathiriya, I.S., Yamagishi, H. and Srivastava, D. (2001) Tbx1, a DiGeorge syndrome candidate gene, is regulated by sonic hedgehog during pharyngeal arch development. *Developmental biology*, **235**, 62-73.
 103. Vitelli, F., Taddei, I., Morishima, M., Meyers, E.N., Lindsay, E.A. and Baldini, A. (2002) A genetic link between Tbx1 and fibroblast growth factor signaling. *Development (Cambridge, England)*, **129**, 4605-11.
 104. Lania, G., Zhang, Z., Huynh, T., Caprio, C., Moon, A.M., Vitelli, F. and Baldini, A. (2009) Early thyroid development requires a Tbx1-Fgf8 pathway. *Developmental biology*, **328**, 109-17.
 105. Fagman, H., Liao, J., Westerlund, J., Andersson, L., Morrow, B.E. and Nilsson, M. (2007) The 22q11 deletion syndrome candidate gene

- Tbx1 determines thyroid size and positioning. *Human molecular genetics*, **16**, 276-85.
106. Parlato, R., Rosica, A., Rodriguez-Mallon, A., Affuso, A., Postiglione, M.P., Arra, C., Mansouri, A., Kimura, S., Di Lauro, R. and De Felice, M. (2004) An integrated regulatory network controlling survival and migration in thyroid organogenesis. *Developmental biology*, **276**, 464-75.
 107. Weinzimer, S.A., McDonald-McGinn, D.M., Driscoll, D.A., Emanuel, B.S., Zackai, E.H. and Moshang, T., Jr. (1998) Growth hormone deficiency in patients with 22q11.2 deletion: expanding the phenotype. *Pediatrics*, **101**, 929-32.
 108. Liao, J., Kochilas, L., Nowotschin, S., Arnold, J.S., Aggarwal, V.S., Epstein, J.A., Brown, M.C., Adams, J. and Morrow, B.E. (2004) Full spectrum of malformations in velo-cardio-facial syndrome/DiGeorge syndrome mouse models by altering Tbx1 dosage. *Human molecular genetics*, **13**, 1577-85.
 109. Wendl, T., Adzic, D., Schoenebeck, J.J., Scholpp, S., Brand, M., Yelon, D. and Rohr, K.B. (2007) Early developmental specification of the thyroid gland depends on hox-expressing surrounding tissue and on FGF signals. *Development (Cambridge, England)*, **134**, 2871-9.
 110. Olivieri, A., Stazi, M.A., Mastroiacovo, P., Fazzini, C., Medda, E., Spagnolo, A., De Angelis, S., Grandolfo, M.E., Taruscio, D., Cordeddu, V. *et al.* (2002) A population-based study on the frequency of additional congenital malformations in infants with congenital hypothyroidism: data from the Italian Registry for Congenital Hypothyroidism (1991-1998). *The Journal of clinical endocrinology and metabolism*, **87**, 557-62.
 111. Mjaatvedt, C.H., Nakaoka, T., Moreno-Rodriguez, R., Norris, R.A., Kern, M.J., Eisenberg, C.A., Turner, D. and Markwald, R.R. (2001) The outflow tract of the heart is recruited from a novel heart-forming field. *Developmental biology*, **238**, 97-109.
 112. Kelly, R.G., Brown, N.A. and Buckingham, M.E. (2001) The arterial pole of the mouse heart forms from Fgf10-expressing cells in pharyngeal mesoderm. *Developmental cell*, **1**, 435-40.
 113. Waldo, K.L., Kumiski, D.H., Wallis, K.T., Stadt, H.A., Hutson, M.R., Platt, D.H. and Kirby, M.L. (2001) Conotruncal myocardium arises from a secondary heart field. *Development (Cambridge, England)*, **128**, 3179-88.
 114. Cai, C.L., Liang, X., Shi, Y., Chu, P.H., Pfaff, S.L., Chen, J. and Evans, S. (2003) Isl1 identifies a cardiac progenitor population that

- proliferates prior to differentiation and contributes a majority of cells to the heart. *Developmental cell*, **5**, 877-89.
115. Xu, J., Zheng, S.L., Hawkins, G.A., Faith, D.A., Kelly, B., Isaacs, S.D., Wiley, K.E., Chang, B., Ewing, C.M., Bujnovszky, P. *et al.* (2001) Linkage and association studies of prostate cancer susceptibility: evidence for linkage at 8p22-23. *American journal of human genetics*, **69**, 341-50.
 116. Jiang, X., Rowitch, D.H., Soriano, P., McMahon, A.P. and Sucov, H.M. (2000) Fate of the mammalian cardiac neural crest. *Development (Cambridge, England)*, **127**, 1607-16.
 117. Kirby, M.L. and Waldo, K.L. (1995) Neural crest and cardiovascular patterning. *Circulation research*, **77**, 211-5.
 118. Li, J., Chen, F. and Epstein, J.A. (2000) Neural crest expression of Cre recombinase directed by the proximal Pax3 promoter in transgenic mice. *Genesis*, **26**, 162-4.
 119. Kelly, R.G. and Buckingham, M.E. (2002) The anterior heart-forming field: voyage to the arterial pole of the heart. *Trends Genet*, **18**, 210-6.
 120. Xu, H., Morishima, M., Wylie, J.N., Schwartz, R.J., Bruneau, B.G., Lindsay, E.A. and Baldini, A. (2004) Tbx1 has a dual role in the morphogenesis of the cardiac outflow tract. *Development (Cambridge, England)*, **131**, 3217-27.
 121. Barald, K.F. and Kelley, M.W. (2004) From placode to polarization: new tunes in inner ear development. *Development (Cambridge, England)*, **131**, 4119-30.
 122. Fekete, D.M. and Wu, D.K. (2002) Revisiting cell fate specification in the inner ear. *Current opinion in neurobiology*, **12**, 35-42.
 123. Liu, M., Pereira, F.A., Price, S.D., Chu, M.J., Shope, C., Himes, D., Eatock, R.A., Brownell, W.E., Lysakowski, A. and Tsai, M.J. (2000) Essential role of BETA2/NeuroD1 in development of the vestibular and auditory systems. *Genes & development*, **14**, 2839-54.
 124. Kim, W.Y., Frittsch, B., Serls, A., Bakel, L.A., Huang, E.J., Reichardt, L.F., Barth, D.S. and Lee, J.E. (2001) NeuroD-null mice are deaf due to a severe loss of the inner ear sensory neurons during development. *Development (Cambridge, England)*, **128**, 417-26.
 125. Raft, S., Nowotschin, S., Liao, J. and Morrow, B.E. (2004) Suppression of neural fate and control of inner ear morphogenesis by Tbx1. *Development (Cambridge, England)*, **131**, 1801-12.
 126. Vitelli, F., Viola, A., Morishima, M., Pramparo, T., Baldini, A. and Lindsay, E. (2003) TBX1 is required for inner ear morphogenesis. *Human molecular genetics*, **12**, 2041-8.

127. Alencar, A.P., Iorio, M.C. and Morales, D.S. (2005) Equivalent volume: study in subjects with chronic otitis media. *Brazilian journal of otorhinolaryngology*, **71**, 644-8.
128. Xu, H., Viola, A., Zhang, Z., Gerken, C.P., Lindsay-Iltingworth, E.A. and Baldini, A. (2007) Tbx1 regulates population, proliferation and cell fate determination of otic epithelial cells. *Developmental biology*, **302**, 670-82.
129. Keithley, E.M., Ma, C.L., Ryan, A.F., Louis, J.C. and Magal, E. (1998) GDNF protects the cochlea against noise damage. *Neuroreport*, **9**, 2183-7.
130. Yamagishi, H., Maeda, J., Hu, T., McAnally, J., Conway, S.J., Kume, T., Meyers, E.N., Yamagishi, C. and Srivastava, D. (2003) Tbx1 is regulated by tissue-specific forkhead proteins through a common Sonic hedgehog-responsive enhancer. *Genes & development*, **17**, 269-81.
131. Kaufmann, E. and Knochel, W. (1996) Five years on the wings of fork head. *Mechanisms of development*, **57**, 3-20.
132. Kaestner, K.H., Knochel, W. and Martinez, D.E. (2000) Unified nomenclature for the winged helix/forkhead transcription factors. *Genes & development*, **14**, 142-6.
133. Weinstein, D.C., Ruiz i Altaba, A., Chen, W.S., Hoodless, P., Prezioso, V.R., Jessell, T.M. and Darnell, J.E., Jr. (1994) The winged-helix transcription factor HNF-3 beta is required for notochord development in the mouse embryo. *Cell*, **78**, 575-88.
134. Iida, K., Koseki, H., Kakinuma, H., Kato, N., Mizutani-Koseki, Y., Ohuchi, H., Yoshioka, H., Noji, S., Kawamura, K., Kataoka, Y. *et al.* (1997) Essential roles of the winged helix transcription factor MFH-1 in aortic arch patterning and skeletogenesis. *Development (Cambridge, England)*, **124**, 4627-38.
135. Winnier, G.E., Hargett, L. and Hogan, B.L. (1997) The winged helix transcription factor MFH1 is required for proliferation and patterning of paraxial mesoderm in the mouse embryo. *Genes & development*, **11**, 926-40.
136. Winnier, G.E., Kume, T., Deng, K., Rogers, R., Bundy, J., Raines, C., Walter, M.A., Hogan, B.L. and Conway, S.J. (1999) Roles for the winged helix transcription factors MF1 and MFH1 in cardiovascular development revealed by nonallelic noncomplementation of null alleles. *Developmental biology*, **213**, 418-31.
137. Kume, T., Deng, K.Y., Winfrey, V., Gould, D.B., Walter, M.A. and Hogan, B.L. (1998) The forkhead/winged helix gene Mfl is disrupted

- in the pleiotropic mouse mutation congenital hydrocephalus. *Cell*, **93**, 985-96.
138. Kume, T., Jiang, H., Topczewska, J.M. and Hogan, B.L. (2001) The murine winged helix transcription factors, *Foxc1* and *Foxc2*, are both required for cardiovascular development and somitogenesis. *Genes & development*, **15**, 2470-82.
 139. Chiang, C., Litington, Y., Lee, E., Young, K.E., Corden, J.L., Westphal, H. and Beachy, P.A. (1996) Cyclopia and defective axial patterning in mice lacking Sonic hedgehog gene function. *Nature*, **383**, 407-13.
 140. Helms, J.A., Kim, C.H., Hu, D., Minkoff, R., Thaller, C. and Eichele, G. (1997) Sonic hedgehog participates in craniofacial morphogenesis and is down-regulated by teratogenic doses of retinoic acid. *Developmental biology*, **187**, 25-35.
 141. Maeda, J., Yamagishi, H., McAnally, J., Yamagishi, C. and Srivastava, D. (2006) *Tbx1* is regulated by forkhead proteins in the secondary heart field. *Dev Dyn*, **235**, 701-10.
 142. Hu, T., Yamagishi, H., Maeda, J., McAnally, J., Yamagishi, C. and Srivastava, D. (2004) *Tbx1* regulates fibroblast growth factors in the anterior heart field through a reinforcing autoregulatory loop involving forkhead transcription factors. *Development (Cambridge, England)*, **131**, 5491-502.
 143. Zhang, Z., Huynh, T. and Baldini, A. (2006) Mesodermal expression of *Tbx1* is necessary and sufficient for pharyngeal arch and cardiac outflow tract development. *Development (Cambridge, England)*, **133**, 3587-95.
 144. Kattman, S.J., Huber, T.L. and Keller, G.M. (2006) Multipotent flk-1+ cardiovascular progenitor cells give rise to the cardiomyocyte, endothelial, and vascular smooth muscle lineages. *Developmental cell*, **11**, 723-32.
 145. Moretti, A., Caron, L., Nakano, A., Lam, J.T., Bernshausen, A., Chen, Y., Qyang, Y., Bu, L., Sasaki, M., Martin-Puig, S. *et al.* (2006) Multipotent embryonic isl1+ progenitor cells lead to cardiac, smooth muscle, and endothelial cell diversification. *Cell*, **127**, 1151-65.
 146. Wu, S.M., Fujiwara, Y., Cibulsky, S.M., Clapham, D.E., Lien, C.L., Schultheiss, T.M. and Orkin, S.H. (2006) Developmental origin of a bipotential myocardial and smooth muscle cell precursor in the mammalian heart. *Cell*, **127**, 1137-50.

147. Chen, L., Fulcoli, F.G., Tang, S. and Baldini, A. (2009) Tbx1 regulates proliferation and differentiation of multipotent heart progenitors. *Circulation research*, **105**, 842-51.
148. Vitelli, F., Huynh, T. and Baldini, A. (2009) Gain of function of Tbx1 affects pharyngeal and heart development in the mouse. *Genesis*, **47**, 188-95.
149. Saga, Y., Miyagawa-Tomita, S., Takagi, A., Kitajima, S., Miyazaki, J. and Inoue, T. (1999) MesP1 is expressed in the heart precursor cells and required for the formation of a single heart tube. *Development (Cambridge, England)*, **126**, 3437-47.
150. Naya, F.J., Wu, C., Richardson, J.A., Overbeek, P. and Olson, E.N. (1999) Transcriptional activity of MEF2 during mouse embryogenesis monitored with a MEF2-dependent transgene. *Development (Cambridge, England)*, **126**, 2045-52.
151. Rennel, E. and Gerwins, P. (2002) How to make tetracycline-regulated transgene expression go on and off. *Analytical biochemistry*, **309**, 79-84.
152. Roberts, C., Ivins, S.M., James, C.T. and Scambler, P.J. (2005) Retinoic acid down-regulates Tbx1 expression in vivo and in vitro. *Dev Dyn*, **232**, 928-38.
153. Agarwal, P., Wylie, J.N., Galceran, J., Arkhitko, O., Li, C., Deng, C., Grosschedl, R. and Bruneau, B.G. (2003) Tbx5 is essential for forelimb bud initiation following patterning of the limb field in the mouse embryo. *Development (Cambridge, England)*, **130**, 623-33.
154. Biermanns, M. and Gartner, J. (2000) Genomic organization and characterization of human PEX2 encoding a 35-kDa peroxisomal membrane protein. *Biochemical and biophysical research communications*, **273**, 985-90.
155. Waterham, H.R., Titorenko, V.I., Swaving, G.J., Harder, W. and Veenhuis, M. (1993) Peroxisomes in the methylotrophic yeast *Hansenula polymorpha* do not necessarily derive from pre-existing organelles. *The EMBO journal*, **12**, 4785-94.
156. Tsukamoto, T., Miura, S. and Fujiki, Y. (1991) Restoration by a 35K membrane protein of peroxisome assembly in a peroxisome-deficient mammalian cell mutant. *Nature*, **350**, 77-81.
157. Shimozawa, N., Tsukamoto, T., Suzuki, Y., Orii, T., Shirayoshi, Y., Mori, T. and Fujiki, Y. (1992) A human gene responsible for Zellweger syndrome that affects peroxisome assembly. *Science (New York, N.Y.)*, **255**, 1132-4.

158. Berteaux-Lecellier, V., Picard, M., Thompson-Coffe, C., Zickler, D., Panvier-Adoutte, A. and Simonet, J.M. (1995) A nonmammalian homolog of the PAF1 gene (Zellweger syndrome) discovered as a gene involved in caryogamy in the fungus *Podospora anserina*. *Cell*, **81**, 1043-51.
159. Faust, P.L., Banka, D., Siriratsivawong, R., Ng, V.G. and Wikander, T.M. (2005) Peroxisome biogenesis disorders: the role of peroxisomes and metabolic dysfunction in developing brain. *Journal of inherited metabolic disease*, **28**, 369-83.
160. Faust, P.L. and Hatten, M.E. (1997) Targeted deletion of the PEX2 peroxisome assembly gene in mice provides a model for Zellweger syndrome, a human neuronal migration disorder. *The Journal of cell biology*, **139**, 1293-305.
161. Hermansky, F. and Pudlak, P. (1959) Albinism associated with hemorrhagic diathesis and unusual pigmented reticular cells in the bone marrow: report of two cases with histochemical studies. *Blood*, **14**, 162-9.
162. Spritz, R.A. (1999) Multi-organellar disorders of pigmentation: intracellular traffic jams in mammals, flies and yeast. *Trends Genet*, **15**, 337-40.
163. Spritz, R.A. (1999) Multi-organellar disorders of pigmentation: tied up in traffic. *Clinical genetics*, **55**, 309-17.
164. Spritz, R.A. and Oh, J. (1999) HPS gene mutations in Hermansky-Pudlak syndrome. *American journal of human genetics*, **64**, 658.
165. Bennett, D.C. (1993) Genetics, development, and malignancy of melanocytes. *International review of cytology*, **146**, 191-260.
166. Swank, R.T., Novak, E.K., McGarry, M.P., Rusiniak, M.E. and Feng, L. (1998) Mouse models of Hermansky Pudlak syndrome: a review. *Pigment cell research / sponsored by the European Society for Pigment Cell Research and the International Pigment Cell Society*, **11**, 60-80.
167. Wendland, B., Emr, S.D. and Riezman, H. (1998) Protein traffic in the yeast endocytic and vacuolar protein sorting pathways. *Current opinion in cell biology*, **10**, 513-22.
168. Pelham, H.R. (1999) The Croonian Lecture 1999. Intracellular membrane traffic: getting proteins sorted. *Philosophical transactions of the Royal Society of London*, **354**, 1471-8.
169. Huizing, M., Didier, A., Walenta, J., Anikster, Y., Gahl, W.A. and Kramer, H. (2001) Molecular cloning and characterization of human VPS18, VPS 11, VPS16, and VPS33. *Gene*, **264**, 241-7.

170. Gissen, P., Johnson, C.A., Gentle, D., Hurst, L.D., Doherty, A.J., O'Kane, C.J., Kelly, D.A. and Maher, E.R. (2005) Comparative evolutionary analysis of VPS33 homologues: genetic and functional insights. *Human molecular genetics*, **14**, 1261-70.
171. Suzuki, T., Oiso, N., Gautam, R., Novak, E.K., Panthier, J.J., Suprabha, P.G., Vida, T., Swank, R.T. and Spritz, R.A. (2003) The mouse organellar biogenesis mutant buff results from a mutation in Vps33a, a homologue of yeast vps33 and Drosophila carnation. *Proceedings of the National Academy of Sciences of the United States of America*, **100**, 1146-50.
172. Pardo, P.S., Leung, J.K., Lucchesi, J.C. and Pereira-Smith, O.M. (2002) MRG15, a novel chromodomain protein, is present in two distinct multiprotein complexes involved in transcriptional activation. *The Journal of biological chemistry*, **277**, 50860-6.
173. Leung, J.K., Berube, N., Venable, S., Ahmed, S., Timchenko, N. and Pereira-Smith, O.M. (2001) MRG15 activates the B-myb promoter through formation of a nuclear complex with the retinoblastoma protein and the novel protein PAM14. *The Journal of biological chemistry*, **276**, 39171-8.
174. Tominaga, K., Leung, J.K., Rookard, P., Echigo, J., Smith, J.R. and Pereira-Smith, O.M. (2003) MRGX is a novel transcriptional regulator that exhibits activation or repression of the B-myb promoter in a cell type-dependent manner. *The Journal of biological chemistry*, **278**, 49618-24.
175. Yochum, G.S. and Ayer, D.E. (2002) Role for the mortality factors MORF4, MRGX, and MRG15 in transcriptional repression via associations with Pfl, mSin3A, and Transducin-Like Enhancer of Split. *Molecular and cellular biology*, **22**, 7868-76.
176. Ikura, T., Ogryzko, V.V., Grigoriev, M., Groisman, R., Wang, J., Horikoshi, M., Scully, R., Qin, J. and Nakatani, Y. (2000) Involvement of the TIP60 histone acetylase complex in DNA repair and apoptosis. *Cell*, **102**, 463-73.
177. Cai, Y., Jin, J., Tomomori-Sato, C., Sato, S., Sorokina, I., Parmely, T.J., Conaway, R.C. and Conaway, J.W. (2003) Identification of new subunits of the multiprotein mammalian TRRAP/TIP60-containing histone acetyltransferase complex. *The Journal of biological chemistry*, **278**, 42733-6.
178. Tominaga, K., Kirtane, B., Jackson, J.G., Ikeno, Y., Ikeda, T., Hawks, C., Smith, J.R., Matzuk, M.M. and Pereira-Smith, O.M. (2005)

- MRG15 regulates embryonic development and cell proliferation. *Molecular and cellular biology*, **25**, 2924-37.
179. Tominaga, K., Matzuk, M.M. and Pereira-Smith, O.M. (2005) MrgX is not essential for cell growth and development in the mouse. *Molecular and cellular biology*, **25**, 4873-80.
 180. Pena, A.N. and Pereira-Smith, O.M. (2007) The role of the MORF/MRG family of genes in cell growth, differentiation, DNA repair, and thereby aging. *Annals of the New York Academy of Sciences*, **1100**, 299-305.
 181. Derynck, R. and Feng, X.H. (1997) TGF-beta receptor signaling. *Biochimica et biophysica acta*, **1333**, F105-50.
 182. ten Dijke, P. and Hill, C.S. (2004) New insights into TGF-beta-Smad signalling. *Trends in biochemical sciences*, **29**, 265-73.
 183. Piek, E., Heldin, C.H. and Ten Dijke, P. (1999) Specificity, diversity, and regulation in TGF-beta superfamily signaling. *Faseb J*, **13**, 2105-24.
 184. Massague, J., Blain, S.W. and Lo, R.S. (2000) TGFbeta signaling in growth control, cancer, and heritable disorders. *Cell*, **103**, 295-309.
 185. Elliott, R.L. and Blobe, G.C. (2005) Role of transforming growth factor Beta in human cancer. *J Clin Oncol*, **23**, 2078-93.
 186. Bierie, B. and Moses, H.L. (2006) Tumour microenvironment: TGFbeta: the molecular Jekyll and Hyde of cancer. *Nature reviews*, **6**, 506-20.
 187. Keeton, M.R., Curriden, S.A., van Zonneveld, A.J. and Loskutoff, D.J. (1991) Identification of regulatory sequences in the type 1 plasminogen activator inhibitor gene responsive to transforming growth factor beta. *The Journal of biological chemistry*, **266**, 23048-52.
 188. Macias-Silva, M., Abdollah, S., Hoodless, P.A., Pirone, R., Attisano, L. and Wrana, J.L. (1996) MADR2 is a substrate of the TGFbeta receptor and its phosphorylation is required for nuclear accumulation and signaling. *Cell*, **87**, 1215-24.
 189. Song, K., Wang, H., Krebs, T.L. and Danielpour, D. (2006) Novel roles of Akt and mTOR in suppressing TGF-beta/ALK5-mediated Smad3 activation. *The EMBO journal*, **25**, 58-69.
 190. Remy, I., Montmarquette, A. and Michnick, S.W. (2004) PKB/Akt modulates TGF-beta signalling through a direct interaction with Smad3. *Nature cell biology*, **6**, 358-65.
 191. Kamaraju, A.K. and Roberts, A.B. (2005) Role of Rho/ROCK and p38 MAP kinase pathways in transforming growth factor-beta-

- mediated Smad-dependent growth inhibition of human breast carcinoma cells in vivo. *The Journal of biological chemistry*, **280**, 1024-36.
192. Yu, L., Hebert, M.C. and Zhang, Y.E. (2002) TGF-beta receptor-activated p38 MAP kinase mediates Smad-independent TGF-beta responses. *The EMBO journal*, **21**, 3749-59.
 193. Moustakas, A. and Heldin, C.H. (2005) Non-Smad TGF-beta signals. *Journal of cell science*, **118**, 3573-84.
 194. Tian, F., Byfield, S.D., Parks, W.T., Stuelten, C.H., Nemani, D., Zhang, Y.E. and Roberts, A.B. (2004) Smad-binding defective mutant of transforming growth factor beta type I receptor enhances tumorigenesis but suppresses metastasis of breast cancer cell lines. *Cancer research*, **64**, 4523-30.
 195. Watanabe, H., de Caestecker, M.P. and Yamada, Y. (2001) Transcriptional cross-talk between Smad, ERK1/2, and p38 mitogen-activated protein kinase pathways regulates transforming growth factor-beta-induced aggrecan gene expression in chondrogenic ATDC5 cells. *The Journal of biological chemistry*, **276**, 14466-73.
 196. Lopez-Casillas, F., Wrana, J.L. and Massague, J. (1993) Betaglycan presents ligand to the TGF beta signaling receptor. *Cell*, **73**, 1435-44.
 197. Deng, X., Bellis, S., Yan, Z. and Friedman, E. (1999) Differential responsiveness to autocrine and exogenous transforming growth factor (TGF) beta1 in cells with nonfunctional TGF-beta receptor type III. *Cell Growth Differ*, **10**, 11-8.
 198. Brown, C.B., Boyer, A.S., Runyan, R.B. and Barnett, J.V. (1999) Requirement of type III TGF-beta receptor for endocardial cell transformation in the heart. *Science (New York, N.Y.)*, **283**, 2080-2.
 199. Stenvers, K.L., Tursky, M.L., Harder, K.W., Kountouri, N., Amatayakul-Chantler, S., Grail, D., Small, C., Weinberg, R.A., Sizeland, A.M. and Zhu, H.J. (2003) Heart and liver defects and reduced transforming growth factor beta2 sensitivity in transforming growth factor beta type III receptor-deficient embryos. *Molecular and cellular biology*, **23**, 4371-85.
 200. You, H.J., Bruinsma, M.W., How, T., Ostrander, J.H. and Blobe, G.C. (2007) The type III TGF-beta receptor signals through both Smad3 and the p38 MAP kinase pathways to contribute to inhibition of cell proliferation. *Carcinogenesis*, **28**, 2491-500.
 201. Blobe, G.C., Liu, X., Fang, S.J., How, T. and Lodish, H.F. (2001) A novel mechanism for regulating transforming growth factor beta (TGF-beta) signaling. Functional modulation of type III TGF-beta

- receptor expression through interaction with the PDZ domain protein, GIPC. *The Journal of biological chemistry*, **276**, 39608-17.
202. Pollock, R. and Treisman, R. (1991) Human SRF-related proteins: DNA-binding properties and potential regulatory targets. *Genes & development*, **5**, 2327-41.
 203. Martin, J.F., Miano, J.M., Hustad, C.M., Copeland, N.G., Jenkins, N.A. and Olson, E.N. (1994) A Mef2 gene that generates a muscle-specific isoform via alternative mRNA splicing. *Molecular and cellular biology*, **14**, 1647-56.
 204. Suzuki, E., Guo, K., Kolman, M., Yu, Y.T. and Walsh, K. (1995) Serum induction of MEF2/RSRF expression in vascular myocytes is mediated at the level of translation. *Molecular and cellular biology*, **15**, 3415-23.
 205. Breitbart, R.E., Liang, C.S., Smoot, L.B., Laheru, D.A., Mahdavi, V. and Nadal-Ginard, B. (1993) A fourth human MEF2 transcription factor, hMEF2D, is an early marker of the myogenic lineage. *Development (Cambridge, England)*, **118**, 1095-106.
 206. Leifer, D., Krainc, D., Yu, Y.T., McDermott, J., Breitbart, R.E., Heng, J., Neve, R.L., Kosofsky, B., Nadal-Ginard, B. and Lipton, S.A. (1993) MEF2C, a MADS/MEF2-family transcription factor expressed in a laminar distribution in cerebral cortex. *Proceedings of the National Academy of Sciences of the United States of America*, **90**, 1546-50.
 207. Molkenin, J.D., Firulli, A.B., Black, B.L., Martin, J.F., Hustad, C.M., Copeland, N., Jenkins, N., Lyons, G. and Olson, E.N. (1996) MEF2B is a potent transactivator expressed in early myogenic lineages. *Molecular and cellular biology*, **16**, 3814-24.
 208. Molkenin, J.D., Black, B.L., Martin, J.F. and Olson, E.N. (1996) Mutational analysis of the DNA binding, dimerization, and transcriptional activation domains of MEF2C. *Molecular and cellular biology*, **16**, 2627-36.
 209. Yu, Y.T. (1996) Distinct domains of myocyte enhancer binding factor-2A determining nuclear localization and cell type-specific transcriptional activity. *The Journal of biological chemistry*, **271**, 24675-83.
 210. Edmondson, D.G., Lyons, G.E., Martin, J.F. and Olson, E.N. (1994) Mef2 gene expression marks the cardiac and skeletal muscle lineages during mouse embryogenesis. *Development (Cambridge, England)*, **120**, 1251-63.

211. Lyons, G.E., Micales, B.K., Schwarz, J., Martin, J.F. and Olson, E.N. (1995) Expression of mef2 genes in the mouse central nervous system suggests a role in neuronal maturation. *J Neurosci*, **15**, 5727-38.
212. Firulli, A.B., Miano, J.M., Bi, W., Johnson, A.D., Casscells, W., Olson, E.N. and Schwarz, J.J. (1996) Myocyte enhancer binding factor-2 expression and activity in vascular smooth muscle cells. Association with the activated phenotype. *Circulation research*, **78**, 196-204.
213. Swanson, B.J., Jack, H.M. and Lyons, G.E. (1998) Characterization of myocyte enhancer factor 2 (MEF2) expression in B and T cells: MEF2C is a B cell-restricted transcription factor in lymphocytes. *Molecular immunology*, **35**, 445-58.
214. Lin, Q., Lu, J., Yanagisawa, H., Webb, R., Lyons, G.E., Richardson, J.A. and Olson, E.N. (1998) Requirement of the MADS-box transcription factor MEF2C for vascular development. *Development (Cambridge, England)*, **125**, 4565-74.
215. Olson, E.N., Perry, M. and Schulz, R.A. (1995) Regulation of muscle differentiation by the MEF2 family of MADS box transcription factors. *Developmental biology*, **172**, 2-14.
216. Arceci, R.J., King, A.A., Simon, M.C., Orkin, S.H. and Wilson, D.B. (1993) Mouse GATA-4: a retinoic acid-inducible GATA-binding transcription factor expressed in endodermally derived tissues and heart. *Molecular and cellular biology*, **13**, 2235-46.
217. Ross, R.S., Navankasattusas, S., Harvey, R.P. and Chien, K.R. (1996) An HF-1a/HF-1b/MEF-2 combinatorial element confers cardiac ventricular specificity and established an anterior-posterior gradient of expression. *Development (Cambridge, England)*, **122**, 1799-809.
218. Lints, T.J., Parsons, L.M., Hartley, L., Lyons, I. and Harvey, R.P. (1993) Nkx-2.5: a novel murine homeobox gene expressed in early heart progenitor cells and their myogenic descendants. *Development (Cambridge, England)*, **119**, 969.
219. Morrissey, E.E., Ip, H.S., Lu, M.M. and Parmacek, M.S. (1996) GATA-6: a zinc finger transcription factor that is expressed in multiple cell lineages derived from lateral mesoderm. *Developmental biology*, **177**, 309-22.
220. Morrissey, E.E., Ip, H.S., Tang, Z. and Parmacek, M.S. (1997) GATA-4 activates transcription via two novel domains that are conserved within the GATA-4/5/6 subfamily. *The Journal of biological chemistry*, **272**, 8515-24.

221. Morrissey, E.E., Ip, H.S., Tang, Z., Lu, M.M. and Parmacek, M.S. (1997) GATA-5: a transcriptional activator expressed in a novel temporally and spatially-restricted pattern during embryonic development. *Developmental biology*, **183**, 21-36.
222. Lin, M.H., Bour, B.A., Abmayr, S.M. and Storti, R.V. (1997) Ectopic expression of MEF2 in the epidermis induces epidermal expression of muscle genes and abnormal muscle development in *Drosophila*. *Developmental biology*, **182**, 240-55.
223. De Val, S., Anderson, J.P., Heidt, A.B., Khiem, D., Xu, S.M. and Black, B.L. (2004) Mef2c is activated directly by Ets transcription factors through an evolutionarily conserved endothelial cell-specific enhancer. *Developmental biology*, **275**, 424-34.
224. Lin, X., Shah, S. and Bulleit, R.F. (1996) The expression of MEF2 genes is implicated in CNS neuronal differentiation. *Brain research*, **42**, 307-16.
225. Leifer, D., Golden, J. and Kowall, N.W. (1994) Myocyte-specific enhancer binding factor 2C expression in human brain development. *Neuroscience*, **63**, 1067-79.
226. Masui, S., Shimosato, D., Toyooka, Y., Yagi, R., Takahashi, K. and Niwa, H. (2005) An efficient system to establish multiple embryonic stem cell lines carrying an inducible expression unit. *Nucleic acids research*, **33**, e43.
227. Lewandoski, M. (2001) Conditional control of gene expression in the mouse. *Nat Rev Genet*, **2**, 743-55.
228. Gossen, M. and Bujard, H. (2002) Studying gene function in eukaryotes by conditional gene inactivation. *Annual review of genetics*, **36**, 153-73.
229. Gossen, M. and Bujard, H. (1992) Tight control of gene expression in mammalian cells by tetracycline-responsive promoters. *Proceedings of the National Academy of Sciences of the United States of America*, **89**, 5547-51.
230. Gossen, M., Freundlieb, S., Bender, G., Muller, G., Hillen, W. and Bujard, H. (1995) Transcriptional activation by tetracyclines in mammalian cells. *Science (New York, N.Y.)*, **268**, 1766-9.
231. Wu, H., Naya, F.J., McKinsey, T.A., Mercer, B., Shelton, J.M., Chin, E.R., Simard, A.R., Michel, R.N., Bassel-Duby, R., Olson, E.N. *et al.* (2000) MEF2 responds to multiple calcium-regulated signals in the control of skeletal muscle fiber type. *The EMBO journal*, **19**, 1963-73.

232. Li, H. and Capetanaki, Y. (1994) An E box in the desmin promoter cooperates with the E box and MEF-2 sites of a distal enhancer to direct muscle-specific transcription. *The EMBO journal*, **13**, 3580-9.
233. Soriano, P. (1999) Generalized lacZ expression with the ROSA26 Cre reporter strain. *Nature genetics*, **21**, 70-1.
234. Liao, J., Aggarwal, V.S., Nowotschin, S., Bondarev, A., Lipner, S. and Morrow, B.E. (2008) Identification of downstream genetic pathways of Tbx1 in the second heart field. *Developmental biology*, **316**, 524-37.
235. Dodou, E., Xu, S.M. and Black, B.L. (2003) mef2c is activated directly by myogenic basic helix-loop-helix proteins during skeletal muscle development in vivo. *Mechanisms of development*, **120**, 1021-32.
236. Olson, E.N. (1990) MyoD family: a paradigm for development? *Genes & development*, **4**, 1454-61.
237. Weintraub, H. (1993) The MyoD family and myogenesis: redundancy, networks, and thresholds. *Cell*, **75**, 1241-4.
238. Andres, V. and Walsh, K. (1996) Myogenin expression, cell cycle withdrawal, and phenotypic differentiation are temporally separable events that precede cell fusion upon myogenesis. *The Journal of cell biology*, **132**, 657-66.
239. Zhang, Z. and Baldini, A. (2008) In vivo response to high-resolution variation of Tbx1 mRNA dosage. *Human molecular genetics*, **17**, 150-7.
240. Fine, S.E., Weissman, A., Gerdes, M., Pinto-Martin, J., Zackai, E.H., McDonald-McGinn, D.M. and Emanuel, B.S. (2005) Autism spectrum disorders and symptoms in children with molecularly confirmed 22q11.2 deletion syndrome. *Journal of autism and developmental disorders*, **35**, 461-70.
241. Niklasson, L., Rasmussen, P., Oskarsdottir, S. and Gillberg, C. (2001) Neuropsychiatric disorders in the 22q11 deletion syndrome. *Genet Med*, **3**, 79-84.
242. Bassett, A.S., Hodgkinson, K., Chow, E.W., Correia, S., Scutt, L.E. and Weksberg, R. (1998) 22q11 deletion syndrome in adults with schizophrenia. *American journal of medical genetics*, **81**, 328-37.
243. Murphy, K.C., Jones, L.A. and Owen, M.J. (1999) High rates of schizophrenia in adults with velo-cardio-facial syndrome. *Archives of general psychiatry*, **56**, 940-5.

244. Bassett, A.S., Chow, E.W., AbdelMalik, P., Gheorghiu, M., Husted, J. and Weksberg, R. (2003) The schizophrenia phenotype in 22q11 deletion syndrome. *The American journal of psychiatry*, **160**, 1580-6.
245. Braff, D.L., Geyer, M.A. and Swerdlow, N.R. (2001) Human studies of prepulse inhibition of startle: normal subjects, patient groups, and pharmacological studies. *Psychopharmacology*, **156**, 234-58.
246. Sobin, C., Kiley-Brabeck, K. and Karayiorgou, M. (2005) Lower prepulse inhibition in children with the 22q11 deletion syndrome. *The American journal of psychiatry*, **162**, 1090-9.
247. McAlonan, G.M., Daly, E., Kumari, V., Critchley, H.D., van Amelsvoort, T., Suckling, J., Simmons, A., Sigmundsson, T., Greenwood, K., Russell, A. *et al.* (2002) Brain anatomy and sensorimotor gating in Asperger's syndrome. *Brain*, **125**, 1594-606.
248. Paylor, R., Glaser, B., Mupo, A., Ataliotis, P., Spencer, C., Sobotka, A., Sparks, C., Choi, C.H., Oghalai, J., Curran, S. *et al.* (2006) Tbx1 haploinsufficiency is linked to behavioral disorders in mice and humans: implications for 22q11 deletion syndrome. *Proceedings of the National Academy of Sciences of the United States of America*, **103**, 7729-34.
249. Shimozawa, N., Imamura, A., Zhang, Z., Suzuki, Y., Orii, T., Tsukamoto, T., Osumi, T., Fujiki, Y., Wanders, R.J., Besley, G. *et al.* (1999) Defective PEX gene products correlate with the protein import, biochemical abnormalities, and phenotypic heterogeneity in peroxisome biogenesis disorders. *Journal of medical genetics*, **36**, 779-81.
250. Wanders, R.J., Mooijer, P.A., Dekker, C., Suzuki, Y. and Shimozawa, N. (1999) Disorders of peroxisome biogenesis: complementation analysis shows genetic heterogeneity with strong overrepresentation of one group (PEX1 deficiency). *Journal of inherited metabolic disease*, **22**, 314-8.
251. Faust, P.L. (2003) Abnormal cerebellar histogenesis in PEX2 Zellweger mice reflects multiple neuronal defects induced by peroxisome deficiency. *The Journal of comparative neurology*, **461**, 394-413.
252. Chintala, S., Novak, E.K., Spornyak, J.A., Mazurchuk, R., Torres, G., Patel, S., Busch, K., Meeder, B.A., Horowitz, J.M., Vaughan, M.M. *et al.* (2009) The Vps33a gene regulates behavior and cerebellar Purkinje cell number. *Brain Res*, **1266**, 18-28.
253. Maynard, T.M., Haskell, G.T., Peters, A.Z., Sikich, L., Lieberman, J.A. and LaMantia, A.S. (2003) A comprehensive analysis of 22q11

- gene expression in the developing and adult brain. *Proceedings of the National Academy of Sciences of the United States of America*, **100**, 14433-8.
254. Bi, W., Drake, C.J. and Schwarz, J.J. (1999) The transcription factor MEF2C-null mouse exhibits complex vascular malformations and reduced cardiac expression of angiopoietin 1 and VEGF. *Developmental biology*, **211**, 255-67.
 255. Lin, Q., Schwarz, J., Bucana, C. and Olson, E.N. (1997) Control of mouse cardiac morphogenesis and myogenesis by transcription factor MEF2C. *Science (New York, N.Y.)*, **276**, 1404-7.
 256. Bour, B.A., O'Brien, M.A., Lockwood, W.L., Goldstein, E.S., Bodmer, R., Taghert, P.H., Abmayr, S.M. and Nguyen, H.T. (1995) Drosophila MEF2, a transcription factor that is essential for myogenesis. *Genes & development*, **9**, 730-41.
 257. Lilly, B., Zhao, B., Ranganayakulu, G., Paterson, B.M., Schulz, R.A. and Olson, E.N. (1995) Requirement of MADS domain transcription factor D-MEF2 for muscle formation in Drosophila. *Science (New York, N.Y.)*, **267**, 688-93.
 258. Ranganayakulu, G., Zhao, B., Dokidis, A., Molkenin, J.D., Olson, E.N. and Schulz, R.A. (1995) A series of mutations in the D-MEF2 transcription factor reveal multiple functions in larval and adult myogenesis in Drosophila. *Developmental biology*, **171**, 169-81.
 259. Firulli, A.B. and Olson, E.N. (1997) Modular regulation of muscle gene transcription: a mechanism for muscle cell diversity. *Trends Genet*, **13**, 364-9.
 260. Molkenin, J.D. and Olson, E.N. (1996) Combinatorial control of muscle development by basic helix-loop-helix and MADS-box transcription factors. *Proceedings of the National Academy of Sciences of the United States of America*, **93**, 9366-73.
 261. Molkenin, J.D. and Olson, E.N. (1996) Defining the regulatory networks for muscle development. *Current opinion in genetics & development*, **6**, 445-53.
 262. Davis, R.L., Weintraub, H. and Lassar, A.B. (1987) Expression of a single transfected cDNA converts fibroblasts to myoblasts. *Cell*, **51**, 987-1000.
 263. Braun, T., Rudnicki, M.A., Arnold, H.H. and Jaenisch, R. (1992) Targeted inactivation of the muscle regulatory gene Myf-5 results in abnormal rib development and perinatal death. *Cell*, **71**, 369-82.
 264. Edmondson, D.G. and Olson, E.N. (1989) A gene with homology to the myc similarity region of MyoD1 is expressed during myogenesis

- and is sufficient to activate the muscle differentiation program. *Genes & development*, **3**, 628-40.
265. Rhodes, S.J. and Konieczny, S.F. (1989) Identification of MRF4: a new member of the muscle regulatory factor gene family. *Genes & development*, **3**, 2050-61.
 266. von Both, I., Silvestri, C., Erdemir, T., Lickert, H., Walls, J.R., Henkelman, R.M., Rossant, J., Harvey, R.P., Attisano, L. and Wrana, J.L. (2004) Foxh1 is essential for development of the anterior heart field. *Developmental cell*, **7**, 331-45.
 267. Sun, Y., Liang, X., Najafi, N., Cass, M., Lin, L., Cai, C.L., Chen, J. and Evans, S.M. (2007) Islet 1 is expressed in distinct cardiovascular lineages, including pacemaker and coronary vascular cells. *Developmental biology*, **304**, 286-96.
 268. Guris, D.L., Duester, G., Papaioannou, V.E. and Imamoto, A. (2006) Dose-dependent interaction of Tbx1 and Crkl and locally aberrant RA signaling in a model of del22q11 syndrome. *Developmental cell*, **10**, 81-92.
 269. Nowotschin, S., Liao, J., Gage, P.J., Epstein, J.A., Campione, M. and Morrow, B.E. (2006) Tbx1 affects asymmetric cardiac morphogenesis by regulating Pitx2 in the secondary heart field. *Development (Cambridge, England)*, **133**, 1565-73.
 270. Evans, M.J. and Kaufman, M.H. (1981) Establishment in culture of pluripotential cells from mouse embryos. *Nature*, **292**, 154-6.
 271. Martin, G.R. (1981) Isolation of a pluripotent cell line from early mouse embryos cultured in medium conditioned by teratocarcinoma stem cells. *Proceedings of the National Academy of Sciences of the United States of America*, **78**, 7634-8.
 272. Rideout, W.M., 3rd, Hochedlinger, K., Kyba, M., Daley, G.Q. and Jaenisch, R. (2002) Correction of a genetic defect by nuclear transplantation and combined cell and gene therapy. *Cell*, **109**, 17-27.
 273. Takahashi, K., Tanabe, K., Ohnuki, M., Narita, M., Ichisaka, T., Tomoda, K. and Yamanaka, S. (2007) Induction of pluripotent stem cells from adult human fibroblasts by defined factors. *Cell*, **131**, 861-72.
 274. Lowry, W.E., Richter, L., Yachechko, R., Pyle, A.D., Tchieu, J., Sridharan, R., Clark, A.T. and Plath, K. (2008) Generation of human induced pluripotent stem cells from dermal fibroblasts. *Proceedings of the National Academy of Sciences of the United States of America*, **105**, 2883-8.

275. Park, I.H., Lerou, P.H., Zhao, R., Huo, H. and Daley, G.Q. (2008) Generation of human-induced pluripotent stem cells. *Nature protocols*, **3**, 1180-6.
276. Yu, J., Vodyanik, M.A., Smuga-Otto, K., Antosiewicz-Bourget, J., Frane, J.L., Tian, S., Nie, J., Jonsdottir, G.A., Ruotti, V., Stewart, R. *et al.* (2007) Induced pluripotent stem cell lines derived from human somatic cells. *Science (New York, N.Y.)*, **318**, 1917-20.
277. Park, I.H., Arora, N., Huo, H., Maherali, N., Ahfeldt, T., Shimamura, A., Lensch, M.W., Cowan, C., Hochedlinger, K. and Daley, G.Q. (2008) Disease-specific induced pluripotent stem cells. *Cell*, **134**, 877-86.
278. Dimos, J.T., Rodolfa, K.T., Niakan, K.K., Weisenthal, L.M., Mitumoto, H., Chung, W., Croft, G.F., Saphier, G., Leibel, R., Goland, R. *et al.* (2008) Induced pluripotent stem cells generated from patients with ALS can be differentiated into motor neurons. *Science (New York, N.Y.)*, **321**, 1218-21.
279. Ebert, A.D., Yu, J., Rose, F.F., Jr., Mattis, V.B., Lorson, C.L., Thomson, J.A. and Svendsen, C.N. (2009) Induced pluripotent stem cells from a spinal muscular atrophy patient. *Nature*, **457**, 277-80.
280. Hotta, A., Cheung, A.Y., Farra, N., Vijayaragavan, K., Seguin, C.A., Draper, J.S., Pasceri, P., Maksakova, I.A., Mager, D.L., Rossant, J. *et al.* (2009) Isolation of human iPS cells using EOS lentiviral vectors to select for pluripotency. *Nature methods*, **6**, 370-6.
281. Maehr, R., Chen, S., Snitow, M., Ludwig, T., Yagasaki, L., Goland, R., Leibel, R.L. and Melton, D.A. (2009) Generation of pluripotent stem cells from patients with type 1 diabetes. *Proceedings of the National Academy of Sciences of the United States of America*, **106**, 15768-73.
282. Ye, Z., Zhan, H., Mali, P., Dowey, S., Williams, D.M., Jang, Y.Y., Dang, C.V., Spivak, J.L., Moliterno, A.R. and Cheng, L. (2009) Human-induced pluripotent stem cells from blood cells of healthy donors and patients with acquired blood disorders. *Blood*, **114**, 5473-80.
283. Soldner, F., Hockemeyer, D., Beard, C., Gao, Q., Bell, G.W., Cook, E.G., Hargus, G., Blak, A., Cooper, O., Mitalipova, M. *et al.* (2009) Parkinson's disease patient-derived induced pluripotent stem cells free of viral reprogramming factors. *Cell*, **136**, 964-77.
284. Amit, M. and Itskovitz-Eldor, J. (2006) Derivation and maintenance of human embryonic stem cells. *Methods in molecular biology (Clifton, N.J.)*, **331**, 43-53.

285. Akutsu, H., Cowan, C.A. and Melton, D. (2006) Human embryonic stem cells. *Methods in enzymology*, **418**, 78-92.
286. Adewumi, O., Aflatoonian, B., Ahrlund-Richter, L., Amit, M., Andrews, P.W., Beighton, G., Bello, P.A., Benvenisty, N., Berry, L.S., Bevan, S. *et al.* (2007) Characterization of human embryonic stem cell lines by the International Stem Cell Initiative. *Nature biotechnology*, **25**, 803-16.
287. Nichols, J., Zevnik, B., Anastassiadis, K., Niwa, H., Klewe-Nebenius, D., Chambers, I., Scholer, H. and Smith, A. (1998) Formation of pluripotent stem cells in the mammalian embryo depends on the POU transcription factor Oct4. *Cell*, **95**, 379-91.
288. Loh, Y.H., Wu, Q., Chew, J.L., Vega, V.B., Zhang, W., Chen, X., Bourque, G., George, J., Leong, B., Liu, J. *et al.* (2006) The Oct4 and Nanog transcription network regulates pluripotency in mouse embryonic stem cells. *Nature genetics*, **38**, 431-40.
289. Draper, J.S., Moore, H.D., Ruban, L.N., Gokhale, P.J. and Andrews, P.W. (2004) Culture and characterization of human embryonic stem cells. *Stem cells and development*, **13**, 325-36.
290. Ginis, I., Luo, Y., Miura, T., Thies, S., Brandenberger, R., Gerecht-Nir, S., Amit, M., Hoke, A., Carpenter, M.K., Itskovitz-Eldor, J. *et al.* (2004) Differences between human and mouse embryonic stem cells. *Developmental biology*, **269**, 360-80.
291. Badcock, G., Pigott, C., Goepel, J. and Andrews, P.W. (1999) The human embryonal carcinoma marker antigen TRA-1-60 is a sialylated keratan sulfate proteoglycan. *Cancer research*, **59**, 4715-9.
292. Cooper, S., Bennett, W., Andrade, J., Reubinoff, B.E., Thomson, J. and Pera, M.F. (2002) Biochemical properties of a keratan sulphate/chondroitin sulphate proteoglycan expressed in primate pluripotent stem cells. *Journal of anatomy*, **200**, 259-65.
293. Lee, G., Papapetrou, E., Kim, H., Chambers, S., Tomishima, M., Fasano, C., Ganat, Y., Menon, J., Shimizu, F., *et al.* (2009) Modelling pathogenesis and treatment of familial dysautonomia using patient-specific iPSCs. *Nature*, 10.1038/nature08320.
294. Raya, A., Rodriguez-Piza, I., Guenechea, G., Vassena, R., Navarro, S., Barrero, M.J., Consiglio, A., Castella, M., Rio, P., Sleep, E., *et al.* (2009) disease-corrected haematopoietic progenitors from fanconi anaemia induced pluripotent stem cells. *Nature*, **460**, 53-59.
295. Moretti, A., Caron, L., Nakano, A., Lam, J.T., Bernshausen, A., Chen, Y., Qyang, Y., Bu, L., Sasaki, M., Martin-Puig, S., Sun, Y., Evans, S.M., Laugwitz, K.L., and Chie, K.R., (2006) Multipotent embryonic

- isl1+ progenitors cells lead to cardiac, smooth muscle, and endothelial cell diversification. *Cell* **127**, 1151-1165.
296. Kattman, S.J., Huber, T.L., and Keller, G.M. (2006) Multipotent flk1+ cardiovascular progenitor cells give rise to the cardiomyocyte, endothelial, and vascular smooth muscle lineages. *Dev. Cell* **11**, 723-732.
 297. Sun, Y., Liang, X., Najafi, N., Cass, M., Lin, L., Cai, C.L., Chen, J., and Evans, S.M. (2007) Islet1 is expressed in distinct cardiovascular lineages, including pacemaker and coronary vascular cells. *Dev. Biol.* **304**, 286-296.
 298. Moretti, A., Bellin, M., Jung, C.B., Thies, T., takashima, Y., Bernshausen, A., Schiemann, M. *et al.* (2010) Mouse and human induced pluripotent stem cells as a source for multipotent Isl1+ cardiovascular progenitor. *The FASEB Journal*, **24**, 1-12.